Pacific Northwest
NATIONAL LABORATORY

Proudly Operated by **Battelle** *Since 1965*

PNNL Measurement Results for the 2016 Criticality Accident Dosimetry Exercise at the Nevada National Security Site (IER-148)

May 2017

BA Rathbone
SM Morley
JA Stephens

PNNL Measurement Results for the 2016 Criticality Accident Dosimetry Exercise at the Nevada National Security Site (IER-148)

BA Rathbone
SM Morley
JA Stephens

May 2017

Pacific Northwest National Laboratory
Richland, Washington 99352

Abstract

The Pacific Northwest National Laboratory (PNNL) participated in a criticality accident dosimetry intercomparison exercise held at the Nevada National Security Site (NNSS) May 24-27, 2016. The exercise was administered by Lawrence Livermore National Laboratory (LLNL) and utilized the Godiva-IV critical assembly housed in the Device Assembly Facility (DAF) situated on the NNSS site. The exercise allowed participants to test the ability of their nuclear accident dosimeters to meet the performance criteria in ANSI/HPS N13.3-2013, *Dosimetry for Criticality Accidents* and to obtain new measurement data for use in revising dose calculation methods and quick sort screening methods where appropriate.   PNNL participated with new prototype Personal Nuclear Accident Dosimeter (PNAD) and Fixed Nuclear Accident Dosimeter (FNAD) designs as well as the existing historical PNAD design. The new prototype designs incorporate optically stimulated luminescence (OSL) dosimeters in place of thermoluminescence dosimeters (TLDs), among other design changes, while retaining the same set of activation foils historically used.   The default dose calculation methodology established decades ago for use with activation foils in PNNL PNADs and FNADs was used to calculate neutron dose results for both the existing and prototype dosimeters tested in the exercise. The results indicate that the effective cross sections and/or dose conversion factors used historically need to be updated to accurately measure the operational quantities recommended for nuclear accident dosimetry in ANSI/HPS N13.3-2013 and to ensure PNAD and FNAD performance meets the performance criteria given in the standard. The operational quantities recommended for nuclear accident dosimetry are personal absorbed dose, $D_p(10)$, and ambient absorbed dose, $D^*(10)$.

Summary

The Pacific Northwest National Laboratory (PNNL) participated in a criticality accident dosimetry intercomparison exercise held at the Nevada National Security Site (NNSS) May 24-27, 2016. The exercise was administered by Lawrence Livermore National Laboratory (LLNL) and consisted of three exposures performed using the Godiva-IV critical assembly which is part of the Nuclear Criticality Experimental Research Center (NCERC) situated on the NNSS site. The exercise allowed participants to test the ability of their nuclear accident dosimeters to meet the performance criteria in ANSI/HPS N13.3-2013, *Dosimetry for Criticality Accidents* and to obtain new measurement data for use in revising dose calculation methods and quick sort screening methods where appropriate. PNNL participated with new prototype Personal Nuclear Accident Dosimeter (PNAD) and Fixed Nuclear Accident Dosimeter (FNAD) designs as well as the existing historical Hanford PNAD design. The new prototype PNNL designs incorporate optically stimulated luminescence (OSL) dosimeters in place of thermoluminescence dosimeters (TLDs), among other design changes, while retaining the same set of activation foils used historically.   The prototype PNAD incorporates the Landauer InLight® OSLN four element whole body dosimeter which provides the primary gamma dose and an estimate of neutron dose to supplement the primary neutron dose information obtained from the activation foils. The prototype FNAD incorporates Landauer OSL and OSLN nanoDot dosimetrs to provide the primary gamma dose information and supplemental neutron dose information.

The default dose calculation methodology established decades ago for use with activation foils in PNNL PNADs and FNADs was used to calculate neutron dose results for both the existing and prototype dosimeters tested in the exercise. Neutron absorbed dose results calculated from foil activities using this methodology were consistently low. The bias in reported personal neutron absorbed dose, $D_p(10)_n$ for PNADs exposed on phantom was -0.40. Similarly, the bias in reported ambient neutron absorbed dose, $D^*(10)_n$ for FNADs exposed in air was -0.42. Even when the the under estimated neutron dose is combined with the over estimated gamma dose (bias = 1.59), nearly half of the PNADs exposed on phantom failed to meet the ANSI/HPS N13.3-2013 $\pm$ 25% accuracy requirement for total gamma+neutron dose. These results indicate that the effective cross sections and dose conversion factors used historically need to be updated to accurately measure the operational quantities recommended for nuclear accident dosimetry in ANSI/HPS N13.3-2013 and to ensure PNAD and FNAD performance meets the performance criteria given in the standard. The operational quantities recommended for nuclear accident dosimetry are personal absorbed dose, $D_p(10)$, and ambient absorbed dose, $D^*(10)$. Current dose calculation methodology is based on measurement of tissue kerma which is typically 70% - 80% of the absorbed dose value.

The foil activity measurements documented in this report have acceptable uncertainty and are consistent across measurement locations exhibiting relatively low variability. Combined with the reference dosimetry for the exercise provided by LLNL, and the fluence/spectrum characterization work performed by AWE, the activity measurements documented in this report should be suitable for use in validating and/or revising the activity-to-fluence conversion factors, and the fluence-to-dose conversion factors for unmoderated criticality events. The revised dose calculation methodology will also need to to accommodate the neutron energy spectrum expected in a solution type criticality event at PNNL. The OSL/OSLN response data obtained during the exercise indicate that OSL gamma dose calculations need to be revised to correct for the influence of neutrons on gamma dose response. The response data also indicate that OSL/OSLN nanoDot pairs in the FNAD can provide accurate $D^*(10)_n$ dose results and the InLight OSLN dosimeter in the PNAD can potentially provide accurate gamma dose results and unbiased *estimates* of neutron dose with proper calibration to a specific source spectrum.

Acknowledgments

Acronyms and Abbreviations

ABS	acrylonitrile butadiene styrene
ANSI	American National Standards Institute
AWE	Atomic Weapons Establishment (U.K.)
BOMAB	BOttle MAnnikin Absorber
DAF	device assembly facility
EOB	end of burst
EPD	electronic personal dosimeter
FNAD	fixed nuclear accident dosimeter
FWHM	full width at half maximum
GM	Geiger-Mueller tube
HD	high dose
HPGe	high purity germanium
HPRR	Health Physics Research Reactor
HPS	Health Physics Society
IAEA	International Atomic Energy Agency
ICRP	International Commission on Radiation Protection
ICP-MS	inductively coupled plasma-mass spectrometry
LANL	Los Alamos National Laboratory
LCD	liquid crystal display
LD	low dose
LED	light emitting diode
LLNL	Lawrence Livermore National Laboratory
MCA	multi-channel analyzer
mil	one thousandth of an inch
NAD	nuclear accident dosimeter
NCERC	Nuclear Criticality Experimental Research Center
NNSS	National Nuclear Security Site
NRC	Nuclear Regulatory Commission (U.S.)
OSL	optically stimulated luminescence
OSLN	optically stimulated luminescence (neutron sensitive)
PMMA	polymethylmethacrylate
PNAD	personal nuclear accident dosimeter
PSSS	passive single sphere spectrometer
TLD	thermoluminescence dosimeter
XRF	X-ray flurorescence

Contents

Appendices

1.0 Introduction

An international nuclear accident dosimetry exercise was conducted at the Nevada National Security Site (NNSS) on May 24-27, 2016 using the Godiva-IV critical assembly. The exercise was administered by Lawrence Livermore National Laboratory (LLNL) and included participation by LLNL, Los Alamos National Laboratory (LANL), the U.S. Naval Dosimetry Center (NDS), NNSS, Pacific Northwest National Laboratory (PNNL), Sandia National Laboratory (SNL), Savannah River Site (SRS), the Atomic Weapons Establishment (AWE) from the United Kingdom, and the Institute for Radiological Protection and Nuclear Safety (IRSN) from France. The final planned experimental design is described in IER-148 CED-2 Report (Heinrichs, et. al. 2014). The primary purpose of the exercise was to allow participants to test the ability of their criticality accident dosimetry systems to meet the performance criteria in ANSI/HPS N13.3-2013. The exercise also afforded participants the opportunity to evaluate their measurement methods and collect measurement data for use in revising dose calculation methodology where appropriate. The primary purpose of this report is to document in detail the measurements made by the PNNL team during the exercise, and the doses calculated from the measurement data using default calibration factors and historical dose calculation formulae. Any revisions to the dose calculation methodology which stem from the results of this report will be documented in a separate report.

This exercise presented an opportunity for PNNL to test prototypes of new personal nuclear accident dosimeter (PNAD) and fixed nuclear accident dosimeter (FNAD) designs planned for implementation at PNNL in 2017 as well as the existing PNAD design. The new designs incorporate optically stimulated luminescence (OSL) dosimeters in place of thermoluminescence dosimeters (TLDs), activation foils and sulfur pellets with larger mass to increase sensitivity, and sealed sulfur pellet packets with sufficient mass to allow direct beta counting without the need for melting, crushing or handling of dispersible activity. The new designs were developed to address a number of issues with the current dosimeter design and to capitalize on the transition of PNNL from a TLD based external dosimetry program with its associated infrastructure to an OSL based external dosimetry program. The new PNAD and FNAD designs and the existing PNAD design are described in greater detail in Section 2 of this report. Some of the issues with existing PNAD and FNAD designs that are addressed by the new PNAD and FNAD designs are the following:

- Oxidation of indium foils over time to a dispersible powder state with significant reduction in mass of the metal foil over time and increased potential for contamination of equipment and cross contamination of other samples being analyzed.
- Fracturing and crumbling of sulfur pellets to a dispersible form that is difficult to retrieve and analyze and increases the potential for contamination of equipment and cross contamination of other samples being analyzed.
- Welded plastic PNAD cases that require destructive opening to retrieve foils.
- Insufficient sulfur mass for reliable measurement of 10 rad dose without performing time consuming sublimation to negligible residue on metal planchet.
- Detector elements that are not pre-labeled with unique identifiers with increased risk for handling and labeling errors during a criticality event.
- Cumbersome time consuming handling and analysis procedures that prevent adequate dosimeter throughput to provide initial dose results on significantly exposed individuals within 24 hours.
- Difficult detection of In-115m peaks in thin 0.005" indium foils.

The IER-148 CED-2 Report was finalized in September 2014 and included descriptions of the dosimeters planned for testing by each participant. The prototype PNAD design described in that report as the "PNNL PNAD" was replaced with the design described in this report. Because of issues related to handling of flammable and dispersible radioactive materials at the NAD lab in Mercury, NV, the availability of only one hood for all participants desiring to melt or crush their sulfur pellets, and the limited number of PNADs that could be tested if time consuming radiochemistry were required, PNNL developed a new prototype PNAD that did not require crushing or melting of sulfur. The shortened analysis time was also considered advantageous to the program at PNNL by simplifying handling procedures, reducing equipment and lab space requirements, and by increasing capacity to analyze dosimeters from 20 or more significantly exposed individuals in the event of an actual criticality. The FNAD design described in the IER-148 CED-2 Report also does not reflect the actual FNAD design tested. For similar reasons as those described above, the prototype FNAD design described in this report was tested instead of the standard FNAD design described in the IER-148 CED-2 Report. The new PNAD and FNAD designs utilize the same activation materials and activation reactions for determining neutron dose as the existing designs, and differ primarily in material dimensions and packaging.

PNNL has participated in a number of nuclear accident dosimetry (NAD) intercomparison exercises in the past. These include some of the exercises in the series conducted by the Oak Ridge National Laboratory (ORNL) with the health physics research reactor (HPRR) (Sims 1988, Swaja et. al. 1986) as well as more recent DOE sponsored exercises at the CED Valduc Silene and Caliban Reactors (Hill and Conrady 2010, Hill and Conrady 2011). Although the reference dosimetry was well established for these exercises (Sims and Killough 1981, Sims and Ragan 1987, Asselineau et. al. 2004), the activity measurement data obtained from foils in the PNNL dosimeters is no longer available for review or use in re-evaluating dose calculation formulae. Consequently, an important objective of the present report is to document the measurements made during this Godiva-IV exercise with sufficient detail to allow meaningful use in evaluating and/or revising as necessary, the effective cross sections, dose conversion factors and dose calculation methodology to be used for the new PNNL PNAD and FNAD designs.

A large number of measurements were made over a three day period and an extensive volume of data was generated, including 339 activity measurements on 245 foils, 118 readings on 36 nanoDot dosimeters, 159 readings on 50 InLight® dosimeters, 10 readings on 10 electronic personal dosimeters (EPD)s, and 104 direct survey readings on 52 PNADs. Gamma and neutron dose results are reported for 52 PNADs, and 3 FNADs. Neutron dose results are reported on the basis of both the foil measurements and the OSLN (neutron sensitive OSL) measurements.

2.0 Dosimeter Descriptions

Three different dosimeter designs were tested during the Godiva-IV exercise.

- Hanford PNAD (5 mil foil and 10 mil foil versions)
- PNNL PNAD (10 mil foils)
- PNNL FNAD (10 mil foils)

The actual dosimeters tested were prototypes of dosimeters already in service or slight variants thereof (Hanford PNAD), or prototypes of dosimeters planned for implementation (PNNL PNAD and PNNL FNAD). At the time of this writing, the Hanford FNAD had been removed from service.

The prototype dosimeters built for the exercise were assembled from the PNNL NAD program inventory of sulfur pellets, indium foils and copper foils which was used to build the actual dosimeters that will be put into field use. With the exception of the 10 mil indium foils, all activation materials had certifications by the supplier for 99% or better purity. The 10 mil indium foils were manufactured from an old inventory that did not have purity certification. This stock was sampled and tested for impurities at PNNL using X-ray Fluorescence (XRF) and Inductively Coupled Plasma - Mass Spectrometry (ICP-MS) analytical methods. Analysis results determined that the indium foils are >99.9% pure.

2.1 Hanford PNAD

Figure 1 shows the actual Hanford PNAD in current use and the test model used for the Godiva-IV exercise. The test model duplicates the radiologically significant features of the Hanford PNAD currently in the field. The foil thickness, cadmium filter thickness in front of and behind each element, and polymethyl methacrylate (PMMA) plastic thickness in front of and behind each detector in the test model are the same as the field version. The PMMA front and back plastic plates are held together with nylon screws for easy disassembly. The activation detectors are (A) sulfur pellet, (B) cadmium covered copper, (C) cadmium covered indium, and (D), bare indium. Each sulfur pellet is sealed in a 0.038 mm thick (1.5 mil) polyethylene bag to prevent dispersible powder. Each foil and pellet pack are pre-labeled with the detector mass, and a unique ID indicating the both the dosimeter number and detector position within the dosimeter. The foil dimensions are shown in **Table 1**. Two versions of this PNAD were tested. One version contained 0.127 mm thick (5 mil) indium and copper foils, duplicating the foil thickness in the Hanford field PNADs. The second version contained 0.254 mm thick (10 mil) foils which is the thickness used in the LANL and NNSS PNADs manufactured by Shieldwerx (Rio Rancho, NM) and is the thickness used for the PNNL PNAD. Sulfur pellet dimensions were the same in both versions. The primary reason for testing two foil thicknesses was to measure the effects of self-shielding in the foils for thermal and epithermal neutrons on the ^{115}In(n,γ)^{116m}In and ^{63}Cu(n,γ)^{64}Cu reactions. A secondary reason was to assess the potential for improved minimum detectable activity (MDA) for ^{115m}In and ^{64}Cu with increased foil thickness.

Table 1. Description of test models of Hanford PNAD used in Godiva-IV exercise.

Hanford PNAD Description (test model)	Hanford PNAD (5 mil foils)				Hanford PNAD (10 mil foils)			
detector name	A	B	C	D	A	B	C	D
detector composition	S	Cu	In	In	S	Cu	In	In
detector thickness (mm)	1.91	0.127	0.127	0.127	1.91	0.254	0.254	0.254
detector diameter (cm)	1.27	1.27	1.27	1.27	1.27	1.27	1.27	1.27
filter composition	none	Cd	Cd	none	none	Cd	Cd	none
filter thickness (mm)	none	0.533	0.533	none	none	0.533	0.533	none
Case composition	PMMA	PMMA	PMMA	PMMA	PMMA	PMMA	PMMA	PMMA
Case thickness (cm)	0.15	0.15	0.15	0.15	0.15	0.15	0.15	0.15

For gamma dosimetry, a second pair of PMMA plates loaded with three Landauer OSL nanoDots was attached to the test model of the Hanford PNAD. The combined gamma+neutron PNAD assembly as tested during the exercise is shown in **Figure 2**, mounted on an aluminum plate that was hung on a dosimeter tree. The use of OSL nanoDots allowed onsite processing with a Landauer microStar® reader to obtain gamma dose results for the PNAD while at the exercise. Since PNNL has moved to an OSL based external dosimetry program it was also desirable to obtain response information for the Al_2O_3:C OSL nanoDot detectors which will be used in the PNNL FNAD (described below). Two LiF:Mg,Ti (TLD 700) chips were also loaded into the gamma dosimeter half of the PNAD assembly but not processed.

The use of actual Hanford PNADs in the intercomparison exercise was impractical for several reasons. The plastic case is permanently welded together and requires destructive techniques for opening. The actual Hanford PNADs were manufactured 30 years ago with the sulfur pellets having fractured and crumbled over time and the indium foils having degraded due to oxidation. The degraded state of the activation components made the risk of spreading dispersible radioactive materials with a destructive opening process unacceptable.
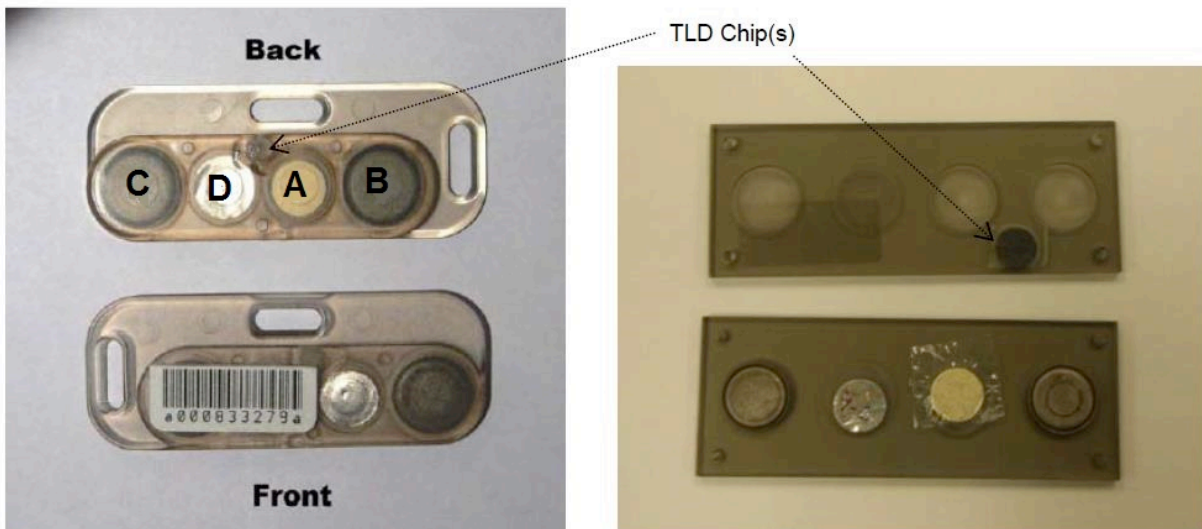
Figure 1. Actual Hanford PNAD (left) and test model used in exercise (right).
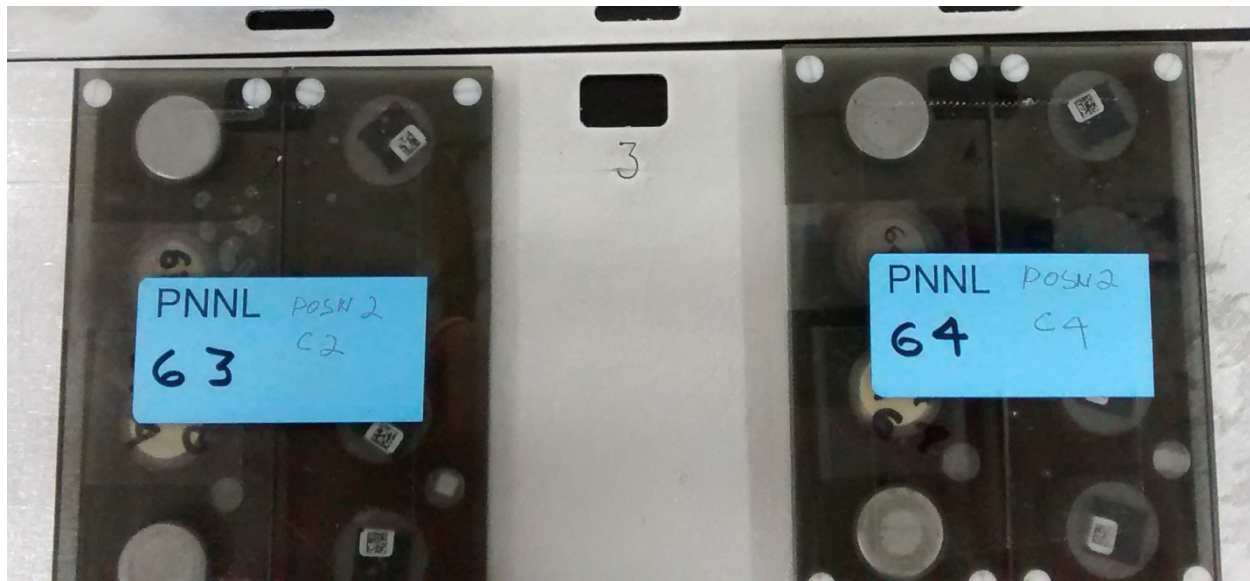
Figure 2. Test model of Hanford PNAD as tested with added holder for OSL nanoDots.

2.2 PNNL PNAD

The PNNL PNAD uses the same types of neutron activation detectors, and activation reactions for neutron dose assessment as the Hanford PNAD. For the purpose of this exercise, the same effective cross sections, dose conversion factors, and dose calculation formulae were used for deriving neutron dose as were used for the Hanford PNAD. The PNNL PNAD differs from the Hanford PNAD in that the foils and sulfur pellets are housed inside a Landauer InLight® Model 2 dosimeter clear polycarbonate shell together with an InLight® Model 2 OSLN dosimeter case ("BA" type case) and slide ("N" type slide). Other differences include the use of 10 mil foils instead of 5 mil foils, and the use of 6 sulfur pellets sealed in a polyethylene bag for direct beta counting on a standard 50 mm planchet with commonly available beta counting equipment. The InLight® OSLN dosimeter is read on a Landauer microStar® reader specially modified with a neutral density filter for readout of accident level dosimeters. The InLight® OSLN dosimeters may also be read on a standard microStar® if the dose is sufficiently low. The InLight® OSLN dosimeter provides the primary gamma dose to be used for the PNAD and an albedo neutron dose value that can be used as an initial estimate of neutron dose. The albedo neutron dose response is highly energy dependent and not suitable for final reporting of neutron dose. **Appendix A** contains detailed design information for the PNNL PNAD. Components of a disassembled PNNL PNAD are shown in **Figure A.1** and an exploded view of the dosimeter is shown in **Figure A.2**. Component dimensions and composition are given in **Table A.1**. The prototype PNNL PNAD that was used for the exercise was identical to the PNNL PNAD in **Appendix A** except as follows: 1) a single sulfur pellet was added behind the bare indium foil (detector D), a thinner blue paper label was used on the PNAD shell exterior instead of the orange paper label inside the PNAD shell and 3) flat strap loop type hangers were used instead of alligator clips. Photos of the front and back side of the prototype PNNL PNAD used in the exercise are shown in **Figure 3 and Figure 4**. A simplified table of the detector dimensions for the PNNL PNAD is shown in **Table 2**.

Figure 3. PNNL PNAD front side (without label) **Figure 4**. PNNL PNAD back side (w/added S pellet)

Table 2. Prototype PNNL PNAD detector dimensions and composition

PNNL PNAD Activation Elements (test model)					
detector name	A	B	C	D	n/a
detector description	sulfur pellet (sixpack)	10 mil copper foil (Cd covers)	10 mil indium foil (Cd covers)	10 mil indium foil (bare)	sulfur pellet (single)
detector composition	S	Cu	In	In	S
detector thickness (mm)	1.91	0.254	0.254	0.254	1.91
detector mass (g)	2.61	0.281	0.236	0.236	0.435
detector density thickness (g/cm^2)	0.343	0.228	0.186	0.186	0.343
detector diameter (cm)	n/a	1.27	1.27	1.27	1.27
detector L (cm) x W (cm)	3.81 x 2.54	n/a	n/a	n/a	n/a
filter composition	none	Cd	Cd	none	none
filter thickness (mm)	none	0.533	0.533	none	none

The single sulfur pellet shown in **Figure 4** was included in the test model of the PNNL PNAD to provide the option for independent analysis by sublimation should the opportunity present itself, and as a method for comparing relative sensitivity for counting of a single sulfur pellet whole vs. a packet of six pellets. Count results from the sulfur pellet six pack afforded improved sensitivity and shortened count times and were used for dose determination.

2.3 PNNL FNAD

The PNNL FNAD is a new design based on the Hanford FNAD which has been used since the 1960s at both Hanford and PNNL. The historical Hanford FNAD is described in Hanford historical documents (Bramson 1963, Glen and Bramson 1977). The new PNNL FNAD design uses the same types of neutron activation detectors, and activation reactions for neutron dose assessment as the Hanford FNAD. The new design differs from the old design primarily in the replacement of TLDs with OSL dosimeters. Landauer OSL and OSLN nanoDots have replaced the TLD 700 and TLD 600 chips respectively, and are read on the same modified Landauer microStar® reader used for reading the InLight® dosimeters in the PNNL PNADs. The new design also differs in the dimensions of foils used, in the packaging used, and in the arrangement of foils within the packaging (metal foils are no longer stacked on top of each other). The PNNL FNAD inner and outer dosimetry packages have been re-designed for easier loading and unloading. The PNNL FNAD is described in greater detail in **Appendix B**. An exploded view of the dosimeter is shown in **Figures B.1** through B.**4**. Component dimensions and composition are given in **Table B.1**.

Unfortunately, the outer dosimetry package design for the PNNL FNAD had not been finalized by the time of the exercise and printed plastic case parts were not available. As a result, the outer dosimetry package used at the exercise was a crude prototype made with existing plastic case parts from the Hanford FNAD outer dosimetry package.   The prototype PNNL FNAD as tested in the exercise is shown in **Figure 5**. The prototype outer dosimetry package used in the PNNL FNAD is shown in **Figure 6** (the rectangular cadmium plate is missing from front half in the photo). The exercise version differed from the final design version documented in **Appendix B** as follows: 1) A single 10 mil copper foil 2.54 cm diameter and 0.254 mm thick was used for detector B instead of two 1.27 cm diameter x 0.254 cm thick copper foils, 2) Square indium foils 1 cm x 1 cm x 0.254 cm thick were used for detectors C and D instead of round foils 1 cm dia. x 0.254 cm thick.   3) A pair of rectangular cadmium plates 3.2 cm x 2.2 cm x 0.114 cm thick were used as filters to cover the copper (B), indium (C) and gold (F) foils in the outer package (see note below regarding letter labeling) rather than round cadmium cups. 4) The OSL-OSLN nanoDot pair (dots 1 and 2) were stacked on top of each other instead of being side by side. 5) The hexagonal sulfur pellet pack was supported between thin cardboard disks and taped to the top of the outer dosimetry package rather than being enclosed in the outer dosimetry package plastic case.

The configuration of the inner dosimetry package used in the exercise differed from the final design by using two OSL nanoDots and two OSLN nanoDots rather than the final design configuration of one OSL nanoDot and 3 OSLN nanoDots. The OSL-OSLN nanoDot combination in the inner package was changed in the final design to reduce uncertainty in the net neutron signal. **Figure 7** shows the inner dosimetry package used in the exercise prototype.

Figure 8 shows an assembled FNAD candle as used for the exercise.   A simplified table of the detector dimensions for the version of the PNNL FNAD used in the exercise is shown in **Table 3**. The dimensions given are for the sensitive volume of the detector.

NOTE: *For the purposes of the exercise, the bare gold foil and cadmium covered gold foil in the outer dosimetry package were tracked with the letters **F** and **G** respectively. In the inner dosimetry package, the gold foil was tracked with the letter **H**. In the final FNAD design documented in **Appendix B**, these three foils have had their letter designations changed from **F,G,H** to **E,F,G** respectively.   The reason for the change in letter designation was the elimination of the single sulfur pellet in the PNAD (designated with the letter **E** for the exercise). For consistency with the component naming conventions used in the final system design documentation provided in **Appendix B**, the letter codes **E,F,G** are used in this report to document the activity measurements associated with these gold foil and are used in **Table 3**.*

Figure 5 Prototype PNNL FNAD as tested

Figure 6. PNNL FNAD Outer Dosimetry Package (test prototype).

Figure 7. PNNL FNAD Inner Dosimetry Package (test prototype)
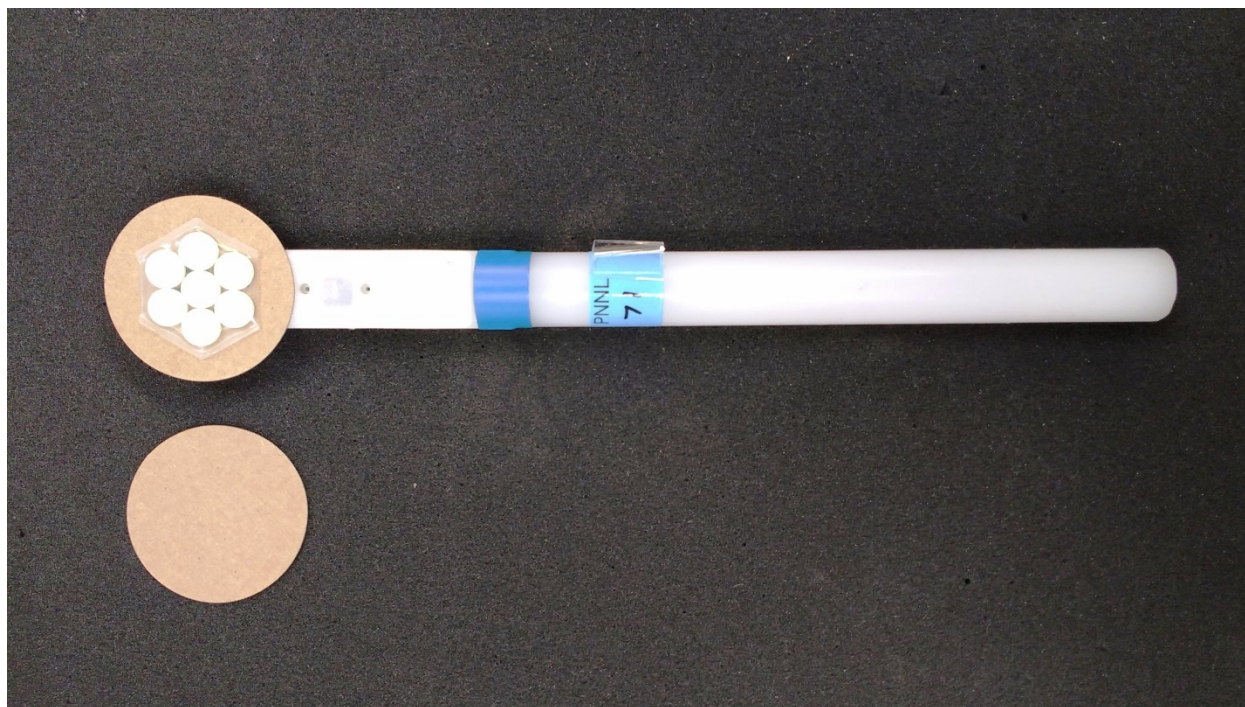
Figure 8. PNNL FNAD Candle (test prototype)

Table 3. Detector dimensions in the prototype PNNL FNAD tested in the exercise

Description	Detector	Mass (g)	Density (g/cm^3)	Dimensions (cm)	Thickness (cm [mil])	Density Thickness (mg/cm^2)
Outer Dosimetry Package	hexagonal sulfur pack (A)	3.07	1.8	3.48 x 3.81	0.190 [75]	343
	round copper foil (B)	0.851	8.96	2.2 dia.	0.025 [10]	224
	square Indium foils (C, D)	0.404	7.31	1.3 by 1.7	0.025 [10]	186
	square gold foils (E, F)	0.245	19.3	1.0 by 1.0	0.0127 [5]	245
	rectangular cadmium filters	6.974	8.69	3.2 by 2.2	0.114 [45]	986
	OSL nanoDot (dot 1)	0.009	1.21	0.5 cm dia.	0.0381 [15]	46
	OSLN nanoDot (dot 2)	0.009	1.21	0.5 cm dia.	0.0381 [15]	46
Inner Dosimetry Package	square gold foil (G)	0.245	19.3	1.0 by 1.0	0.0127 [5]	245
	OSL nanoDot (dots 3, 4)	0.009	1.21	0.5 cm dia.	0.0381 [15]	46
	OSLN nanoDot (dots 5, 6)	0.009	1.21	0.5 cm dia.	0.0381 [15]	46

2.4 Electronic Personal Dosimeters

Four types of electronic personal dosimeters (EPD) were tested during the exercise. These include three (3) Thermo Mark 2.5, three (3) Mirion-MGP DMC2000S, three (3) Mirion-MGP DMC3000 and one (1) Mirion-MGP DMC3000 with added neutron module. Only the DMC3000 with added neutron module included the capability for neutron dose measurement. The primary objective was to measure the "apparent" gamma dose response of the gamma only dosimeters when exposed to very intense short bursts of neutron+gamma radiation, at both protection level doses and accident level doses. A secondary objective was to obtain neutron absorbed dose response information for the DMC3000 for intense bursts of neutron+gamma radiation. All EPDs had been calibrated on a ^{137}Cs well source with response (counts/mrem) cross calibrated to ^{137}Cs response on phantom. The EPD internal calibration factors were set for reporting of $H_p(10)_\gamma$ gamma dose on that basis. In addition, the DMC 3000 had been calibrated on phantom at PNNL using a bare ^{252}Cf source and had internal calibration factors set for reporting of $H_p(10)_n$ neutron dose equivalents on that basis. Readout of the Thermo Mark 2.5 dosimeters was accomplished using a Thermo USB-IR reader controlled by EasyEPD software (version 15) installed on laptop with Windows 7 operating system. Readout of the Mirion-MGP EPDs was accomplished using a LDM-320D USB electronic dosimeter proximity reader with a Windows 7 laptop and Mirion-MGP analysis software (DmcUser Version 1.8). The DMC3000s were in G2 mode, while the DMC3000-neutron was in G3 mode. Readings taken directly from the LCD displays were found to be consistent with those obtained from the software.

3.0 Experiment Design

The source used for the intercomparison exercise was the Godiva-IV critical assembly. The assembly consists of enriched U-235 concentric metal cylinders and has minimal inherent moderation. More information on the Godiva-IV critical assembly, and the neutron energy spectrum produced by it can be found in various technical reports (Casson et. al 1996a, Casson et.al 1996b, IAEA 1978, IAEA 1990, Kimpland, 1996, Mosteller and Goda 2009). The Godiva-IV critical assembly is housed in the device assembly facility (DAF) situated on the NNSS site. Godiva-IV was moved from LANL to NNSS in 2005. It is one of many critical assemblies at the National Criticality Experiments Research Center located on the NNSS site (Hutchinson et. al. 2012). The exercise consisted of 3 irradiations from the unmoderated Godiva-IV critical assembly, each being administered on a separate day with a new set of dosimeters being exposed each day. The reactor was operated in the pulse mode and the burst intensity was varied on each day to achieve the desired number of fissions and range of doses at dosimeter locations in the DAF. Each pulse consisted of a super-prompt-critical excursion lasting approximately 50 microseconds (pulse FWHM $\approx$ 25 microseconds). Pulse 1 occurred on 5/24/2016 at 10:11 am. Pulse 2 occurred on 5/25/2016 at 9:42 am. Pulse 3 occurred on 5/26/2016 at 11:35 am. The exact dimensions of the room in which the reactor is housed and the irradiations took place were not provided to participants. However, it was revealed that the room is heavily shielded with concrete walls, floor and ceiling. Dosimeters were irradiated either in air or on phantom. To simulate irradiations in air, PNADs and EPDs were mounted on thin aluminum plates suspended on portable racks called "trees", or in the case of the FNADs, placed on low mass stands. The phantoms used were saline filled Bottle Manikin Absorption (BOMAB) phantoms and 30 x 30 x 15 cm polymethyl methacrylate (PMMA) slab phantoms. PNADs were mounted on the front and back of the phantoms. No EPDs were mounted on phantoms. For the third pulse, one BOMAB was placed in a lateral orientation with respect to the source with PNADS mounted on the front and back of the phantom to provide lateral irradiation geometry. For each pulse, the phantoms, dosimeter trees, and FNAD stands were placed at designated locations numbered 1 through 12, having distances of either 2 meters, 2.5 meters, 3 meters, 4 meters or 9 meters. The single location at 9 meters (location 10) was described as an "alcove" location. Maps of the locations and types of phantoms/trees at each location for each pulse are shown in **Appendix C**, **Figures C.1-C.3**. The identities of the individual dosimeters placed on each phantom or tree are also documented in **Appendix C**, in **Table C.1**.

The BOMAB phantoms complied with the standard dimensions and fill volumes documented ANSI/HPS N13.35-2009 (HPS 2009) for a phantom representing a contemporary adult male. The cylinders in each phantom were filled with Ringer's lactate solution. Samples were drawn from one of the phantoms and provided to participants in 10 ml sample vials after each pulse for counting by those participants who requested samples. After each pulse, the BOMAB phantoms were made available to participants to make quick-sort measurements with hand held instruments.

Each designated test location (except for the alcove location, no. 10) had been previously characterized for neutron fluence, neutron energy spectrum (Wilson et. al. 2014) and various neutron dose quantities including personal absorbed dose from neutrons, $D_p(10)_n$ and ambient absorbed dose from neutrons, $D^*(10)_n$ which are recommended operational quantities to use for calibration of PNADs and FNADs

respectively.   Gamma doses at each location except the alcove location had also been characterized.
Neutron dose measurements were made for the alcove position during pulse 2 of the exercise by AWE
using a passive single sphere spectrometer (PSSS) (Gomez-Roz et. al. 2012) employing gold foils at
multiple depths across multiple axes within a 30 cm diameter polyethylene sphere. The AWE report of
these measurements has not been finalized. Preliminary reference fluence and dose information provided
by LLNL is shown in **Appendix D**, **Tables D.1.1-D.3.3**. One noteworthy conclusion from the Godiva-IV
characterization report by AWE is the fact that the neutron energy spectrum varied significantly as a
function of height above the floor. To the extent practicable, PNNL dosimeters were placed at a uniform
height across the locations used.

After each pulse, the trees and phantoms loaded with dosimeters were returned to the NAD lab in
Mercury, NV, surveyed and dosimeters provided to participants for breakdown and analysis. After each
pulse, at least one BOMAB phantom was made available for participants to make direct measurements
with hand held survey instruments.   After Pulse 1 and Pulse 2, the participants were provided with
reference doses to allow them to verify their measurement methods. After Pulse 3, the participants were
asked to provide initial estimates of dose for their dosimeters within 24 hours of the pulse, without being
provided reference doses. Reference doses for Pulse 3 were provided after reporting of results by all
participants.

4.0 Activity Measurements

Participants in the IER-148 International Intercomparison Exercise for Nuclear Accident Dosimetry at the DAF Using Godiva-IV were required to bring their own counting equipment for analyzing the foils in their nuclear accident dosimeters. For PNNL, this meant bringing gamma counting equipment, beta counting equipment, and associated shielding. A brief list of the major counting equipment is shown in **Table 4**. The equipment is described in greater detail in the context of the measurements being made in Sections 4.1 – 4.4.   All of the counting equipment was tested and calibrated at PNNL before being shipped. All activity measurements on PNNL dosimeters for the purpose of assessing dose were made in the NAD lab in Mercury using the PNNL equipment.   The activation reactions and product radionuclides used for determining dose in PNNL PNADs and FNADS are shown in **Table 5**.

Table 4. Counting Equipment used for Foil Activity Analysis

Name	Description	Radiations Detected	Samples Analyzed	radionuclides analyzed	Detector	Scaler/MCA	Analysis Software
GM #1	shielded pancake GM	beta	sulfur pellets	^{32}P	Ludlum 44-40 lead shielded pancake GM probe	Ludlum Model 3 meter with digital scaler option	Excel spreadsheet
GM #2	shielded pancake GM	beta	sulfur pellets	^{32}P	Ludlum 44-40 lead shielded pancake GM probe	Thermo RadEye meter with digital scaler	Excel spreadsheet
iSolo	bench top beta counter	beta, alpha	sulfur pellets	^{32}P	Canberra 300 μm PIPS® silicon detector, with guard detector	Canberra iSolo benchtop alpha/beta counter, Model SOLO300G	Canberra iLink software
NaI #1	NaI	photon	copper foils	^{64}Cu	REXON NaI Probe 1.0" dia. X 1.0" deep	Ludlum Model 2200	Excel spreadsheet
NaI #2	NaI	photon	copper foils	^{64}Cu	REXON NaI Probe 1.0" dia. X 1.125" deep	Ludlum Model 2200	Excel spreadsheet
falcon	HPGe	photon	indium, copper and gold foils	^{115m}In, ^{116m}In, ^{64}Cu, ^{198}Au	Canberra HPGe BE2830 60 x 30 mm, 18% rel. eff.	Canberra Falcon 5000	Genie 2000
dx1	HPGe	photon	indium, copper and gold foils	^{115m}In, ^{116m}In, ^{64}Cu, ^{198}Au	Ortec HPGe, P-type, 50 mm dia. x 33 mm deep, coaxial	Ortec microDetective DX	Genie 2000
dx2	HPGe	photon	indium, copper and gold foils	^{115m}In, ^{116m}In, ^{64}Cu, ^{198}Au	Ortec HPGe, P-type, 50 mm dia. x 33 mm deep, coaxial	Ortec microDetective DX	Genie 2000

Table 5. Activation Reactions used in FNADs and PNADs

Energy range	Reaction	Effective Threshold or resonance energy (approx.) [1]	Filter	Product half-life	Principal radiations for assay (MeV)	Other principle radiations (MeV)
Thermal	^{63}Cu(n,γ)^{64}Cu	-	-	12.701 h	γ(0.511) [2]	β^- (0.578)
	^{197}Au(n,γ)^{198}Au	-	-	2.696 d	γ(0.412)	β^- (0.961)
	^{115}In(n,γ)^{116m}In	-	-	54.2 m	γ(0.417) γ(1.097) γ(1.294)	β^- (0.189 avg) β^- (0.294 avg) β^- (0.351 avg)
Intermediate	^{63}Cu(n,γ)^{64}Cu	580 eV	Cd	12.701 h	γ(0.511) [2]	β^- (0.578)
	^{197}Au(n,γ)^{198}Au	4.9 eV	Cd	2.696 d	γ(0.412)	β^- (0.961)
Fast	^{32}S(n,p)^{32}P	3.3 MeV	-	14.29 d	β^- (1.711)	-
	^{115}In(n,n$'$)^{115m}In	1.2 MeV	-	4.486 h	γ(0.336)	ce (0.308) [3]

1. from Delafield, 1988. (Resonance energy for intermediate range. Threshold energy for fast range)
2. annihilation photon
3. conversion electron

The instrumentation used to make activity measurements, how it was calibrated, and the analytical methods used are described for each foil type in the subsections below.

4.1 Sulfur Pellets (^{32}P)

The traditional method for analyzing for ^{32}P in sulfur pellets providing the greatest sensitivity is to melt the pellet slowly on metal planchet in a beaker with watch glass cover, at carefully controlled temperature. However this method is cumbersome, time consuming and limits the number of dosimeters that can be analyzed during a 24 hour period. During the planning stages of the exercise, it became apparent that there would be only one fume hood available in the NAD lab for melting of sulfur pellets and the hood would only be available during limited hours and would need to be shared by all participants. To maximize the number of dosimeters that could be tested and the response data that could be obtained from the exercise, PNNL decided to investigate alternative methods of analyzing sulfur pellets for ^{32}P. It was determined that sealed bags containing either six or seven whole pellets in a single layer 0.190 cm thick could be counted on standard 50 mm sample counting planchets in standard

benchtop beta counters and provide adequate count rates for measuring a 10 rad dose of unmoderated fission neutrons.

Three beta counting systems were used to analyze the sulfur pellet packs used in the PNAD and FNAD. These were

- Canberra iSolo alpha beta sample counter
- Ludlum 44-40 Lead Shielded Pancake GM Probe with Ludlum Model 3 Meter with digital scaler option
- Ludlum 44-40 Lead Shielded Pancake GM Probe with Thermo RadEyeGX Meter with digital scaler

The lead shielded GM probes were housed in lead brick caves affording 2 inches of lead shielding in addition to that contained in the probe. The shielded GM counting setup is shown in **Figure 9**. Background count rates during the exercise varied between 23 and 26 cpm for GM #1 and between 18 and 22 cpm for GM #2. Sulfur pellet packs were counted on stainless steel planchets that were placed in aluminum counting fixtures adapted to fit the Ludlum probes. The planchet counting fixture used with the Ludlulm 44-40 GM probes is shown **Figure 10.** For the iSolo, sulfur pellet packs were counted on the same style planchet. Background count rates for the iSolo varied between 15 and 16 cpm. The iSolo beta counting system setup is shown in **Figure 11**.

Figure 9. Lead Shielded Pancake GM Beta Counting Systems

Figure 10. Planchete Counting Fixture used with Ludlum 44-40 Pancake GM Probe

Figure 11. iSolo Beta Counting System

Counting efficiencies for the rectangular sulfur pellet "6 pack" and hexagonal "7 pack" were determined for the Pancake GM detectors and the iSolo by a series of measurements at PNNL in which uniformly irradiated packets were first counted whole with each type of instrument. Each instrument had been nominally calibrated with 47 mm diameter ^{90}Sr/^{90}Y and ^{99}Tc disk sources. For the GM detectors the nominal efficiency during routine annual calibration at a distance of ¼ inch with a 47mm source was approximately 22% for ^{90}Sr/^{90}Y and 13% for ^{99}Tc. The nominal efficiency of the iSolo was approximately 34% for ^{90}Sr/^{90}Y and approximately 11% for ^{99}Tc. The specific activity of the packets contents were then assayed by melting/sublimation on stainless steel planchet followed by counting on a Canberra (Tennelec) gas flow proportional gross alpha beta counting system. The Tennelec system counting efficiency for the sublimated sample residues having negligible mass was established by counting of ^{32}P liquid activity standards evaporated on the same type of stainless steel planchet that was used for the sublimation of sulfur and counting of the ^{32}P residue. Counting efficiencies determined for use with the iSolo, Pancake GMs and NaI detectors are shown for each combination of detector and sample geometry in **Appendix E, Table E.1**. The detector background count rates observed during the exercise are shown in **Table E.2.**

The activation of a sulfur tablet can result in several activation products. These are summarized in **Table 6** below. After a 4-hour decay time from irradiation, the short-lived products, ^{31}S, ^{34}P, and ^{37}S, will have decayed away. The longer-lived beta-emitters, ^{33}P and ^{35}S, will be present in relatively low quantities. ^{35}S beta particles will be mostly attenuated within the sulfur pellet. The ^{33}P beta can be effectively absorbed with a 70 mg/cm^2 aluminum absorber but will also be largely attenuated within the sulfur pellet. Data from sulfur pellet irradiation experiments at PNNL showed that there is not a significant difference in assayed activities when sulfur pellet packs are counted with and without the 70 mg/cm^2 absorber, after taking into account the reduction in counting efficiency for low mass ^{32}P residue with the absorber in place. The primary interference when counting whole sulfur pellets for analysis of ^{32}P comes from the ^{31}Si with a 2.62 h half-life and a penetrating beta particle. The anticipated ^{31}Si/^{32}P activity ratio at end of burst (EOB) for the Godiva-IV neutron energy spectrum was calculated to be 0.524 using the PNNL activation program SCOPER. This program uses the same reaction rate calculation code as the STAYSL_PNNL program (Greenwood and Johnson, 2014). Recommended wait times for counting whole sulfur pellets range from "a few hours" to "six hours" (**IAEA 1982** pages 86 and 68). The post irradiation decay times before counting of the sulfur pellets in the exercise ranged between 4.2 and 10.6 hours. Given the potential for ^{31}S interference in the ^{32}P results, a correction for this influence was incorporated into the decay correction equations used for sulfur pellet raw count data (see **Appendix G**). The ^{32}P specific activity in sulfur pellets calculated with the correction for ^{31}Si interference applied ranged between 88% and 98% of the activity calculated without the correction applied. The mean ratio was 0.93. In other words, without correction for ^{31}Si interference, ^{32}P activity would be overestimated by as much as 14%.

Table 6 - Radioactive Products from Neutron-Induced Reactions in Sulfur

Reaction	Type	Cross Section, mb	Product Half-life	Beta Energy, MeV	Isotopic Abundance of Parent, %
$^{32}S(n,p)^{32}P$	Fast	67 (av)	14.29 d	1.710	95.02
$^{32}S(n,2n)^{31}S$	Fast		2.6 s	44 (β^+)	95.05
$^{33}S(n,p)^{33}P$	Thermal	2.3	25.4 d	0.25	0.75
$^{34}S(n,p)^{34}P$	Fast		12.4 s	5.1, 3.2	4.21
$^{34}S(n,\alpha)^{31}Si$	Fast	3.0	2.62 h	1.49	4.21
$^{34}S(n,\gamma)^{35}S$	Thermal	260	87.4 d	0.17	4.21
$^{36}S(n,\gamma)^{37}S$	Thermal	140	5.0 m	4.7, 1.6	0.02

For each sulfur pellet pack, the identity (dosimeter number and element type) and mass were pre-recorded in a spreadsheet. For each type of detector, counting efficiencies for each type of packet were also pre-recorded in spreadsheet. During the exercise, the count start date and time, count duration, and number of net counts were entered into the spreadsheet for each sulfur packet counted. The date and time of the pulse was also entered into the spreadsheet. All calculated ^{32}P activities (A_o) were decay corrected to EOB including correction for decay during irradiation (negligible), decay between irradiation and start of counting, and decay during counting (negligible for ^{32}P). The raw count data and calculated ^{32}P specific activity, A_o (dpm/g) for each dosimeter are given in **Appendix G, Table G.1**.

4.2 Copper Foils (^{64}Cu)

The activation of copper foils by epithermal neutrons produces ^{64}Cu by the $^{63}Cu(n,\gamma)^{64}Cu$ reaction. The 1346 keV gamma from ^{64}Cu decay by internal conversion has a relatively low yield of only 0.0049 gammas per disintegration. However ^{64}Cu also decays 17.86% of the time by positron emission with a yield of 0.358 gammas per disintegration for the 511 keV annihilation photons. The ½ inch diameter copper foils in the PNADs irradiated during the exercise were analyzed by counting the 511keV annihilation photons using 1" x 1" NaI detectors coupled with Ludlum Model 2200 scalers with adjustable threshold and window. To the extent practical, the pulse height thresholds were set to reject Compton events within the crystal that were below the 511 keV photo peak energy. The detectors were housed inside makeshift lead caves assembled from lead bricks, affording approximately 2 inches of lead shielding on the sides and bottom and 4 inches of shielding on top. For the purpose of counting, the foils were sandwiched between two aluminum plates 2.54 cm x 1.91 cm x 0.076 cm (1" x 0.75" x 0.030") to ensure complete annihilation of all positrons in close proximity to the foil. The foil-plate assemblies were centered on contact with the flat face of the detector housing. The NaI counting setup is shown in **Figure 12**.

Figure 12. Ludlum 2200 Scalers with NaI Probes in Lead Cave

Although the counting efficiencies for the NaI systems had been initially determined at PNNL prior to the exercise, the initial efficiencies were revised after careful analysis of exercise data. The reasons for revision of NaI counting efficiencies are discussed in **Appendix F**. For each NaI detector, the corrected ^{64}Cu counting efficiency was determined by comparison of results for copper foils counted on the NaI detector and on one of the HPGe detectors. The ^{64}Cu activity determined from the HPGe detector was used as the reference activity the purpose of determining the NaI counting efficiency. The HPGe systems (two Ortec microDetective DX systems and one Canberra Falcon 5000 system) were used during the exercise primarily for counting of indium and gold foils but were also used for counting a small set of copper foils. Prior to the exercise, the HPGe detectors had energy and efficiency calibrations performed at PNNL for a 1.27 cm diameter disk sample centered on contact with the detector housing, using a sealed calibration source of the same dimensions. The calibration source was prepared at PNNL by uniformly depositing known activity from a NIST-traceable multi-nuclide gamma standard solution (source no 1868-34) purchased from Eckert and Ziegler Isotope Products, Inc. (Valencia, CA), onto a paper disk 1.27 cm in diameter. The corrected ^{64}Cu counting efficiencies for the two NaI detectors used to count copper foils at the exercise are shown in **Appendix E, Table E.1.** The detector background count rates observed during the exercise are shown in **Table E.2.**

The 2.54 cm diameter copper foils in the FNADs were analyzed by counting the 511 keV annihilation photons using the Falcon 5000 HPGe system. Foils were counted between 30 mil thick aluminum plates in contact with and centered on the face of the detector. The detector efficiency for the 2.54 cm disk geometry in contact with the detector was determined using a 2.54 cm diameter paper source prepared at PNNL in the same manner as the 1.27 cm diameter source, using the same Eckert and Ziegler Isotope Products activity standard.

The raw count data and final calculated ^{64}Cu specific activity, A_o (dpm/g) for copper foils from each PNAD and FNAD are given in **Appendix G, Table G.2.**

4.3 Indium Foils (^{115m}In, ^{116m}In)

Indium foils are activated by thermal and epithermal neutrons via the ^{115}In(n,γ)^{116m}In reaction. Indium foils are also activated by fast neutrons via the ^{115}In(n,n')^{115m}In reaction. The ^{115m}In and ^{116m}In activities in the foils exposed during the exercise were determined from gamma spectra acquired with HPGe detectors. Peak search, peak area and activity calculations for all HPGe systems were performed using the Canberra Genie™ 2000 gamma spectrometry software (suite). The data files from the Ortec microDetective DX systems were converted and exported into Genie for analysis. In general, the ^{116m}In activity was determined using the weighted mean of the individual activities determined from identified full energy absorption peaks, primarily the 417 keV, 1097 keV and 1294 keV gamma lines. The ^{115m}In activity was determined from the peak area of the single 336 keV gamma line. The acquired spectra for all indium foils, whether cadmium covered or bare, were analyzed for both ^{115m}In and ^{116m}In, using the Genie 2000™ software. The setup of the Falcon 5000, and two microDetective DX systems with makeshift lead shields is shown in **Figure 13**. Each detector was calibrated for a reference source in contact with and centered on the face of the detector housing (with plastic end cap removed) at PNNL. The reference source was a 1.27 cm paper disk with a uniformly deposited known activity aliquot from a NIST-traceable multi-nuclide gamma standard solution. The indium foils from the FNADs were 1 cm x 1 cm square foils but the disk geometry was considered adequate for counting of these as well as the round foils. The cadmium covered indium foils had decayed a minimum of 262 minutes before counting. The bare indium foils had decayed a minimum of 330 minutes before counting. Allowing six hours for decay of the ^{116m}In before counting, particularly in unshielded foils, helps reduce Compton background from ^{116m}In and improve detectability of the ^{115m}In isotope (IAEA 1982). The indium activity measurement results for the PNADs and FNADs exposed in the exercise are listed in **Appendix G, Table G.3**. For all HPGe analyses, the column labeled "count duration" gives the actual data acquisition time (i.e. the real time, not live time). All calculated activities are based on the live times captured in the microDetective DX or Falcon 5000 MCA data files. Detector dead times were 11% or less for all samples counted. It should be noted that corrections for cascade summing were not applied to the ^{116m}In activity results. Based on cascade summing corrections calculated for 1.27 cm diameter indium foils counted on the detector face with fixed HPGe systems at PNNL, the ^{116m}In activities in **Table G.3** may underestimate the actual activities by 10% -15%.

Figure 13. HPGe Gamma Spectroscopy Counting System Setup

4.4 Gold Foils (^{198}Au)

Gold foils are used in the inner and outer dosimetry packages of FNADs. Gold foils are activated by thermal and epithermal neutrons via the ^{197}Au(n,γ)^{198}Au reaction. The ^{198}Au activity in the foils was determined from gamma spectra acquired with one of the three HPGe detectors listed in **Table 4**. The HPGe detectors were calibrated for a 1.27 cm disk source as described in the previous sections above. Although the gold foils from the FNADs were 1 cm x 1 cm square foils, the disk geometry was considered adequate. Peak search, peak area and activity calculations for all HPGe systems were performed using the Canberra Genie™ 2000 software. The data files from the Ortec micro Detective DX systems were converted and exported into Genie for analysis. The ^{198}Au activity was based on the peak area of the 412 keV gamma line. The ^{198}Au activity measurement results for gold foils in the FNADs are listed in **Appendix G, Table G.4**.

4.5 Specific Activity per Unit Fluence

For the purpose of assessing consistency of foil activity measurement data and validating reaction cross sections, foil activity data generated under similar neutron energy spectra and exposure geometry were grouped together, and activity expressed as specific activity per unit fluence. According to the Godiva-IV spectrum characterization report by AWE (Wilson et. al. 2016), the neutron fluence and energy spectrum vary little among locations at the same distance but do vary significantly as a function of distance. The measured specific activity per unit fluence for each combination of distance and exposure geometry (phantom front, phantom back, air) are shown in **Appendix G, Table G.5.** and **Table G.6.**

5.0 Methodology for Calculating Neutron Dose from Foil Activity

The fluence-to-dose conversion factors in **equation 9** and **equation 13** below are assumed to be valid for calculating tissue kerma from neutrons. The exact origin of these fluence-to-dose conversion factors is not entirely clear from existing historical documentation. However, a comparison of these values with values published in the peer reviewed literature for unmoderated fission spectra in the energy regions nominally being assessed with this methodology, indicates that some of these factors are consistent with first collision dose and some with tissue kerma (PNNL 2017). Revision of these conversion factors for use in accurately calculating the operational quantities $D_p(10)_n$ and $D*(10)_n$ adopted in ANSI/HPS N13.11-2013 (ANSI, 2013) will be the subject of a follow-on report to this report. For the purpose of assessing the performance of the PNADs and FNADs exposed in this Godiva-IV exercise, the kerma values obtained from **equation 9** are compared against the preliminary reference values for $D_p(10)_n$ and $D*(10)_n$ given for the exercise, since the standard calls for NAD systems to capable of measuring and reporting these quantities.

5.1 Neutron Fluence Calculation

The reactions in **Table 5**, are used to calculate neutron fluence in the following energy ranges:

- thermal to 0.4 eV
- 0.4 eV to 2 eV
- 0.4 eV to 10 eV
- 2 eV to 0.5 MeV
- above 1.2 MeV
- above 2.9 MeV.

The neutron fluences are calculated from the initial specific activities, A_o, (dpm/g) of the foils using effective cross sections, $\boldsymbol{\sigma}$, that have been calculated and/or determined by experiment at HPRR in Oak Ridge and other facilities (Anderson 1964; IAEA 1982; Swaja and Ragan 1985). The currently used values of $\boldsymbol{\sigma}$ for detectors in the PNAD and FNAD are shown in **Table 7**.

Table 7. Activity-to-Fluence Conversion Factors, C_x and Supporting Data.

Energy Region [a]	Reaction	Foil Combination	Decay Constant λ (min^{-1}) [b]	Isotopic Abundance of Target Atom	Foil Atomic Weight (AMU)	Cross Section σ (barns)	C_x (min-g/cm^2)
0.025 eV − 0.4 eV	^{197}Au(n,γ)^{198}Au	Au(bare) - Au(Cd)	1.785 x 10^{-4}	1.000	196.97	98.8 [c]	1.86 x 10^4
0.4 eV − 10 eV	^{197}Au(n,γ)^{198}Au	Au(Cd)	1.785 x 10^{-4}	1.000	196.97	1560 [c,d]	1.18 x 10^3
0.025 eV − 0.4 eV	^{115}In(n,γ)^{116m}In	In(bare) - In(Cd)	1.280 x 10^{-2}	0.957	114.82	161 [d]	9.68 x 10^1
0.4 eV − 2 eV	^{115}In(n,γ)^{116m}In	In(Cd)	1.280 x 10^{-2}	0.957	114.82	2600 [d]	6.00
> 1.2 MeV	^{115}In(n,n')^{115m}In	In(Cd) or In(bare)	2.575 x 10^{-3}	0.957	114.82	0.188 [d]	4.11 x 10^5
2 eV − 0.5 MeV	^{63}Cu(n,γ)^{64}Cu	Cu(Cd)	9.094 x 10^{-4}	0.692	63.546	0.341 [e]	4.92 x 10^5
> 2.9 MeV	^{32}S(n,p)^{32}P	S (pellet)	3.368 x 10^{-5}	0.9493	32.066	0.238 [f]	6.98 x 10^6

a.   From Hanford External Dosimetry Internal Technical Documentation, Vol. IV – Nuclear Accident Dosimetry, a manual in use in the 1980s and last updated December 1990.

b.   From ICRP Publication 38 (ICRP 1983)

c.   From IAEA Technical Report 211, page 177 (IAEA 1982).

d.   From IAEA Technical Report 211, Table in Section A.3.4 (IAEA 1982).

e.   From Anderson, 1964, for the 0.68 eV to 100 keV region of the spectrum. This region covers from the essentially the cadmium cutoff through the major resonance region to 100 keV. Above 100 keV the cross-section decreases sufficiently to be ignorable.

f.   From Swaja and Ragan, 1985.

Using the foil activity at time zero, $\mathbf{A_0}$ (dpm/g), and the activity to fluence conversion factor $\mathbf{C_x}$, from **Table 7**, a fluence, Φ, for each energy region is calculated using **Eq. 1.**

$$\Phi = C_x A_0 \qquad\qquad \text{Eq. 1}$$

where:

Φ = fluence (cm^{-2})

C_x = activity-to-fluence conversion factor $(min\ g\ cm^{-2})$

A_O = initial activity as dpm *per gram* $(min^{-1}\ g^{-1})$

The specific equations used for calculating fluence (cm^{-2}) for each region are described below. The equations involving gold foil activities are used only for the FNAD.

Thermal to 0.4 eV

The difference between the ^{198}Au activity in the bare gold foil E, (outer dosimetry package) and the ^{198}Au activity in the cadmium covered gold foil F (outer dosimetry package) can be used to estimate the thermal neutron fluence as follows:

$$\Phi_{th} = 1.86 \times 10^4\ [A_O\ (\text{bare gold }\mathbf{E})\ -\ A_O\ (\text{Cd-covered gold }\mathbf{F})] \qquad \text{Eq. 2}$$

The difference between the ^{116m}In activity in the bare indium foil (outer dosimetry package) and the ^{116m}In activity in the cadmium covered indium foil (outer dosimetry package) *also* can be used to estimate the thermal neutron fluence as follows:

$$\Phi_{th} = 9.68 \times 10^1\ [A_O\ (\text{bare indium }\mathbf{D})\ -\ A_O\ (\text{Cd-covered indium }\mathbf{C})] \qquad \text{Eq.3}$$

Equations 2 and 3 provide two independent measurements of the thermal fluence, one (the indium) being more sensitive but decaying away much more rapidly. Calculating thermal fluence for PNADs requires use of equation 3.

0.4 eV to 2 eV

The cadmium-covered indium becomes activated primarily from neutrons between 0.4 and 2 eV due to the ^{115}In$(n,\gamma)^{116m}$In reaction. Fluence in this energy region can be calculated from the ^{116m}In activity in the foil as follows:

$$\Phi_{epi} = 6.00\ A_O\ (\text{Cd-covered indium }\mathbf{C}). \qquad\qquad \text{Eq. 4}$$

0.4 eV to 10 eV

The cadmium-covered gold becomes activated primarily due to neutrons between 0.4 and 10 eV. The cross section can reach 3×10^4 barns for 4.9 eV, which is the resonance energy. The fluence for this energy region can be calculated from the ^{198}Au activity as follows:

$$\Phi_{epi} = 1.18 \times 10^3\ A_O\ (\text{Cd-covered gold }\mathbf{F}). \qquad\qquad \text{Eq. 5}$$

Equations 4 and 5 provide two independent measurements of the epithermal fluence, Φ_{epi}. For the FNAD, either result or the average of the two can be used for this energy region when calculating dose. For the PNAD, equation 4 must be used.

2 eV to 0.5 MeV

The fluence calculation equation for this energy region is based on a cross section of 0.341 barn for the copper foil. Fluence for this energy region can be calculated from the ^{64}Cu activity as follows:

$$\Phi_{Cu} = 4.92 \text{ x } 10^5 \text{ A}_O \quad \text{(Cd-covered copper } \textbf{B}). \qquad\qquad \text{Eq. 6}$$

(Some activation will be due to neutrons in the cadmium cutoff to 2 eV region also)

Above 1.2 MeV

Measurement of the 336-keV photon emission from ^{115m}In provides an estimate of the neutron fluence exceeding 1.2 MeV, the threshold for the ^{115}In (n, n') ^{115m}In reaction. This measurement is best made between 2 and 10 hours after exposure (IAEA 1982). This will allow the ^{116m}In activity to decay. The higher energy gammas and high count rates from ^{116m}In can elevate the Compton background in the detector making detection and measurement of the lower energy 336 keV photons from the lower activity of ^{115m}In potentially more difficult. The fluence in this energy region can be calculated from the ^{115m}In activity as follows:

$$\Phi_{In} = 4.11 \text{ x } 10^5 \text{ A}_O \quad \text{(Cd-covered indium } \textbf{C}, \text{ or bare indium } \textbf{D}). \qquad\qquad \text{Eq. 7}$$

Above 2.9 MeV

Sulfur-32 has a reaction threshold beginning at approximately 2.5 MeV, producing ^{32}P, with the cross section becoming significant for energies exceeding 3.0 MeV. The effective cross section is assumed to be 238 millibarns. The fluence in this energy region can be calculated from the ^{32}P activity as follows:

$$\Phi_S = 6.98 \text{ x } 10^6 \text{ A}_O \text{ (sulfur pellet pack } \textbf{A}). \qquad\qquad \text{Eq. 8}$$

5.2 Neutron Dose Calculation

For both PNADs and FNADs, the tissue kerma K, from neutrons is calculated from fluence results for each energy region using spectrum weighted fluence to kerma conversion factors.

$$K \quad = \quad (0.022\ \Phi_{th} + 0.004\Phi_{epi} + 0.28\Phi_{Cu} + 2.87\ (\Phi_{In} - \Phi_S) + 3.84\Phi_S)\ 10^{-9} \qquad \text{Eq. 9}$$

where Φ_{th}, Φ_{epi}, Φ_{Cu}, Φ_{In}, and Φ_S are the values of neutron fluence (cm^{-2}) as determined by each foil and the kerma K, is in cGy (rads). As can be seen from the above equation, measurement of ^{32}P activity in the sulfur pellet and ^{115m}In activity in the indium foil are the most important contributors to the dose calculations.

With PNADs and FNADs, a first-approximation of *absorbed dose* in tissue D, can be made by the ^{32}P activity on the sulfur pellets, which assumes exposure to a standard fission spectrum with no moderation, as follows:

$$D \quad = \quad 8.32 \text{ x } 10^{-2} \text{ } A_0 \quad\quad\quad\quad\quad\quad\quad\quad\quad \text{Eq. 12}$$

where A_0 is the initial specific activity on the sulfur pellet in dpm/g and D is in rads (IAEA 1982). This is the charged particle dose only. The dose from hydrogen capture gamma will add approximately 6.5% to this value assuming the same standard fission spectrum with no moderation.

With FNADs, the neutron tissue kerma can be calculated from the ^{198}Au activity in the bare gold foil (**G**) located in the *inner* dosimetry package using the following empirically derived formula:

$$K \quad = \quad k \text{ } A_O \quad\quad\quad\quad\quad\quad\quad\quad\quad\quad\quad \text{Eq. 13}$$

where K is tissue kerma in rad, A_o is the ^{198}Au activity in $g^{-1} \text{ min}^{-1}$ (i.e. dpm/g), and k is a kerma conversion factor. The conversion factor k has the numeric value of 4.76 x 10^{-5} and has units of rad-min-g [i.e. (rad)/(dpm/g)] (Bramson 1963).

6.0 Neutron Dose Results Calculated from Foil Activity

Neutron kerma results for the PNADs and FNADs exposed during the exercise were calculated in an Excel workbook using equations 1 through 9 above. For each PNAD and each FNAD, the foil activities, calculated fluence in each energy region, and corresponding tissue kerma in each energy region, and total tissue kerma are shown in **Appendix H, Tables H.1 and H.2** respectively. Absorbed dose estimates based on the sulfur pellet pack in the outer dosimetry package of the FNAD using **equation 12** and tissue kerma estimates based on the bare gold foil in the inner dosimetry package of the FNAD, using **equation 13**, are also shown in **Table H.2**. The foil based kerma response and neutron dose response are shown for each PNAD in **Table H.3**. The response and bias are summarized by distance and exposure geometry in **Table 8** and **Table H.4**. The foil based kerma response and neutron dose response are shown for each FNAD in **Table H.5** and are summarized below in **Table 9**. The bias in reported neutron dose for the PNAD was calculated using kerma as the reported $D_p(10)_n$. The bias in reported neutron dose for the FNAD was calculated using kerma as the reported $D^*(10)_n$.

Table 8. Summary of PNAD Kerma and Dose Response Using Foils

distance (m)	phantom type	location on phantom	foil thickness	Kerma K		Neutron Dose $D_p(10)_n$	
				Measured / Given	B	Reported / Given	B
2.0	Tree A-D	air	10 mil	0.87	-0.13	0.65	-0.35
2.0	Tree A-D	air	5 mil	0.85	-0.15	0.64	-0.36
2.5	Tree A-D	air	10 mil	0.86	-0.14	0.63	-0.37
4.0	Tree A-H	air	10 mil	0.73	-0.27	0.53	-0.47
3.0	BOMAB	front	10 mil	0.75	-0.25	0.55	-0.45
4.0	BOMAB	front	10 mil	0.78	-0.22	0.57	-0.43
9.0	BOMAB	front	10 mil	0.59	-0.41	0.19	-0.81
2.0	PMMA	front	10 mil	0.95	-0.05	0.71	-0.29
4.0	PMMA	front	10 mil	0.78	-0.22	0.56	-0.44
3.0	BOMAB - LAT	side	10 mil	0.45	-0.55	0.33	-0.67
3.0	BOMAB	back	10 mil	0.14	-0.86	0.10	-0.90
4.0	BOMAB	back	10 mil	0.15	-0.85	0.11	-0.89
9.0	BOMAB	back	10 mil	0.10	-0.90	0.03	-0.97
2.0	PMMA	back	10 mil	0.17	-0.83	0.13	-0.87
4.0	PMMA	back	10 mil	0.21	-0.79	0.15	-0.85

Table 9. Summary of FNAD Kerma and Dose Response Using Foils

distance (m)	Kerma K		Neutron Dose $D^*(10)_n$	
	Measured / Given	B	Reported / Given	B
4.0	0.77	-0.23	0.58	-0.42

7.0 InLight® OSL/OSLN Measurements

The Landauer InLight® OSLN dosimeter is used in the PNNL PNAD to provide the primary gamma dose information and supplemental neutron dose information used in the event of a criticality. Because of the highly energy dependent nature of the albedo neutron response, the neutron dose result from the OSLN dosimeter is suitable for use only as an initial estimate (i.e. first approximation) of neutron dose until the results of foil analysis become available. The OSL technology allows repeated readout of the InLight® dosimeter with minimal signal loss (< 0.5% per reading with strong beam). The InLight® OSLN dosimeter used in the PNNL PNAD consists of a BA-type case loaded with an N-type slide containing three gamma sensitive OSL elements (E1, E3, E4) and one gamma + neutron sensitive OSLN element (E2). The BA case filtration in front of and behind each element is symmetrical and consists of an open window (E1), plastic filter (E2), copper filter (E3), and aluminum filter (E4). The InLight® OSLN dosimeter is described in greater detail in **Appendix A** and in Landauer internal documentation (Landauer, 2010). For accident level doses, the InLight® OSLN dosimeters are first on an accident level Landauer microStar® reader (a reader that has been modified with a neutral density filter to extend the dynamic range to 20,000 cGy). After initial readout on the modified reader, the InLight® OSLN dosimeter may be read on a standard microStar® for more accurate readings if the dose is sufficiently low (E2 < 3000 cGy and E1, E3 and E4 less than 1000 cGy). This limit is necessary to avoid damage to the protection level reader's one inch diameter PM tube and to avoid PM tube saturation. The microStar® reader is described in greater detail in the microStar® User Manual (Landauer 2016).   The unmodified and modified readers used during the exercise were interfaced with a Dell Windows 7 laptop running the microStar® 5.0 reader operating system (Software version 5.00.5382.18308, Data Base Version 10.1.0.0, Reader Communication Version 1.1.0.3).   The accident level dosimeter reader setup with laptop and bar code scanner is shown in **Figure 14**.
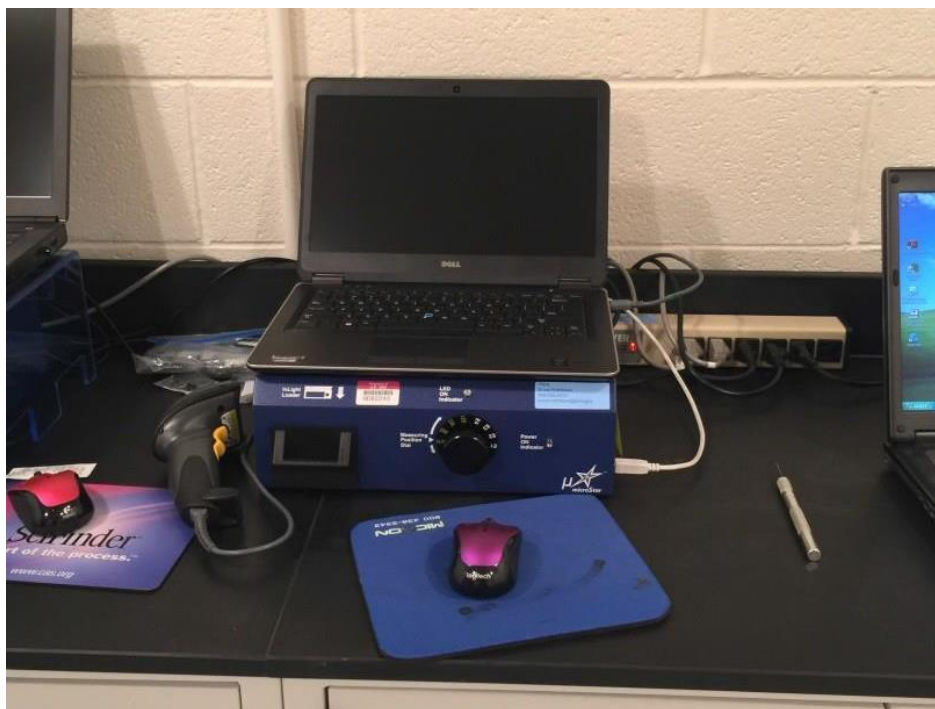
Figure 14. Accident Level microStar® Reader with Laptop

7.1 microStar® Reader Calibration

For the purpose of reading the InLight® OSLN dosimeters exposed in PNADs during the exercise, the microStar® readers were calibrated using sets of InLight® reader calibration dosimeters (CC case type) that had been exposed to protection and accident level doses using a ^{60}Co beam irradiator at PNNL. The CC type dosimeter contains four OSL gamma sensitive elements, with equal amounts of ABS plastic filtration (178 mg/cm^2) covering each element front and back. The CC calibration dosimeters were exposed on 30 cm x 30 cm x 15 cm PMMA slab phantoms with 30 cm x 30 cm x 3.2 mm thick PMMA cover plates covering the dosimeters and front faces of the phantoms. The calibration dosimeters were irradiated to known levels of personal absorbed dose, $D_p(10)_\gamma$. During readout, the microStar® readers use two different power levels for optical stimulation of OSL elements with green colored LEDs. The two beams of light (weak and strong) are optimized to provide a large dynamic range for the system (5 mrad to 1000 rad ^{60}Co equivalent signal for the unmodified reader and 100 mrad to 20,000 rad for the modified reader). The strong beam is created by turning on all of the LEDs in the array (38 LEDs) and the weak beam is created by turning on only a fraction of the LEDs in the array (6 LEDs). Both beams are calibrated using OSL elements exposed to a known dose from a ^{60}Co photon source. Thus, the reader calibration factors nominally have units of counts/cGy. The microStar® readers use photon counting over the entire dose range but change from 38 LED optical stimulation to 6 LED stimulation at a predetermined crossover point. For the protection level reader, the crossover point is set at approximately10 cGy. For the accident level reader, the crossover point is set at approximately 75 cGy. The use of weak or strong beam is determined by the reader on an element by element basis prior to reading the element for dose, by using a short flash of weak stimulation to estimate the level of dose on the element. Because the light output on the neutron sensitive OSLN element will be much larger than the gamma sensitive OSL elements (particularly in 8:1 neutron:gamma fields), it is possible for both weak and strong beams to be used on a single BA dosimeter. To avoid use of both weak and strong beams when reading elements on a single dosimeter and the possible perturbations in the data due to differing reader calibration biases for the two beams, the default crossover point was temporarily set at a an arbitrarily low level (e.g. 10 counts) to force use of the weak beam on all elements when reading the dosimeters from all pulses. For Pulse 1, the unmodified reader (PNAD LD) was used. For Pulse 2, the modified reader (PNAD HD) was used. For Pulse 3, all dosimeters were read using the modified reader. Those dosimeters receiving lower doses were read again using the unmodified reader. Specifically those dosimeters in Pulse 3 that did not have at least 10,000 counts on each element when read with the PNAD HD reader, were read a second time on the PNAD LD reader to ensure adequate counting statistics. When using either reader, each dosimeter was read three times. Each dosimeter's dose result was thus based on the average of 3 readings.

When calibrating both readers prior to the exercise, the strong beam and weak beam were calibrated independently by adjusting the crossover point as needed to ensure use of the intended beam. Although the weak beam can be used for reading dosimeters with doses much greater than 100 rad, the weak beam was calibrated using dosimeters given doses 100 rad or less to ensure that reader calibration factors were based on linear OSL response. OSL gamma response becomes supralinear above 100 rad (as discussed below). Reader calibrations were performed such that reader calibration factors had units of counts/cGy. The reader calibration factors that were applied by the reader software during the exercise are shown in **Appendix I, Table I.1**.

Raw element readings are recorded as "counts" from the PM tube. Element converted values are readings that have been corrected for element sensitivity and have had the reader calibration factor applied. An InLight® element converted value of 1 cGy results from an element light output (measured as PMT counts) equal to that from an OSL element exposed in a CC case to 1 cGy of ^{60}Co gamma radiation, on phantom under CPE conditions. Element readings may thus be thought of as ^{60}Co cGy equivalent signal.

NOTE: *Although the microStar® software nominally determines reader calibration factors in units of counts/cGy during the reader calibration process, when reading BA type dosimeters, the element readings E1, E2, E3 and E4 recorded in the microStar® database (labeled as "converted values"), are actually given in units of **mrad**. In the formulas below, it is assumed that E1, E2, E3 and E4 have been converted to units of cGy. Thus, the given calibration factors are based on "converted values" that have been converted to units of cGy.*

7.2 InLight® Dose Calculation

For each dosimeter, the personal absorbed dose from photons, $D_p(10)_\gamma$ was calculated as the average of the E3 and E4 converted values, divided by a gamma absorbed dose calibration factor C_γ. No other corrections were applied.

$$D_p(10)_\gamma \ = \ [(E3 + E4) \ / \ 2] \ / \ C_\gamma \qquad\qquad \text{Eq. 14}$$

Where

$$C_\gamma = 1.00 \text{ for dosimeter with 3.2 mm cover exposed to } ^{60}\text{Co photons}$$

For each dosimeter, the personal absorbed dose from neutrons, $D_p(10)_n$, was calculated as the net neutron signal, (E2-E1), divided by a neutron absorbed dose calibration factor, C_n.

$$D_p(10)_n \ = \ (E2\text{-}E1) \ / \ C_n \qquad\qquad \text{Eq. 15}$$

Where

$$C_n = 2.73 \text{ for unmoderated } ^{252}\text{Cf}$$

This default value used for C_n is a preliminary value based on the response of BA cases inside fully assembled PNAD holders, exposed to an unmoderated ^{252}Cf source at a distance of 50 cm on phantom.

NOTE: *A previous value of $C_n = 4.27$ had been determined for use with an earlier prototype of the PNNL PNAD that was documented in the IER-148 CED-2 intercomparison exercise final design report (Heinrichs et. al. 2014). In this earlier prototype, the PNAD case was constructed of machined polycarbonate and had a 3.2 mm thick polycarbonate front cover that was removable for access to the PNAD components. The neutron absorbed dose calibration for this design was based on BA cases exposed to an unmoderated ^{252}Cf source at a distance of 50 cm on phantom with 3.2 mm of PMMA buildup plate covering the dosimeters.*

It is recognized that the appropriate values for C_n are unique to each radiation field and highly energy dependent. It is planned that C_n be accurately evaluated for BA cases inside fully loaded PNAD holders of the final PNNL PNAD design mounted on phantom for the following radiation fields: 1) bare ^{252}Cf, 2) moderated ^{252}Cf 3) Godiva-IV unmoderated, and 4) a field simulating a solution criticality.

Correction factors for non-linearity of element dose response were developed prior to the exercise, for use with element readings when necessary. OSL gamma response linearity from 10 cGy to 10,000 cGy was determined using the accident level reader to read sets of reader calibration dosimeters exposed at 12 dose levels equally distributed across six decades. The OSL gamma response was shown to be supralinear above 100 cGy with a maximum response of 1.44 observed at 4000 cGy delivered dose. OSLN fast neutron dose response linearity was determined using the accident level reader to read sets of specially prepared reader calibration dosimeters (N-type slide in CC case) that had been exposed to a moderated ^{252}Cf source to produce readings equivalent to an absorbed dose between 10 cGy and 1000 cGy from an unmoderated ^{252}Cf source. The "simulated" fast neutron response thus measured was essentially linear from 10 cGy to 1000 cGy. However, in mixed neutron/gamma fields in which the gamma component comprised more than half of the total absorbed dose, the neutron response became non-linear, decreasing as gamma/neutron ratio increases. Corrections for gamma dose response non-linearity were not applied because the needed corrections were <3% and generally negligible. Corrections for neutron dose response non-linearity were also <3% and generally negligible. Because the gamma component of absorbed dose from Godiva-IV (unmoderated) was only 13% of the total, the neutron dose response was assumed to be approximately linear.

For each PNNL PNAD, the average element readings and the gamma and neutron absorbed doses calculated from them using the default gamma and neutron absorbed dose calibration factors described above, are given in **Appendix J, Table J.1**. Gamma and neutron absorbed doses calculated using optimized calibration factors are shown in **Table J.2**. These are gamma and neutron absorbed dose calibration factors determined from dosimeter response on the front face of BOMAB and PMMA phantoms placed at a distance of 3 meters from Godiva-IV. The response was determined using the reference dose values provided for these phantom locations. The optimal gamma absorbed dose calibration factor for Godiva-IV mixed neutron/gamma field at 3 meters was determined to be $C_\gamma = 2.59$. The optimal neutron absorbed dose calibration factor for Godiva-IV neutron/gamma field at 3 meters was determined to be $C_n = 6.09$.

8.0 nanoDot OSL/OSLN Measurements

Landauer OSL and OSLN nanoDots are used in the PNNL FNAD to provide the primary gamma dose information and supplemental neutron dose information. Primary neutron dose information is provided by the activation foils in the PNNL FNAD. Landauer OSL nanoDots were also used in the exercise to provide the primary gamma dose information for the Hanford PNADs tested. The OSL and OSLN nanoDots used in the exercise were read on the unmodified microStar® reader in a reader environment named FNAD LD which was configured for reading nanoDots. The reader calibration factors for this environment were determined from the response of OSL nanoDots that had been exposed on PMMA phantom, under 3.2 mm PMMA cover plate to ^{60}Co photons from a beam irradiator to achieve a known delivered personal absorbed dose, $D_p(10)_\gamma$. Reader calibration factors thus nominally had units of counts/cGy. The modified microStar® reader had also been configured with a reader environment named FNAD that was configured and calibrated in the same manner, but was not used for nanoDot readout.   As with the reader calibrations performed for the PNAD and PNAD LD reader environments, the weak beam and strong beams were calibrated independently. OSL nanoDots given doses larger than 100 cGy were not used, so as to ensure that reader calibration factors would be determined based on linear response of the OSL elements. As with the PNAD environments, the crossover point for the FNAD LD reader was set to correspond to doses of approximately 10 cGy. For the FNAD reader, the crossover point was set to correspond to a dose of approximately 75 cGy. The reader calibration factors for the FNAD HD and FNAD LD reader environments are shown in **Appendix I, Table I.2**.

8.1 nanoDot Gamma Dose Measurement in the Hanford PNAD

As shown in **Figure 2**, the Hanford PNADs tested during the exercise included three OSL nanoDots for the purpose of measuring gamma dose. Each nanoDot was read three times in the FNAD LD reader environment. For the purpose of calculating gamma dose the nanoDot readings referred to as converted values (E1), were used.   Converted value E1 is a raw reading in counts that has been divided by the reader calibration factor (counts/cGy) and divided by the element's relative sensitivity factor.

$$E1 =   \text{(element counts)} / \text{(reader calibration factor x sensitivity)} \qquad \text{Eq. 16}$$

For the Hanford PNAD, the personal absorbed dose from photons, $D_p(10)_\gamma$, was calculated as follows:

$$D_p(10)_\gamma =   E1 / C_\gamma \qquad\qquad \text{Eq. 17}$$

Where

$$C_\gamma = \text{gamma absorbed dose calibration factor}$$

For the purpose of the exercise a default value of 1.00 was used for C_γ. Based on the response of Hanford PNADs exposed in air at the 2 meter distance, an optimized value of 1.31 was determined for C_γ. This is the same optimized value determined for the OSL nanoDot in the outer dosimetry package of the PNNL FNAD (also exposed in air). The nanoDot readings and calculated gamma doses for the Hanford PNADs are shown in **Appendix K, Table K.1** and **Table K.2**

8.2 nanoDot Gamma and Neutron Dose Measurement in the FNAD

The prototype FNAD tested in the exercise included an OSL/OSLN nanoDot pair in the outer dosimetry package and two OSL/OSLN nanoDot pairs in the inner dosimetry package. Each nanoDot was read three times on the unmodified microStar® reader in the FNAD LD reader environment. The individual FNAD nanoDot readings are shown in **Appendix K**, **Table K.3**. For the purpose of the exercise, the ambient absorbed dose from photons $D*(10)_\gamma$ was calculated from the OSL nanoDot in the outer dosimetry package as follows:

$$D*(10)_\gamma = OSL / C_\gamma \qquad \text{Eq. 18}$$

Where

OSL = average nanoDot reading (^{60}Co cGy equivalent signal)

C_γ = gamma absorbed dose calibration factor

For the purpose of the exercise a default value of 1.00 was used for C_γ. [An optimized value of 1.31 was also determined for use in accurately measuring gamma dose in Godiva-IV mixed neutron-gamma fields based on preliminary reference dose information provided by LLNL.]

The ambient absorbed dose from neutrons $D*(10)_n$ was calculated from the nanoDot pairs in the inner dosimetry package as follows:

$$D*(10)_n = (OSLN - OSL) / C_n \qquad \text{Eq. 19}$$

Where

OSLN = average OSLN nanoDot reading (^{60}Co cGy equivalent signal)

OSL = average OSL nanoDot reading (^{60}Co cGy equivalent signal)

C_n = neutron absorbed dose calibration factor

For the purpose of the exercise, a default value of 12.89 was used for C_n. This value was based on calibration of the FNAD with an unmoderated ^{252}Cf source at a distance of 1 meter. This value also provided unbiased neutron absorbed dose results for the exercise.

The OSL and OSLN nanoDot response in the outer and inner dosimetry packages to the Godiva-IV radiation field is shown in **Appendix K, Table K.4**. Gamma and neutron ambient absorbed doses were calculated for the FNAD using the default absorbed dose calibration factors are shown in **Table K.5**. Gamma and neutron ambient absorbed doses calculated for the FNAD using the optimized gamma absorbed dose calibration factor and the default neutron absorbed dose calibration factor are shown in **Table K.6**.

9.0 Dosimeter Performance Evaluation

Gamma doses calculated from OSL readings and neutron doses calculated from both foil activities and OSL/OSLN readings are provided in **Appendices H, J,** and **K**. Dose response values were calculated as Reported/Given (R/G).   The purpose of this section of the report is to consolidate the dose information from different sources and analyze dosimeter performance against the performance criteria in ANSI/HPS N13.3-2013. According to the standard, performance is evaluated for the total (gamma + neutron) absorbed dose on an individual dosimeter basis using the performance statistic B which is calculated as follows:

$$B = (\text{Measured Dose} - \text{Delivered Dose}) / \text{Delivered Dose} \qquad \text{Eq. 20}$$

In the context of this report, the term "bias" has been used both when referring to the value of the statistic, B, calculated for an individual dosimeter result *and* when referring to the average value of B for a group of dosimeter results. In each case, the meaning should be clear from the context. The operational quantity recommended for use with PNADs is personal absorbed dose, $D_p(10)$. The operational quantity recommended for use with FNADs is ambient absorbed dose $D^*(10)$.

The performance testing criteria for PNADs and FNADs are given in ANSI/HPS N13.3 are shown in **Table 10**.

Performance for PNNL PNADs when neutron dose is based on foil activity and gamma dose is based on the default OSL reading (reader calibration to ^{60}Co) is shown in **Appendix L, Table L.1.** As can be seen, the positive bias in reported gamma dose offsets the negative bias in reported neutron dose and most of the dosimeters have passing scores.   Performance for PNNL PNADs when neutron dose is based on foil activity and gamma dose is based on the corrected OSL reading is shown in **Table L.2.** The intent was to show how the dosimeter performs using current cross sections and fluence to absorbed dose conversion factors, assuming unbiased gamma dose measurement. Performance for PNNL PNADs when neutron dose is calculated from OSLN readings is given in **Table L.3**. The intent here was to show the potential performance of the OSL/OSLN albedo dosimeter when properly calibrated for the given neutron energy spectrum and properly calibrated for unbiased gamma dose measurement in the presence of neutrons. Performance for the Hanford PNAD with optimized gamma absorbed dose calibration factor is shown in **Table L.4**. All of the Hanford PNADs were exposed in air, so the gamma absorbed dose calibration factor was optimized for OSL elements exposed in air. Performance for the FNAD is given in **Table M.1** and **Table M.2**. Optimized gamma and neutron absorbed dose calibration factors were applied here as well.

Table 10. ANSI/HPS N13.3 Performance Test Criteria for Criticality Accident Dosimetry Systems

Total absorbed dose range	B
10 to 100 cGy (10 to 100 rad)	-0.50 < B < 0.50
100 to 1000 cGy (100 to 1000 rad)	-0.25 < B < 0.25
> 1000 cGy (1000 rad)	indication of dose > 1000 cGy (1000 rad)

10.0 Electronic Personal Dosimeter Measurements

The primary objective of the EPD irradiations was to measure the "apparent" gamma dose response of the gamma sensitive dosimeters when exposed to very short intense bursts of neutron+gamma radiation, at both protection level gamma doses and accident level gamma doses . The gamma dose response is referred to as "apparent" because of the expected under response to the short Godiva-IV pulse duration (e.g. 50 microseconds) and the potential influence of neutrons on the detector gamma response. (The neutron/gamma absorbed dose ratio was approximately 8-10 for locations within the main room.) A secondary objective was to obtain neutron absorbed dose response information for the DMC3000-neutron module for very short intense bursts of neutron+gamma radiation.   The gamma dose response of individual EPDs and the neutron dose response of the DMC3000-neutron module EPD are shown in **Appendix N, Table N.1.** All EPDs grossly under-responded as expected. The gamma dose response is summarized by model number in **Table N.2**. As can be seen, the response varies relatively little as a function of dose level and is fairly uniform across models of EPD. A summary of EPD response by model is presented in **Table 9**. The potential influences on gamma response in these irradiations and causes for the observed under response are numerous and as of this writing, have not been fully investigated or understood. It should be emphasized that the "response factors" in **Table N.1** are simply a convenient way of displaying response data and are NOT currently intended as actual correction factors that could or should be applied to EPD readings in the event of a criticality. It should also be noted that all of the EPDs in the exercise were exposed in air and may differ significantly from the response on phantom.

Table 11. EPD Gamma Dose Response Factors

Make	Model	Gamma Dose Response		
		Average	stdev	C.V.
Mirion-MGP	DMC2000S	0.18	0.01	0.05
Mirion-MGP	DMC3000	0.21	0.03	0.12
Mirion-MGP	DMC3000-neutron module	0.26	n/a	n/a
Thermo	Mark 2.5	0.23	0.02	0.10

11.0 Quick Sort Measurements

Direct readings were taken on saline filled BOMAB phantoms and on activated PNADs using hand held survey instruments to establish and/or verify quick sort criteria for use in the event of an actual criticality event at PNNL.

11.1 Direct Survey Measurements on BOMAB Phantoms

The BOMAB phantoms used in the exercise were filled with lactated Ringer's solution to simulate blood sodium and chlorine levels. All BOMABs were irradiated in the upright position. The exposed BOMABs were made available to participants for direct measurement with hand held survey instruments after each pulse. Unfortunately the BOMABs were not available to participants until at least 4 hours had passed. Most if not all ^{38}Cl that was initially produced had decayed by the time measurements were started ($T_{1/2} = 37.2$ minutes). So the measurement data obtained is not reflective of quicksort data that would be likely be generated within an hour of an actual criticality accident. Direct measurements were made on the BOMAB upper torso and lower torso while the BOMAB was still assembled (with one exception). Measurements were made using the following survey instruments:

- Bicron microrem meter
- Ludlum Model 43-93 alpha-beta scintillation probe (100 cm^2) with Ludlum Model 2360 meter
- Ludlum 26-1 Pancake GM probe with dose equivalent filter (window cover)

Individual measurement data taken from the BOMABs are tabulated in **Appendix O, Table O.1**. The data were normalized to the delivered dose and plotted as a function of time since irradiation. The plots are shown in **Appendix O, Figure O.1 – Figure O.6.** Data that were taken more than 300 minutes after irradiation when ^{38}Cl activity would be negligible were decay corrected to time of burst using the 14.95 hour half-life for ^{24}Na, then averaged to obtain an additional data point at time zero for the purpose of plotting and curve fitting.

11.2 Direct Survey Measurements on PNADs

Each PNNL PNAD and Hanford PNAD was surveyed with the Ludlum 43-93 alpha-beta scintillation probe before being disassembled. The readings are tabulated in **Appendix P, Table P.1**. PNAD 43 was set aside and surveyed a second and third time in an attempt to obtain a rudimentary decay curve. The data for PNAD 43 are plotted in **Appendix P, Figures P.1 and P.2**. Unfortunately short half-life components had decayed away before the PNADs were available for survey and breakdown. To obtain a more useful PNAD quicksort decay curve, direct measurements will need to be performed starting 30 minutes after irradiation.

12.0 DISCUSSION

Neutron dose results calculated from measured foil activities using the dose calculation methodology described in Section 5 of this report were consistently low. This was true whether the dosimeters were exposed in air or on phantom. This is due in part to the fact that the quantity calculated from foil activities is actually tissue kerma in air and this value was used to report absorbed dose. In general, the quantity kerma is substantially less than the quantity absorbed dose. For the unmoderated Godiva-IV fission spectra in this exercise, the quantity kerma is approximately 70% - 80% of the quantity personal absorbed dose. But even when compared to the *known delivered values* for kerma, the foil calculated values for *kerma* are low, with an average response equal to 83% of the delivered kerma for distances between 2 and 4 meters in air, and 82% for the same distances on phantom (see **Table 8**). The resulting negative bias in reported personal *neutron* absorbed dose, $D_p(10)_n$ for dosimeters exposed on phantom when kerma values are used for dose is -0.40 (see **Table 8**). When the foil reported neutron dose is combined with an accurate gamma dose the bias in *total* reported dose was sufficiently low that the PNNL PNAD, Hanford PNAD and FNAD did not meet the total dose accuracy criteria in ANSI/HPS N13.3 – 2013 (**Table L2**, **Table L.4** and **Table M.1**).

In general, when the OSL system is calibrated to ^{60}Co photons using OSL elements exposed on phantom with a 3.2 mm thick PMMA cover plate, and a default gamma absorbed dose calibration factor of 1.00 is used, the OSL calculated gamma dose exhibits a large over response. For dosimeters exposed on phantom the average response was approximately 250%. For dosimeters exposed in air, the average response was approximately 130% of the given gamma dose. One of the possible reasons for this over response is the small but not insignificant neutron sensitivity of Al_2O_3:C to neutrons. Although negligible for radiation protection dosimetry which involves dose equivalent quantities for neutrons, the response becomes significant when absorbed dose is the quantity of interest. The apparent gamma response of Al_2O_3:C to neutrons is 2-4% of the delivered neutron absorbed dose (IAEA 1982). In the Godiva-IV radiation field with 8:1 neutron/gamma absorbed dose ratio, this neutron sensitivity of the phosphor would in principle, result in a reported gamma dose that is 116% - 132% of the delivered gamma dose. In the 2010 NAD intercomparison exercise at Valduc with the Caliban (bare metal) reactor, the TLD 700 chips in Hanford PNADs exposed on phantom in 3 separate irradiation experiments, measured gamma doses that were 155% , 170% and 230% of the delivered gamma dose. The reference neutron/gamma ratio in those 3 experiments was 4.00, 4.25 and 6.10. The TLD results were corrected for fading and supralinearity. The fact that the OSL gamma over response observed in the Godiva-IV field and the TLD 700 over response in the Caliban field are larger than what would be expected based on the IAEA data suggest that other factors may be at play or the particular conditions under which the IAEA data were generated do not apply to the radiation fields in the Caliban and Godiva-IV exercises. Another possible contributing factor to apparent gamma dose over response could be contribution to dose from capture reactions in nearby hydrogenous materials (e.g. phantoms) that were not present when the gamma dose rate for the location was characterized. Another possible factor could be the inherent over response of Al_2O_3:C to low energy photons combined with a possibly significant low energy photon component to the radiation field. The E3 (Cu filtered element) / E4 (Al filtered element) element reading ratios for the InLight® OSLN dosimeters did not indicate the presence of a significant low energy photon component. However, this ratio is not a strong indicator and would not preclude a measurable influence from this effect. The default gamma dose calculation algorithm prepared for use during the exercise does not attempt to correct for any of the above potential influences. The influences on photon response of OSL

detectors used in neutron fields will need to be further investigated and quantified before adequate methods for correction can be incorporated into future gamma dose calculations.

Interestingly, for PNADs exposed on phantom facing the source at distances between 2 and 4 meters, the overestimated gamma dose in combination with the under estimated neutron dose, gives a total reported dose value for approximately half of the dosimeters that is within the $\pm 25\%$ accuracy requirement of the standard for total absorbed dose (see **Table L.1**). The remaining dosimeters (except for those at location 10) are barely outside the accuracy limit. The bias in reported total dose for the group of 9 dosimeters exposed on the front face of a phantom at distances between 2 and 4 meters is -0.22. *However, performing this type of performance analysis simply to demonstrate compliance with a performance standard, is of limited usefulness since it masks the large counteracting biases involved and would not be applicable in scenarios where the neutron/gamma dose ratio differed significantly from 8, which was the approximate ratio for this exercise.*

For the FNAD, neutron dose results calculated using the OSLN elements inside the cylindrical paraffin moderator were within 10% of the delivered $D^*(10)_n$ values when the default neutron absorbed dose calibration factor $C_n = 12.89$ (based on local calibration with bare ^{252}Cf) was used. However, the gamma dose result based on the response of the OSL element in the outer dosimetry package was approximately 130% of the delivered $D^*(10)_\gamma$ values when the default gamma absorbed dose calibration factor $C_\gamma = 1.00$ (based on ^{60}Co) was used. This gamma dose over response is similar to that observed with PNADs exposed in air.

For the PNNL PNAD, neutron dose results calculated using the OSLN elements in the BA case showed a very large over response when the default neutron absorbed dose calibration factor $C_n = 2.73$ (based on bare ^{252}Cf) was used. Reported doses were between 180% and 300% of the given values. When an optimized Godiva-IV specific neutron absorbed dose calibration factor, $C_n = 6.09$, was used, the OSLN albedo neutron dose results for dosimeters exposed on phantom were within acceptable accuracy limits (except for position 10).

In the gamma and neutron dose performance analyses, the data for position 10 (9 meter distance) differed consistently and significantly from the data for the other positions. This was true whether gamma dose performance or neutron dose performance was being analyzed and was true for neutron dose calculated by foil activation or by OSLN albedo response. It is important to note that this position is described as an "alcove" location implying that it is a smaller space contiguous with the main room, but with narrower dimensions and different scatter conditions. It is also important to note that the reference fluence and dose values in **Appendix D** are *preliminary* and subject to change. Therefore, use of the position 10 data for making revisions to dose calculation methodology, or generalized conclusions about dosimeter response should be limited until final reference values have been published.

The quicksort measurements on BOMAB phantoms were performed after essentially all of the ^{38}Cl activity had decayed away and thus represent only the contribution of ^{24}Na to quicksort survey readings. The ^{38}Cl activity (T $_{1/2}$ = 37.2 minutes) can be as much as half of the total activity in a person immediately after irradiation (Mettler and Voelz 2001). Therefore, the cpm/cGy decay curves are not valid for measurements made within 260 minutes of exposure. Similarly, quicksort measurements on PNADs were made after a significant portion of the shorter half-life activity in the PNAD had decayed away. The cpm/cGy curves obtained from these measurements are also not valid for measurements made

within 260 minutes of exposure. In general, cpm/cGy quicksort dose conversion factors for whole body and PNAD direct survey readings are highly dependent on the neutron energy spectrum which varies by distance and shielding. For PNADs exposed by the unmoderated Godiva-IV critical assembly in air, the cpm/cGy values at a distance of 4 meters were twice as large as those for the 2 meter distance.   Because the energy spectrum also varies significantly with the type of criticality (i.e. bare metal vs. solution criticality) the data obtained from Godiva-IV measurements may not be applicable to a solution type criticality at PNNL.

13.0 CONCLUSIONS

The dose calculation methodology documented in Section 5.0 of this report needs to be revised in order for PNNL PNADs and FNADs to satisfy the accuracy requirements of ANSI/HPS N13.3 – 2013.   The assumed cross sections and associated activity-to-fluence conversion factors may need to be revised. The fluence-to-dose conversion factors clearly need to be revised since they appear to be based on measurement of tissue kerma. The revised values for fluence-to-dose conversion factors will need to be based on the new operational quantities, personal absorbed dose $D_p(10)$ and ambient absorbed dose, $D*(10)$ adopted in ANSI/HPS N13.3 – 2013.   The activity measurements documented in this report have low counting uncertainty and are consistent across measurement locations exhibiting relatively low variability. Combined with the reference dosimetry for the exercise and the fluence and spectrum characterization work performed by AWE, the activity measurements documented in this report should be suitable for use in validating and/or revising the activity-to-fluence conversion factors, and the fluence-to-dose conversion factors. Ultimately, the revised dose calculation methodology will need to accommodate and be validated against the neutron energy spectrum expected in a solution type criticality event at PNNL. OSL gamma dose calculations also need to be revised to account for the influence of neutrons on gamma dose response. The response data obtained during the exercise indicate that with proper calibration to a specific source spectrum, the OSL and OSLN detectors can provide accurate gamma dose results and unbiased estimates of neutron dose for normal exposure geometry. The revised gamma and neutron dose calculation methodology using these detectors will need to be tailored to the gamma and neutron energy spectra expected in a solution type criticality event at PNNL.

14.0 REFERENCES

Anderson, Lowell L. 1964 *Cross Section of Copper-63 for Nuclear Accident Dosimetry* Health Physics, Volume 10, pp.315-322.

Asselineau, B. F. et. al. 2004 *Reference dosimetry measurements for the International intercomparison of criticality Accident Dosimetry Silene 9–21, June 2002.* Radiation Protection Dosimetry (2004), Vol. 110, Nos 1-4, pp. 459-464.

Bramson, P.E. 1963. *Hanford Criticality Dosimeter*. HW-71710 Revised 2-8-63, General Electric Hanford Atomic Products Operation, Richland, Washington.

Casson, W. H. et. al. 1996a *Measurement of the neutron energy spectrum on the Godiva IV fast burst assembly for application to neutron dosimetry studies*, Health Physics; Journal Volume: 70; Journal Issue: Suppl.6; 41st Annual Meeting of the Health Physics Society, Seattle, WA, 21-25 July, 1996;

Casson, W. H. et. al. 1996b *Nuclear Accident Dosimetry Studies at Los Alamos National Laboratory LA-UR 95-3845* Los Alamos National Laboratory 1996.

Dealfield, H. J., 1988. *Nuclear Accident Dosimetry – An Overview*. Radiation Protection Dosimetry, Vol. 23, No. 1 (of 4), pp. 143-149, Nuclear Technology Publishing, 1988.

Glenn, R. D. and P. E. Bramson 1977 *The Hanford Critical Radiation Dosimeter* PNL-2276, Pacific Northwest National Laboratory, November 1997.

Gómez-Ros, J. M. et al 2012 *Designing an Extended Energy Range Single-Sphere Multi-Detector Neutron Spectrometer*. Nuclear Instruments and Methods in Physics Research A 677 (2012) 4-9.

Greenwood, L. R. and C. D. Johnson, 2014 *Least-Squares Spectral Adjustment with STAYSL PNNL*, in 15th International Symposium on Reactor Dosimetry, 18-23 May 2014, Aix-en-Provence, France, EPJ Web of Conferences, Vol. 106, 586-593,2016 DOI:10.1051/epjconf/201610607001

Health Physics Society (HPS) 2009. *ANSI/HPS N13.35-2009 Specifications for the Bottle Manikin Absorption Phantom*, Health Physics Society, 2009.

Health Physics Society (HPS) 2013, ANSI/HPS N13.3 – 2013, *Dosimetry For Criticality Accidents*, , Health Physics Society, 1313 Dolley Madison Blvd. Suite 402, McLean, VA

Heinrichs, D. et. al, 2014 *Final Design for an International Intercomparison Exercise for Nuclear Accident Dosimetry at the DAF Using GODIVA-IV (IER-148 CED-2 Report).* LLNL-TR-661851, Lawrence Livermore National Laboratory, September 30, 2014.

Hill, R. L., Conrady, M. M. 2010 *PNNL Results from 2009 Silene Criticality Accident Dosimeter Intercomparison Exercise*. PNNL-19503 Pacific Northwest National Laboratory, June 2010.

Hill, R. L., Conrady, M. M. 2011 *PNNL Results from 2010 CALIBAN Criticality Accident Dosimeter Intercomparison Exercise*. PNNL 20880 Pacific Northwest National Laboratory, October 2011.

Hutchinson, J. D., D. K. Hayes and W. L. Myers 2012 *National Criticality Experiments Research Center: Capabilities and Experiments*, LA-UR-20701 Los Alamos National Laboratory 2012.

International Atomic Energy Agency (IAEA). 1978 *Compendium of Neutron Spectra in Criticality Accident Dosimetry* Technical Report No. 180, IAEA Vienna, Austria

International Atomic Energy Agency (IAEA). 1982. *Dosimetry for Criticality Accidents, a Manual*. Technical Report Series No. 211, IAEA, Vienna, Austria.

International Atomic Energy Agency (IAEA) 1990 Compendium of Neutron Spectra and Detector Responses for Radiation Protection Purposes, Technical Report No. 318. IAEA 1990

International Commission on Radiological Protection (ICRP). 1983. *Radionuclide Transformations: Energy and Intensity of Emissions*. ICRP Publication 38, Pergamon Press, New York, New York.

Kimpland, R. H. 1996 Preliminary Result of GODIVA-IV Prompt Burst Modeling. LA-UR-96-1498 Los Alamos National Laboratory 1996.

Knoll, G. F. 1979 *Radiation Detection and Measurement*. John Wiley and Sons, 1979

Landauer 2010. *Dosimeter Specification (InLight LDR Model 2 – OSLN Revision 1*, March 4, 2010, Landauer Inc., 2 Science Road, Glenwood, Illinois

Mettler, F. A. and G. Voelz 2001. *Evaluation of Neutron Exposure*. in Medical Management of Radiation Accidents 2nd Edition, (I. Gusev, A. Guskova, and F. Mettler, editors) CRC Press LLC. 2001.

Mosteller, R. D. and J. M. Goda 2009 *Analysis of Godiva-IV Delayed-Critical and Super-Prompt-Critical Conditions*. in proceedings of International Conference on Mathematics, Computational Methods and Reactor Physics (M&C 2009), American Nuclear Society, 2009

U.S. Nuclear Regulatory Commission (NRC) 2011 *VARSKIN 4: A Computer Code for Skin Contamination Dosimetry* (NUREG/CR-6918, Revision 1) June 2011

PNNL 1990. *Hanford External Dosimetry Program Internal Technical Documentation, Volume IV – Nuclear Accident Dosimetry*. Health Physics Department, Pacific Northwest National Laboratory, 1990 (internal document).

PNNL 2017 *PNNL Nuclear Accident Dosimetry Technical Basis Manual Revision 0.1*, Radiation Protection Division, Pacific Northwest National Laboratory, April 2017, (internal document).

Sims, C. S. 1988 *Nuclear Accident Dosimetry Studies*. Health Physics Vol. 57, No. 3, pp. 439-448.

Swaja, R. E., Oyan, R. and Sims, C. S. 1986 *Twenty-Second ORNL Intercomparison of Criticality Accident Dosimetry Systems: August 12-16, 1985*. ORNL-6276 Oak Ridge National Laboratory, May 1986.

Sims, C.S., Killough, G.G. 1981 *Reference Dosimetry for Various Health Physics Research Reactor Spectra*. Rep. ORNL/TM-7748, Oak. Ridge National Laboratory, Oak Ridge, TN (1981).

Sims, C. S., and Ragan, G. E. 1987 *Health Physics Research Reactor Reference Dosimetry.* ORNL-6240 Oak Ridge National Laboratory, June 1987.

Swaja, R. E. and G. E. Ragan. 1985. *Effective Threshold Cross Sections for Sulfur and Indium Fast Neutron Reactions*. Radiation Protection Dosimetry, Volume 12, No 3, pp 303-305.

Wilson, C., Leo Clark, and Phil Angus 2014 *Neutron spectrometry results from phase two of the Godiva-IV characterization*. AWE Report No. 880/14 AWE/NAS/RPG/ADS/CRIT/TR/004 issue 5.

Appendix A

PNNL PNAD Design Features
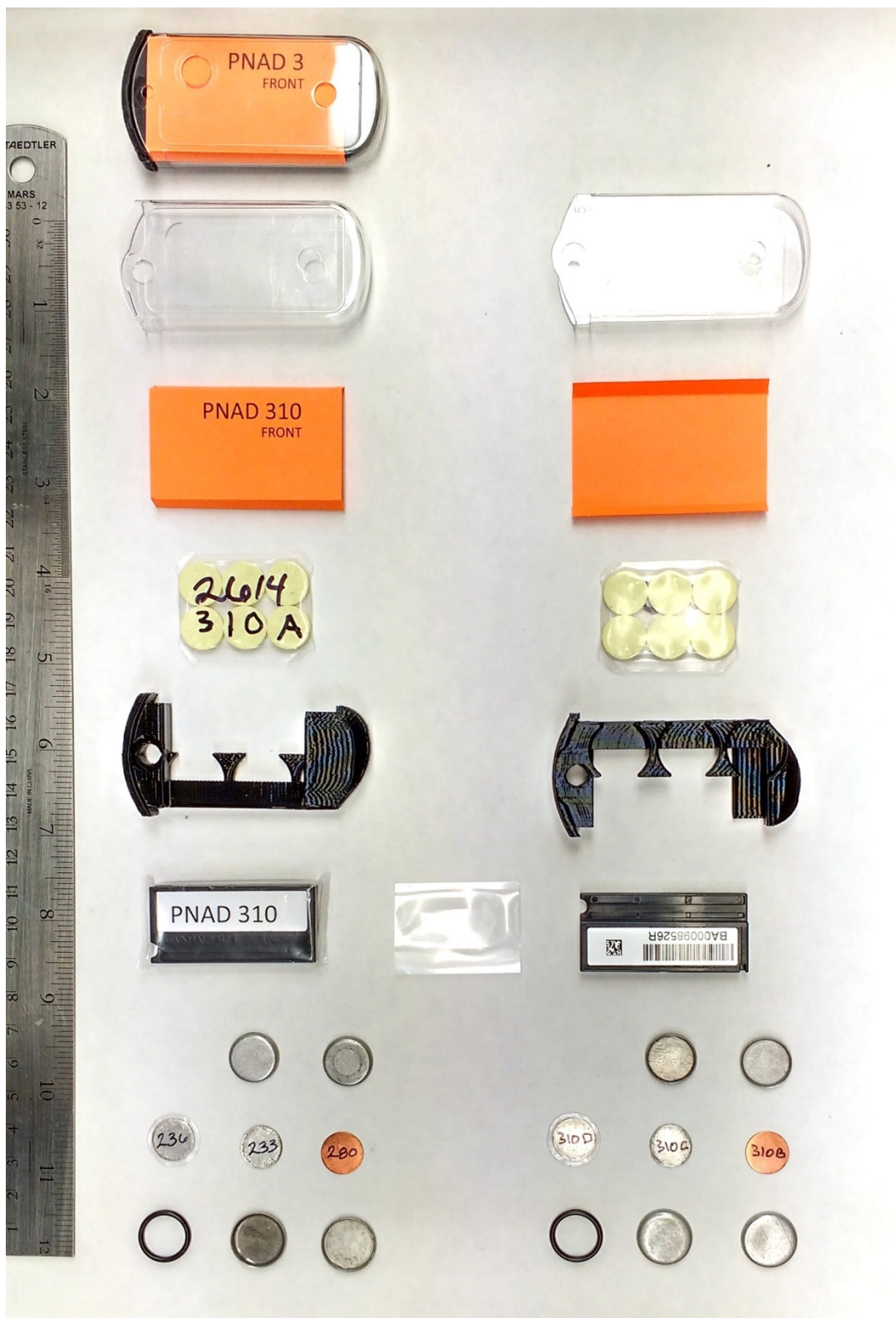
Figure A.1. Disassembled PNNL PNADs with components viewed from front and back sides
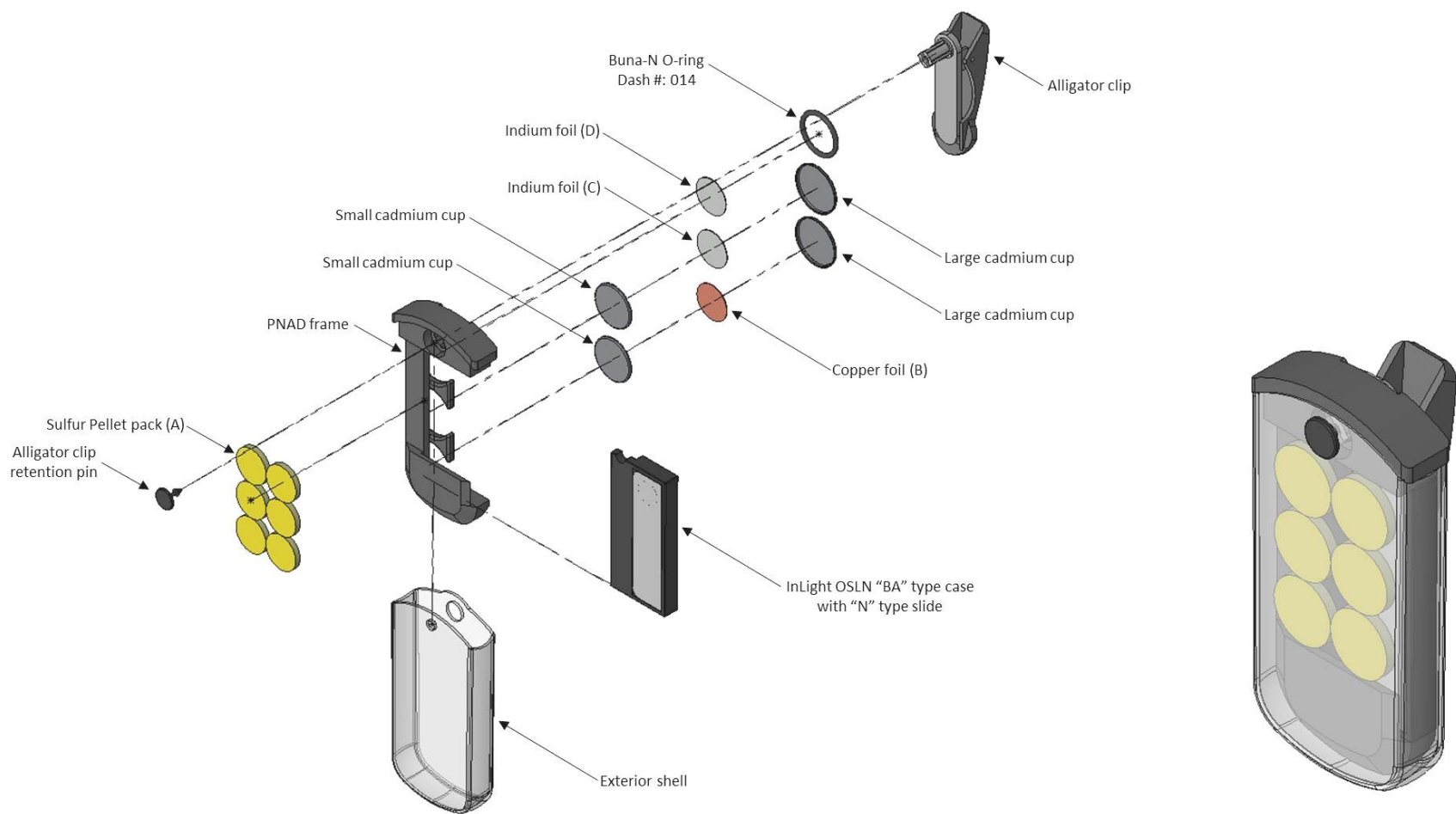
Figure A.2 PNNL PNAD Exploded View

- Buna-N O-ring Dash #: 014
- Alligator clip
- Indium foil (D)
- Indium foil (C)
- Large cadmium cup
- Small cadmium cup
- Large cadmium cup
- Small cadmium cup
- Copper foil (B)
- PNAD frame
- Sulfur Pellet pack (A)
- Alligator clip retention pin
- InLight OSLN "BA" type case with "N" type slide
- Exterior shell

Table A.1 PNNL PNAD Component Dimensions and Composition

Description	Detector	Composition	nominal density (g/cm³)	diameter (cm)	length (cm)	Width (cm)	Nominal Thickness (cm) **	Nominal Mass (g)	nominal density thickness (g/cm²)**
clear tape cover on exterior shell (3M 8412)		PF	1.34	n/a	5.51	2.54	0.015	0.286	0.020
exterior clear plastic shell		PC	1.2	n/a	7.1	3.6	0.089	5.62	0.107
orange cardstock label		paper	0.77	n/a	5.56	4.13	0.023	0.404	0.018
heat sealed bag for sulfur pellets		LDPE	0.902	n/a	3.81	2.9	0.010	n/a	0.00917
sulfur pellet (single) 0.5" dia. x 0.075" thick		S	1.8	1.27	n/a	n/a	0.191	0.435	0.343
sulfur pellet six pack (1" x 1.5" x 0.075")	A	S	1.8	n/a	3.81	2.54	0.191	2.61	0.343
black plastic PNAD frame (overall)		PET	1.15	n/a	n/a	n/a	n/a	4.86	n/a
black plastic PNAD frame (thick section)		PET	1.15	n/a	n/a	n/a	0.508	n/a	0.584
black plastic PNAD frame (thin section)		PET	1.15	n/a	n/a	n/a	0.292	n/a	0.336
lip of black plastic InLight Case		ABS	1.06	n/a	n/a	n/a	0.292	n/a	0.310
small cadmium cup		Cd	8.69	1.52	n/a	n/a	0.051	1.15	0.441
copper foil (inside Cd cups)	B	Cu	8.96	1.27	n/a	n/a	0.025	0.281	0.228
indium foil (inside Cd cups)	C	In	7.31	1.27	n/a	n/a	0.025	0.236	0.186
large cadmium cup		Cd	8.69	1.68	n/a	n/a	0.051	1.22	0.441
Indium foil (bare)	D	In	7.31	1.27	n/a	n/a	0.025	0.236	0.186
clear tape covering on foils (3M 142)		polyester	1.14	1.27	n/a	n/a	0.006	n/a	0.00723
black plastic InLight OSLN case		ABS plastic, Toyolac 10081 black, aluminum filter, copper filter,	1.06	n/a	4.91	2.30	0.554	n/a	n/a
"N" type slide		ABS plastic, black	1.06	n/a	4.70	1.18	0.191	n/a	n/a
Al2O3:C detectors on "N" type slide		Al_2O_3:C, $^6Li_2CO_3$	3.95	0.724	n/a	n/a	0.028	0.021	0.051
Heat sealed bag for InLight BA case		LDPE	1.04	n/a	5.72	2.86	0.004	n/a	0.0040

NOTES:

**	for clear plastic PNAD outer shell and for polyethylene heat sealed bags (sulfur pellet bag and InLight bag), the listed thickness or density thickness is the wall thickness. For adhesive tape, the listed thickness or density thickness is for a single layer and includes the adhesive.
LDPE	low density polyethylene
PET	polyethylene terephthalate
PC	polycarbonate
PF	3M 8412 polyester film tape
S	sulfur pellet
Cu	copper metal
In	indium metal
Cd	cadmium metal
air	dry air at STP
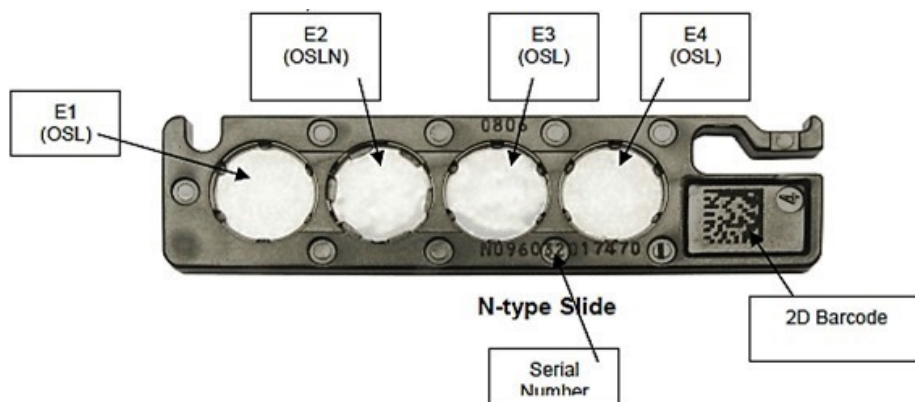
Figure A.3 N-type slide for InLight® OSLN "BA" type case

Figure A.4 InLight® OSLN "BA" type case
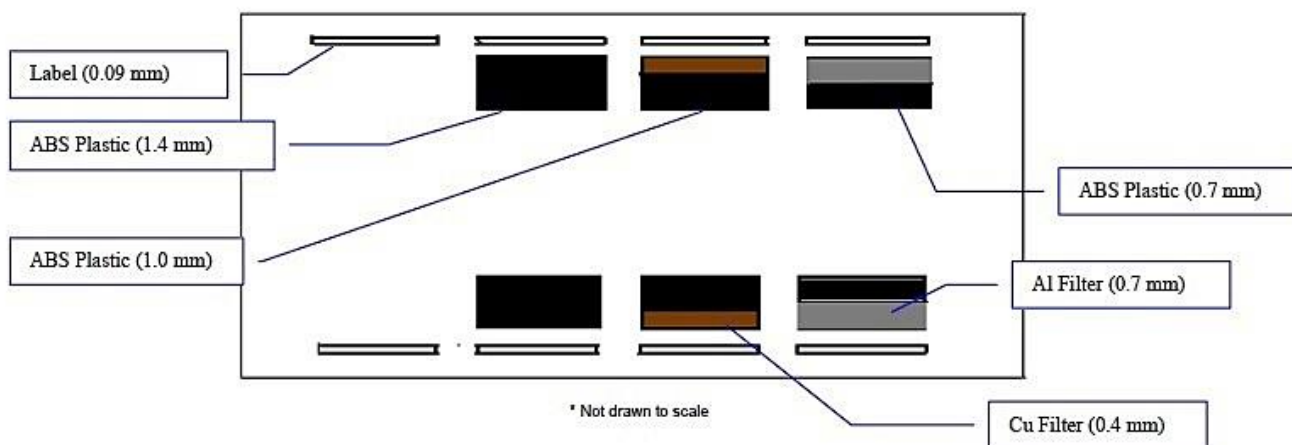
Figure A.4 InLight® OSLN BA case filtration

Table A.2 PNAD Filtration in front of and behind OSL/OSLN elements

Material	Density (g/cm^3)	Thickness (mm)	Density Thickness (mg/cm^2)			
			Element 1 (E1)	Element 2 (E2)	Element 3 (E3)	Element 4 (E4)
FRONTSIDE						
clear polyester film tape (3M 8412)	1.34	0.152	20.4	20.4	20.4	20.4
clear polycarbonate Shell	1.21	0.76	-	92.2	92.2	92.2
orange cardstock paper label	0.77	0.23	17.6	17.6	17.6	17.6
polyethylene bag (wall)	0.90	0.10	9.17	9.17	9.17	9.17
sulfur pellet	1.2	0.02	2.4	2.4	2.4	2.4
polyethylene bag (wall)	0.90	0.10	9.17	9.17	9.17	9.17
paper label (PNAD number)	0.77	0.10	7.8	7.8	7.8	7.8
filter cover label (blank) - polyester	1.01	0.09	9.09	9.09	9.09	9.09
(ABS) plastic case - E2	1.26	0.70	-	88.2	-	-
(ABS) plastic case - E3	1.26	1.00	-	-	126	-
(ABS) plastic case - E4	1.26	0.70	-	-	-	88.2
ABS plastic filter - E2	1.26	0.70	-	88.2	-	-
Cu filter - E3	8.96	0.40	-	-	358.4	-
Al filter - E4	2.7	0.70	-	-	-	189
total in front of OSL or OSLN detector			76	344	652	445

	Material	Density (g/cm^3)	Thickness (mm)	E1	E2	E3	E4
OSL	Al$_2$O$_3$:C dots on "N" type slide	3.95	0.28	51.0	-	51.0	51.0
OSLN	Al$_2$O$_3$:C - ^{6}Li$_2$CO$_3$ dot on "N" type slide	3.95	0.28	-	51.0	-	-

Material	Density (g/cm^3)	Thickness (mm)	E1	E2	E3	E4
BACKSIDE						
Al filter - E4	2.7	0.70	-	-	-	189
Cu filter - E3	8.96	0.40	-	-	358.4	-
ABS plastic filter - E2	1.26	0.70	-	88.2	-	-
(ABS) plastic case - E4	1.26	0.70	-	-	-	88.2
(ABS) plastic case - E3	1.26	1.00	-	-	126	-
(ABS) plastic case - E2	1.26	0.70	-	88.2	-	-
InLight barcode label - polyester	1.01	0.09	9.09	9.09	9.09	9.09
clear polycarbonate shell	1.21	0.76	92.2	92.2	92.2	92.2
total behind OSL or OSLN detector			101	278	586	378

Appendix B

PNNL FNAD Design Features

Figure B.1 PNNL FNAD

Outer dosimetry Package

Polyethylene candlestick
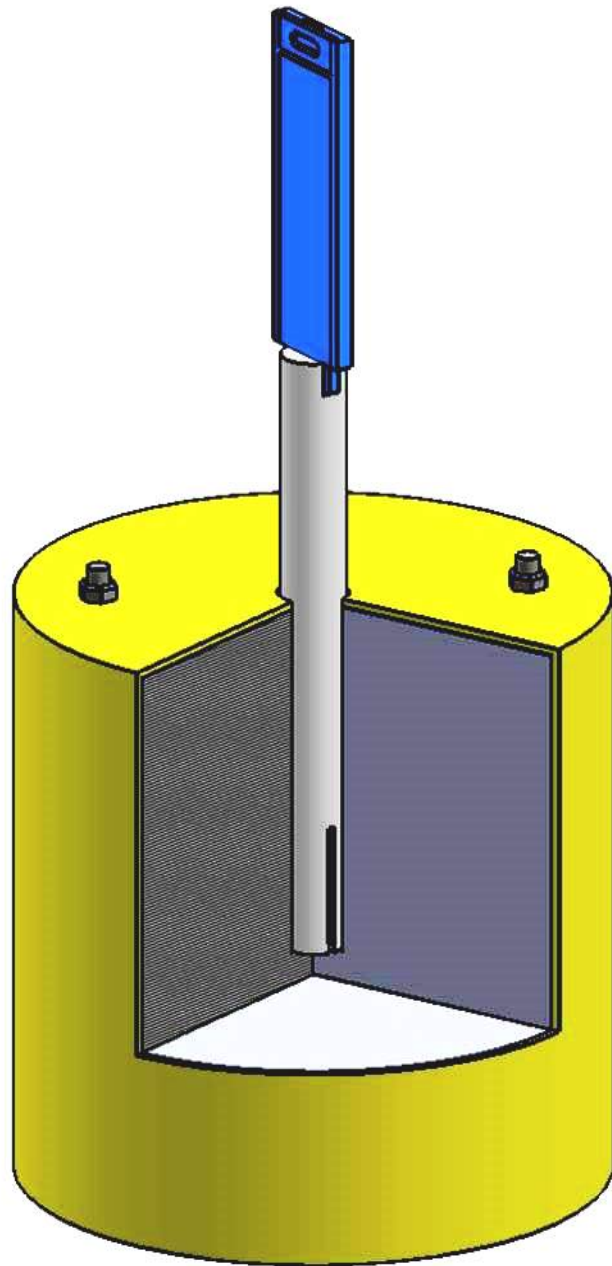
Inner dosimetry Package
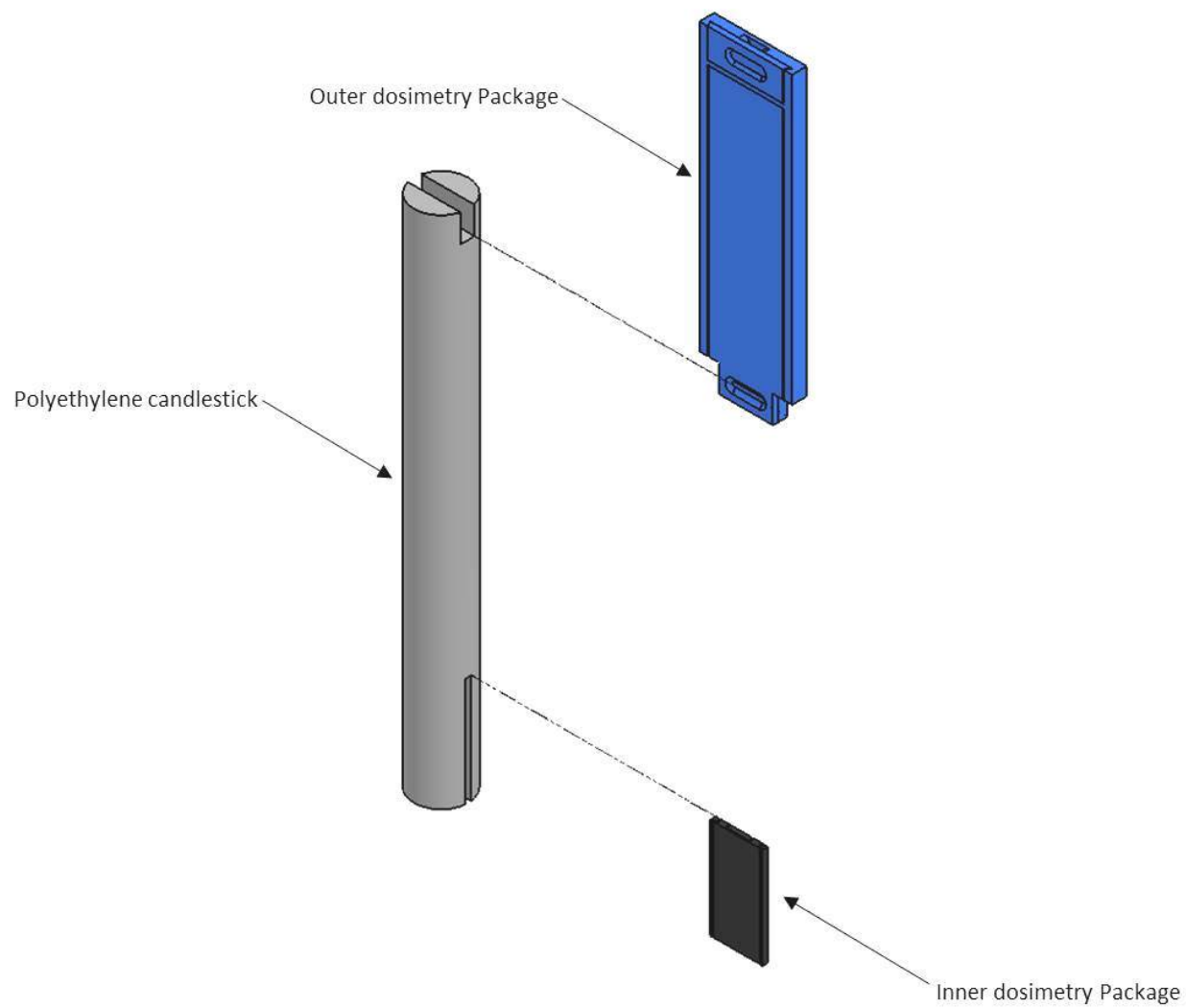
Figure B.2 PNNL FNAD "Candle" Assembly with Inner and Outer Dosimetry Packages
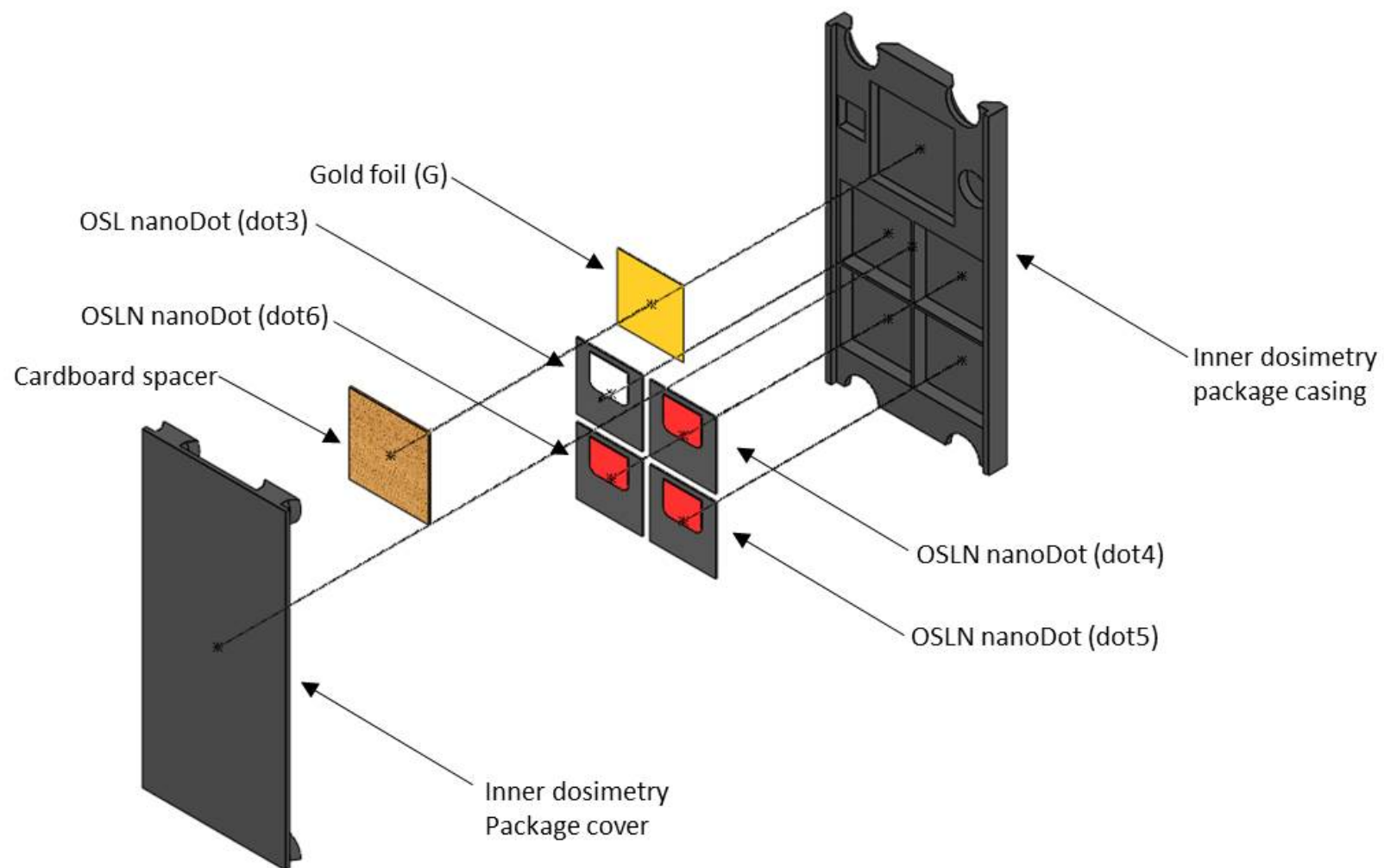
Figure B.3 PNNL FNAD Inner Dosimetry Package (exploded view)
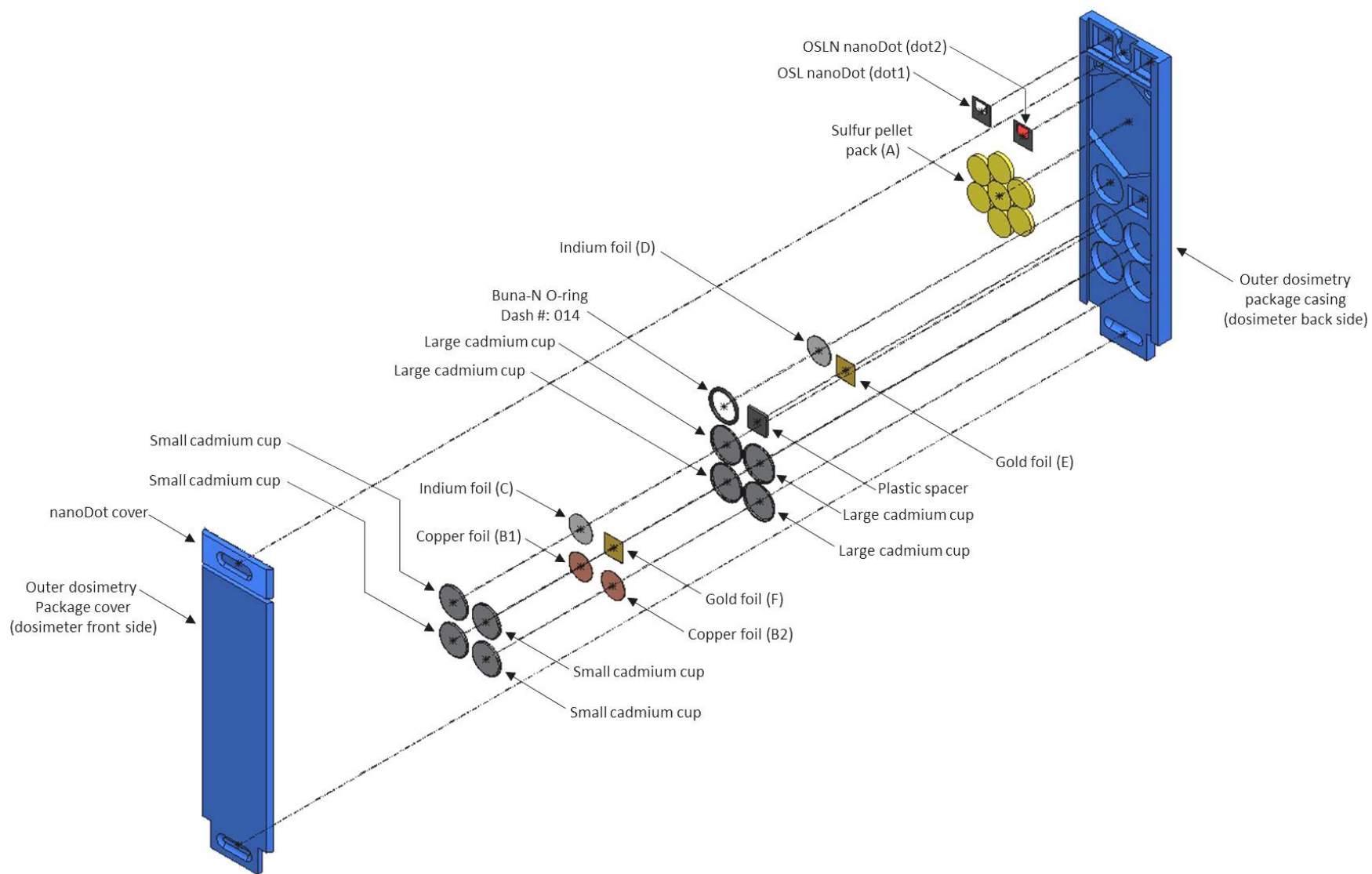
Figure B.4 PNNL FNAD Outer Dosimetry Package (exploded view)

Table B.1 PNNL FNAD Component Dimensions and Composition

Drawing	Component Name	Component Position	Composition	Outer Dimensions (nominal)				Attenuation Thickness[1] (cm)	Nominal density (g/cm^3)	Nominal Mass (g)	Nominal density thickness (g/cm^2)
				Length (cm)	Width (cm)	Thickness (cm)	Diameter (cm)				
Outer Dosimetry Package	sulfur pellet 7 pack	A	S	4.8	4.1	0.191	1.27	0.191	2.07	3.07	0.394
	copper foil (B1)	B1	Cu	n/a	n/a	0.025	1.27	0.025	8.96	0.281	0.228
	large cadmium cup	B1	Cd	n/a	n/a	0.051	1.68	0.051	8.69	1.22	0.441
	small cadmium cup	B1	Cd	n/a	n/a	0.051	1.52	0.051	8.69	1.15	0.441
	copper foil (B2)	B2	Cu	n/a	n/a	0.025	1.27	0.025	8.96	0.281	0.228
	large cadmium cup	B2	Cd	n/a	n/a	0.051	1.68	0.051	8.69	1.22	0.441
	small cadmium cup	B2	Cd	n/a	n/a	0.051	1.52	0.051	8.69	1.15	0.441
	indium foil (C)	C	In	n/a	n/a	0.025	1.27	0.025	7.31	0.236	0.186
	large cadmium cup	C	Cd	n/a	n/a	0.051	1.68	0.051	8.69	1.22	0.441
	small cadmium cup	C	Cd	n/a	n/a	0.051	1.52	0.051	8.69	1.15	0.441
	Indium foil (D)	D	In	n/a	n/a	0.025	1.27	0.025	7.31	0.236	0.186
	O-ring spacer	D	Buna-N rubber	n/a	n/a	0.178	1.60	0.000	1.3	n/a	n/a
	gold foil (E)	E	Au	1	1	0.013	n/a	0.013	19.3	0.250	0.245
	plastic spacer	E	PET	1	1	0.140	n/a	0.140	1.15	0.161	0.161
	gold foil (F)	F	Au	1	1	0.013	n/a	0.013	19.3	0.250	0.245
	large cadmium cup	F	Cd	n/a	n/a	0.051	1.68	0.051	8.69	1.22	0.441
	small cadmium cup	F	Cd	n/a	n/a	0.051	1.52	0.051	8.69	1.15	0.441
	OSL nanoDot	dot1	ABS + Al$_2$O$_3$:C	0.99	1.01	0.191	n/a	0.046	n/a	n/a	n/a
	OSLN nanoDot	dot2	ABS + Al$_2$O$_3$:C	0.99	1.01	0.191	n/a	0.046	n/a	n/a	n/a
	nanoDot Cover Plate	dot1, dot2	PET	1.42	3.78	0.229	n/a	0.229	1.15	n/a	0.263
	Foil Cover Plate	A, B1, B2, C, D, E, F	PET	13.13	3.78	0.254	n/a	0.254	1.15	n/a	0.292
	Detector Tray	A, B1, B2, C, F, dot1, dot2	PET	14.71	4.37	0.711	n/a	0.102	1.15	n/a	0.117
	Detector Tray	D, E	PET	14.71	4.37	0.711	n/a	0.152	1.15	n/a	0.175
Inner Dosimetry Package	gold foil (G)	G	Au	1.00	1.00	0.013	n/a	0.013	19.3	0.250	0.245
	cardboard spacer	G	paper	1.00	1.00	0.058	n/a	0.058	0.75	0.044	0.044
	OSL nanoDot	dot3	ABS + Al$_2$O$_3$:C	0.99	1.01	0.191	n/a	0.046	n/a	n/a	n/a
	OSLN nanoDot	dot4	ABS + Al$_2$O$_3$:C	0.99	1.01	0.191	n/a	0.046	n/a	n/a	n/a
	OSLN nanoDot	dot5	ABS + Al$_2$O$_3$:C	0.99	1.01	0.191	n/a	0.046	n/a	n/a	n/a
	OSLN nanoDot	dot6	ABS + Al$_2$O$_3$:C	0.99	1.01	0.191	n/a	0.046	n/a	n/a	n/a
	Detector Tray	dot3, dot4, dot5, dot6	PET	4.70	2.46	0.208	n/a	0.013	1.15	n/a	0.015
	Detector Tray	G	PET	4.70	2.46	0.208	n/a	0.076	1.15	n/a	0.088
	Detector Cover Plate	G, dot3, dot4, dot5, dot6	PET	4.70	2.20	0.061	n/a	0.061	1.15	n/a	0.070

Notes:

1 Attenuation thickness is the thickness of the part material that lies in the path of a normally incident beam of radiation passing through the sensitive volume of the detector. For foils and pellets, this is the same as the foil or pellet thickness. For detector trays, this will be less than the nominal outer dimension thickness.

Appendix C

Irradiation Locations in the DAF

PULSE 1 : 70 ℃

2m – Blue
2.5m - Brown
3m - Green
4m – Purple
9m - Red

Tree A-D	Position 1, 2, 3, 6
Tree A-H	Position 8, 10
BOMAB AP	Position 4, 5
PMMA/Slab Phantom	Position 7, 9
PNNL/Y-12 FNAD	Position 11, 12
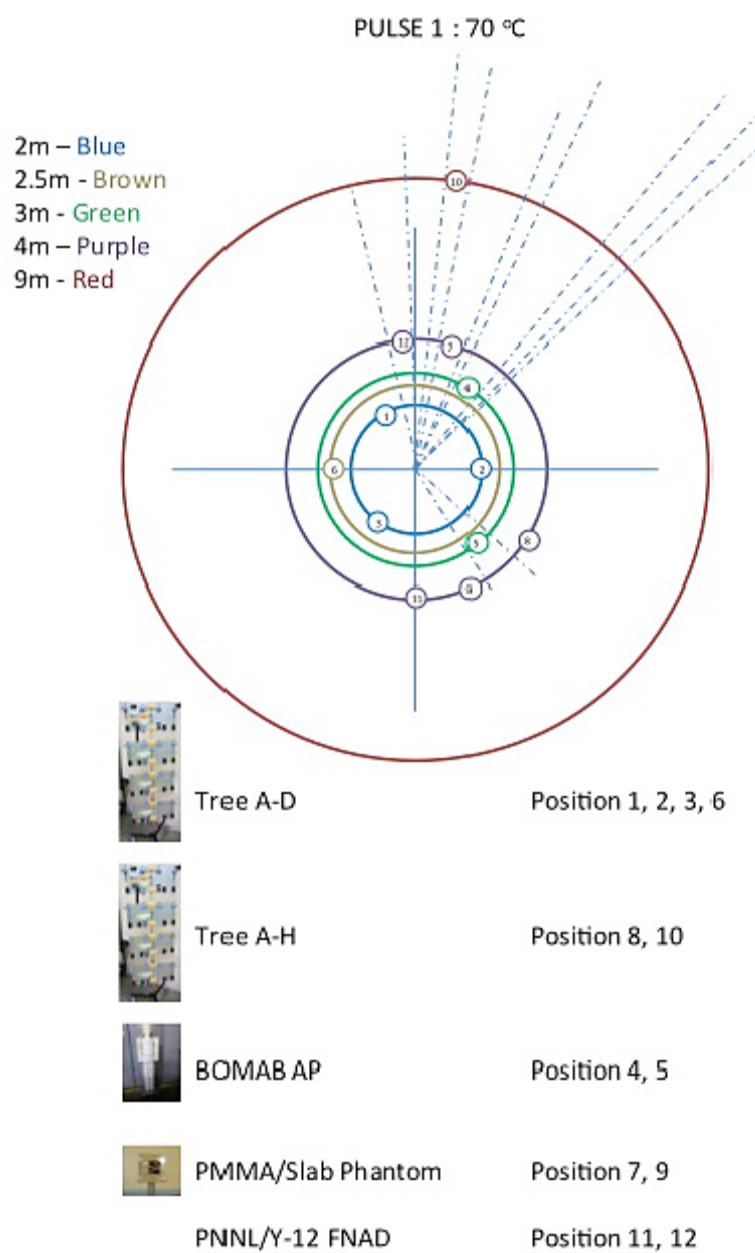
Figure C.1 Irradiation Locations for Pulse 1

PULSE 2 : 250 °C

2m – Blue
2.5m - Brown
3m - Green
4m – Purple
9m - Red

Tree A-D	Position 1, 2, 3, 6
Tree A-H	Position 8
BOMAB AP	Position 4, 5
PMMA/Slab Phantom	Position 7, 9
Single Sphere Spectrometer (SSS AWE)	Position 10
PNNL/Y-12 FNAD	Position 11, 12
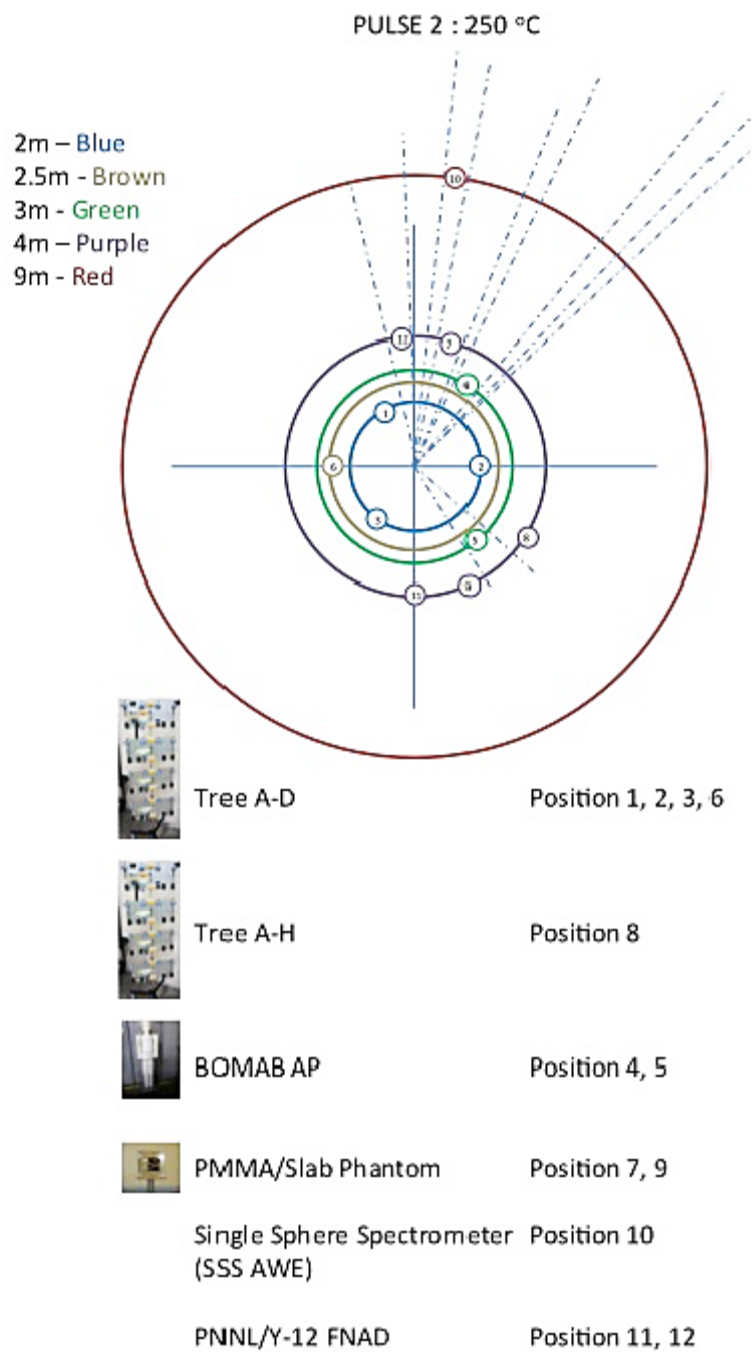
Figure C.2 Irradiation Locations for Pulse 2

PULSE 3: 150 °C

2m – Blue
2.5m - Brown
3m - Green
4m – Purple
9m - Red

Tree A-D	Position 2, 6
Tree A-H	Position 8, 9
BOMAB AP	Position 4, 7, 10
BOMAB LAT	Position 5
PMMA/Slab Phantom	Position 1, 3
PNNL/Y-12 FNAD	Position 11, 12
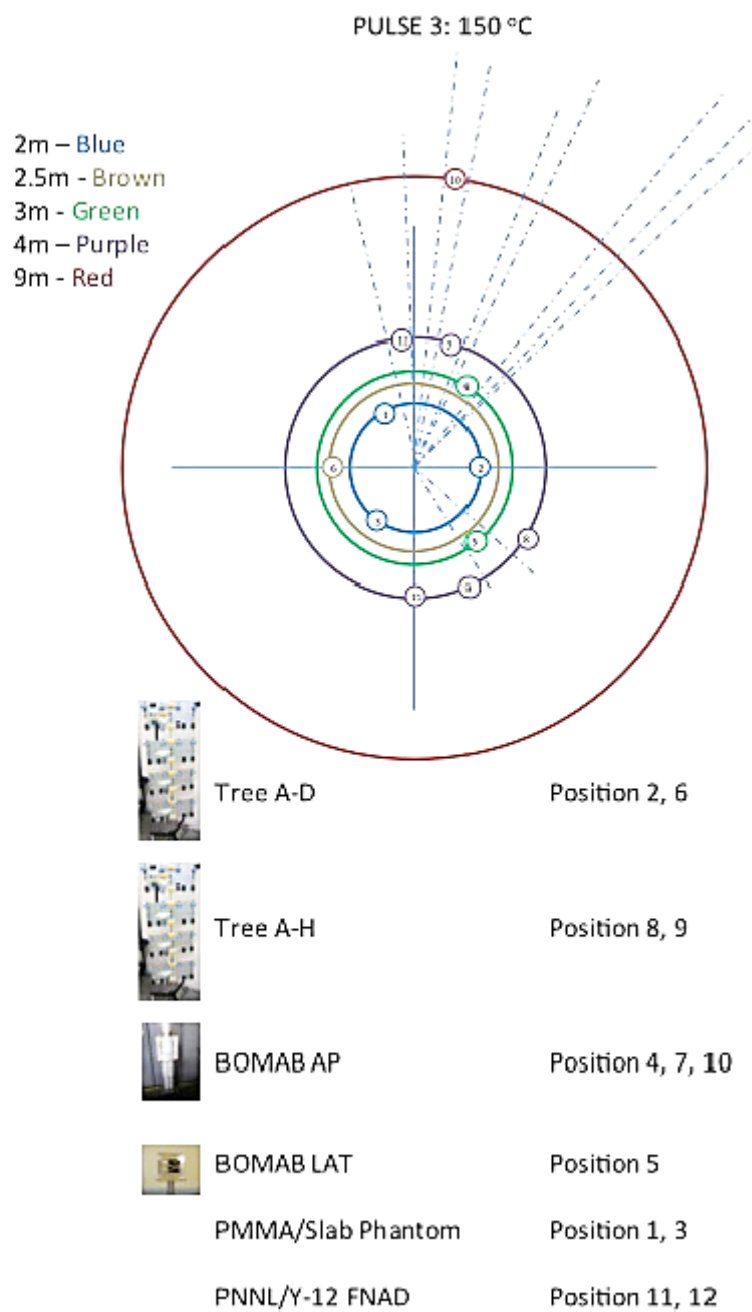
Figure C.3 Irradiation Locations for Pulse 3

Table C.1 Dosimeter Placement at Irradiation Locations for Pulses 1,2 and 3

Pulse #	Position #	distance (m)	phantom type	PNNL PNADs (InLight shell)			Hanford PNADs (flat plate assembly)			EPDs					FNADS	RadWatch Dosimeters
				front	back	total	5mil	10 mil	total	Thermo Mark 2.5	Mirion-MGP DMC3000	Mirion-MGP DMC2000	Miron-MGP DMC3000	Total		
1	1	2	Tree A-D	PNAD1, PNAD2		2			0					0		
	2	2	Tree A-D	PNAD3, PNAD4		2	PNAD61	PNAD62	2					0		
	3	2	Tree A-D			0			0					0		
	4	3	BOMAB	PNAD5	PNAD6	2			0					0		RW1, RW2
	5	3	BOMAB	PNAD7	PNAD8	2			0					0		
	6	2.5	Tree A-D	PNADs 9, 10, 11, 12		4			0					0		
	7	4	PMMA	PNAD13		1			0					0		
	8	4	Tree A-H	PNAD15, PNAD16		2			0					0		
	9	4	PMMA		PNAD 14	1			0					0		
	10	9	Tree A-H			0			0	EPD1	EPD2	EPD3	EPD4	4		
	11	4	FNAD			0			0					0	FNAD71	
	12	4	FNAD			0			0					0		
						16			2					4	1	2
2	1	2	Tree A-D	PNAD17, PNAD18		2			0	EPD5	EPD6			2		
	2	2	Tree A-D			0	PNAD63	PNAD64	2			EPD7		1		
	3	2	Tree A-D	PNAD19, PNAD20		2			0					0		
	4	3	BOMAB	PNAD21	PNAD22	2			0					0		RW3, RW4
	5	3	BOMAB	PNAD23	PNAD24	2			0					0		
	6	2.5	Tree A-D	PNAD27, PNAD28		2			0					0		
	7	4	PMMA	PNAD25		1			0					0		
	8	4	Tree A-H	PNAD29,30	PNAD31, PNAD32	4			0					3		
	9	4	PMMA		PNAD26	1			0					0		
	10	9	SSS-AWE			0			0					0		
	11	4	FNAD			0			0					0	FNAD72	
	12	4	FNAD			0			0					0		
						16			2					6	1	2
3	1	2	PMMA		PNAD44	1			0					0		
	2	2	Tree A-D			0	PNAD65	PNAD66	2					0		
	3	2	PMMA	PNAD45		1			0					0		
	4	3	BOMAB	PNAD34	PNAD35	2			0					0		
	5	3	BOMAB - LAT	PNAD36	PNAD37	2			0					0		
	6	2.5	Tree A-D	PNAD33	PNAD42	2			0					0		
	7	4	BOMAB	PNAD38	PNAD39	2			0					0		RW5, RW6
	8	4	Tree A-H			0			0	EPD8	EPD9	EPD10		3		
	9	4	Tree A-H	PNAD43	PNAD46	2			0					0		
	10	9	BOMAB	PNAD41	PNAD40	2			0					0		
	11	4	FNAD			0			0					0	FNAD73	
	12	4	FNAD			0			0					0		
						14			2					3	1	2
					Exercise Total	46		Exercise Total	6				Exercise Totals	13	3	6

Appendix D

Preliminary Reference Dose Information for Godiva-IV Exercise

Table D.1.1 Pulse 1 Reference Fluence and Dose Values by Location

Pulse 1								
Burst Temperature (°C) :		68.5						
Burst Date/Time:		5/24/2016 10:11						

TOTAL NEUTRON DOSES								
Distance (m)	Position	Total Fluence (n/cm^2)	Tiss. KERMA Dose (Gy)	ANSI 13.3 Dp(10) (Gy)	ANSI 13.3 D*(10) (Gy)	Auxier et. al. Element 57 (Gy)	IAEA 211 (Gy)	NCRP 38 (Gy)
2	1	1.01E+11	1.60	2.14	2.06	2.04	1.98	2.08
2	2	9.59E+10	1.53	2.05	1.98	1.96	1.89	1.99
2	3	1.01E+11	1.59	2.13	2.05	2.03	1.97	2.07
2.5	6	8.58E+10	1.17	1.59	1.53	1.53	1.47	1.56
3	4	6.55E+10	0.90	1.23	1.19	1.19	1.14	1.21
3	5	6.77E+10	0.92	1.26	1.21	1.21	1.17	1.24
4	7	5.10E+10	0.64	0.89	0.86	0.86	0.83	0.88
4	8	5.33E+10	0.66	0.92	0.88	0.89	0.86	0.91
4	9	5.46E+10	0.66	0.92	0.89	0.90	0.86	0.92
9	10	2.86E+10	0.13	0.39	0.38	0.38	0.38	0.40
4	11	5.30E+10	0.65	0.91	0.88	0.88	0.85	0.90

Position 11 fluence, tissue KERMA and dose values estimated from average of Positions 7,8 and 9.

Table D.1.2 Pulse 1 Reference Fluence Values by Distance

	68.5 °C Average Fluence (1.6E-9 to 14 MeV)		
Distance (m)	Total Fluence (n/cm^2)	+/- 1s (%)	Comments
2	9.93E+10	2.78%	@ 156 - 197 cm height to top of 30.5 cm plate(s)
2.5	8.58E+10	NA	@ 169 - 220 cm height to top of plate(s)
3	6.66E+10	2.40%	@ 169 - 220 cm height to top of plate(s)
4	5.30E+10	3.49%	@ 178 - 234 cm height to top of plate(s)
9	2.86E+10	NA	alcove

TableD.1.3 Pulse 1 Reference Tissue Kerma and Gamma Dose Values by Distance

	68.5 °C Average Tissue KERMA Doses (1.6E-9 to 14 MeV)					
Distance (m)	Neutron KERMA (Gy)	+/- 1s (%)	Gamma Dose (Gy)	+/- 1s (%)	Total Dose (Gy)	Comments
2	1.57	2.23%	0.22	19%	1.79	@ 156 - 197 cm height to top of 30.5 cm plate(s)
2.5	1.17	NA	0.17	29%	1.34	@ 169 - 220 cm height to top of plate(s)
3	0.91	1.20%	0.14	43%	1.05	@ 169 - 220 cm height to top of plate(s)
4	0.66	1.62%	0.11	74%	0.77	@ 178 - 234 cm height to top of plate(s)
9	0.13	NA	0.02	NA	0.15	alcove
Gamma dose for 9m distance was estimated from the 4 meter dose using inverse square law.						

65 of 147

Table D.2.1 Pulse 2 Reference Fluence and Dose Values by Location

Pulse 2								
Burst Temperature (°C) :	**244.8**							
Burst Date/Time:	**5/25/2016 9:42**							

TOTAL NEUTRON DOSES								
Distance (m)	Position	Total Fluence (n/cm^2)	Tiss. KERMA Dose (Gy)	ANSI 13.3 Dp(10) (Gy)	ANSI 13.3 D*(10) (Gy)	Auxier et. al. Element 57 (Gy)	IAEA 211 (Gy)	NCRP 38 (Gy)
2	1	3.60E+11	5.70	7.64	7.37	7.29	7.06	7.43
2	2	3.43E+11	5.47	7.32	7.07	6.99	6.77	7.12
2	3	3.60E+11	5.68	7.61	7.34	7.26	7.03	7.40
2.5	6	3.07E+11	4.17	5.70	5.48	5.47	5.26	5.59
3	4	2.34E+11	3.23	4.41	4.24	4.24	4.09	4.33
3	5	2.42E+11	3.29	4.50	4.32	4.32	4.17	4.42
4	7	1.82E+11	2.30	3.19	3.06	3.09	2.97	3.16
4	8	1.91E+11	2.37	3.29	3.16	3.18	3.06	3.26
4	9	1.95E+11	2.37	3.30	3.17	3.20	3.07	3.28
9	10	1.02E+11	0.45	1.41	1.35	1.37	1.35	1.42
4	11	1.89E+11	2.35	3.26	3.13	3.16	3.03	3.23

Position 11 fluence, tissue KERMA and dose values estimated from average of Positions 7,8 and 9.

Table D.2.2 Pulse 2 Reference Fluence Values by Distance

244.8 °C Average Fluence (1.6E-9 to 14 MeV)			
Distance (m)	Total Fluence (n/cm^2)	+/- 1s (%)	Comments
2	3.54E+11	2.78%	@ 156 - 197 cm height to top of 30.5 cm plate(s)
2.5	3.07E+11	NA	@ 169 - 220 cm height to top of plate(s)
3	2.38E+11	2.40%	@ 169 - 220 cm height to top of plate(s)
4	1.89E+11	4.21%	@ 178 - 234 cm height to top of plate(s)
9	1.02E+11	5.50%	alcove

Table D.2.3 Pulse 2 Reference Tissue Kerma and Gamma Dose Values by Distance

244.8 °C Average Tissue KERMA Doses (1.6E-9 to 14 MeV)					
Distance (m)	Neutron KERMA (Gy)	+/- 1s (%)	Gamma Dose (Gy)	+/- 1s (%)	Total Dose (Gy)	Comments
2	5.62	2.23%	0.78	19%	6.40	@ 156 - 197 cm height to top of 30.5 cm plate(s)
2.5	4.17	NA	0.61	29%	4.78	@ 169 - 220 cm height to top of plate(s)
3	3.26	1.20%	0.50	43%	3.76	@ 169 - 220 cm height to top of plate(s)
4	2.35	1.62%	0.40	74%	2.75	@ 178 - 234 cm height to top of plate(s)
9	0.45	NA	0.08	NA	0.53	alcove
Gamma dose for 9m distance was estimated from the 4 meter dose using inverse square law.						

Table D.3.1 Pulse 3 Reference Fluence and Dose Values by Location

Pulse 3								
Burst Temperature (°C) :	**147.7**							
Burst Date/Time:	**5/26/2016 11:35**							
TOTAL NEUTRON DOSES								
Distance (m)	Position	Total Fluence (n/cm^2)	Tiss. KERMA Dose (Gy)	ANSI 13.3 Dp(10) (Gy)	ANSI 13.3 D*(10) (Gy)	Auxier et. al. Element 57 (Gy)	IAEA 211 (Gy)	NCRP 38 (Gy)
2	1	2.17E+11	3.44	4.61	4.45	4.40	4.26	4.48
2	2	2.07E+11	3.30	4.42	4.27	4.22	4.08	4.30
2	3	2.17E+11	3.43	4.59	4.43	4.38	4.24	4.47
2.5	6	1.85E+11	2.52	3.44	3.30	3.30	3.18	3.37
3	4	1.41E+11	1.95	2.66	2.56	2.56	2.47	2.61
3	5	1.46E+11	1.98	2.71	2.61	2.61	2.51	2.67
4	7	1.10E+11	1.39	1.92	1.85	1.86	1.79	1.91
4	8	1.15E+11	1.43	1.99	1.90	1.92	1.84	1.97
4	9	1.18E+11	1.43	1.99	1.91	1.93	1.85	1.98
9	10	6.17E+10	0.27	0.850	0.810	0.83	0.810	0.860
4	11	1.14E+11	1.42	1.97	1.89	1.90	1.83	1.95

Position 11 fluence, tissue KERMA and dose values estimated from average of Positions 7,8 and 9.

Table D.3.2 Pulse 3 Reference Fluence Values by Distance

	147.7 °C Average Fluence (1.6E-9 to 14 MeV)		
Distance (m)	Total Fluence (n/cm2)	+/- 1s (%)	Comments
2	2.14E+11	2.78%	@ 156 - 197 cm height to top of 30.5 cm plate(s)
2.5	1.85E+11	NA	@ 169 - 220 cm height to top of plate(s)
3	1.44E+11	2.40%	@ 169 - 220 cm height to top of plate(s)
4	1.14E+11	3.49%	@ 178 - 234 cm height to top of plate(s)
9	6.17E+10	5.50%	alcove

Table D.3.3 Pulse 3 Reference Tissue Kerma and Gamma Dose Values by Distance

	147.7 °C Average Tissue KERMA Doses (1.6E-9 to 14 MeV)					
Distance (m)	Neutron KERMA (Gy)	+/- 1s (%)	Gamma Dose (Gy)	+/- 1s (%)	Total Dose (Gy)	Comments
2	3.39	2.23%	0.47	19%	3.86	@ 156 - 197 cm height to top of 30.5 cm plate(s)
2.5	2.52	NA	0.37	29%	2.89	@ 169 - 220 cm height to top of plate(s)
3	1.97	1.20%	0.30	43%	2.27	@ 169 - 220 cm height to top of plate(s)
4	1.42	1.62%	0.24	74%	1.66	@ 178 - 234 cm height to top of plate(s)
9	0.27	NA	0.05	NA	0.32	alcove
Gamma dose for 9m distance was estimated from the 4 meter dose using inverse square law.						

Appendix E

Counting Efficiencies and Backgrounds for iSolo, Pancake GM and NaI Detectors

Table E.1 Sample Counting Efficiencies

Foil Type	Sample Configuration	Instrument	70 mg/cm² aluminum absorber?	Sample form	form/ detector	Sample Counting Efficiency (c/d)
sulfur	crushed under mylar	iSolo	N	1crush	1crush_isolo	0.3790
sulfur	sealed bag	GM #1	N	1pk	1pk_gm1	0.1247
sulfur	sealed bag	GM #2	N	1pk	1pk_gm2	0.1074
sulfur	sealed bag	iSolo	N	1pk	1pk_isolo	0.1438
sulfur	sealed bag under Al	iSolo	Y	1pk	1pk_isolo_al	0.0541
sulfur	sealed bag	GM #1	N	6pk	6pk_gm1	0.1130
sulfur	sealed bag	GM #2	N	6pk	6pk_gm2	0.0974
sulfur	sealed bag	iSolo	N	6pk	6pk_isolo	0.1379
sulfur	sealed bag under Al	iSolo	Y	6pk	6pk_isolo_al	0.0537
sulfur	sealed bag	GM #1	N	7pk	7pk_gm1	0.1168
sulfur	sealed bag	GM #2	N	7pk	7pk_gm2	0.1006
sulfur	sealed bag	iSolo	N	7pk	7pk_isolo	0.1337
sulfur	sealed bag under Al	iSolo	Y	7pk	7pk_isolo_al	0.0522
copper	between aluminum plates	NaI #1		Cu disk	Cu_Na1	0.0194
copper	between aluminum plates	NaI #2		Cu disk	Cu_Na2	0.0285
	Original NaI # 1 efficiency measured at PNNL					0.0139
	Original NaI # 2 efficiency measured at PNNL					0.0122
Cu foils exposed at Godiva : NaI #1 Cu-64 activity per unit fluence / HPGe Cu-64 activity per unit fluence						1.40
Cu foils exposed at Godiva : NaI #2 Cu-64 activity per unit fluence / HPGe Cu-64 activity per unit fluence						2.34
	Corrected NaI #1 efficiency for use in Exercise					0.0194
	Corrected NaI #2 efficiency for use in Exercise					0.0285

Table E.2 Detector Background Count Rates Observed During Exercise

Detector	Start Date	Start Time	Count duration (min)	Counts	CPM
iSolo	5/24/2016	am	30	453	15.10
	5/25/2016	am	30	466	15.53
	5/26/2016	am	30	480	16.00
				mean	15.54
				stdev.s	0.45
				C.V.	0.03
GM #1	5/24/2016	am	10	235	23.50
	5/24/2016	18:32	10	264	26.40
	5/24/2016	pm	10	262	26.20
	5/25/2016	am	10	230	23.00
	5/25/2016	pm	10	255	25.50
	5/26/2016	am	10	238	23.80
	5/26/2016	pm	10	233	23.30
				mean	24.53
				stdev.s	1.45
				C.V.	0.06
GM #2	5/24/2016	am	10	208	20.80
	5/24/2016	18:32	10	221	22.10
	5/24/2016	pm	10	204	20.40
	5/25/2016	am	10	200	20.00
	5/25/2016	pm	10	208	20.80
	5/26/2016	am	10	204	20.40
	5/26/2016	pm	10	184	18.40
				mean	20.41
				stdev.s	1.11
				C.V.	0.05
NaI #1	5/24/2016	am	10	87	8.70
	5/25/2016	am	10	80	8.00
	5/26/2016	am	10	90	9.00
	5/26/2016	pm	10	84	8.40
				mean	8.53
				stdev.s	0.43
				C.V.	0.05
NaI #2	5/24/2016	am	10	130	13.00
	5/25/2016	am	10	140	14.00
	5/26/2016	am	10	142	14.20
	5/26/2016	pm	10	136	13.60
				mean	13.70
				stdev.s	0.53
				C.V.	0.04

Appendix F

Re-Calibration of NaI Detectors for ^{64}Cu Measurements Using Exercise Data

Re-Calibration of NaI Detectors for ^{64}Cu Measurements Using Exercise Data

For the purpose of counting copper foils for ^{64}Cu, the foils were sandwiched between two aluminum plates, 2.54 cm x 1.91 cm x 0.076 cm (1" x 0.75" x 0.030") to ensure complete annihilation of all positrons in close proximity to the foil. The foil-plate assemblies were counted in contact with, and centered on the end of a NaI probe coupled to a Ludlum 2200 scaler with threshold set to reject Compton events less than approximately 300 keV.   For each detector, the counting efficiency for this geometry was initially established at PNNL by counting of an irradiated copper foil with a 130% HPGe detector to determine ^{64}Cu activity. The same foil was then counted on contact with the NaI detectors. The HPGe assayed ^{64}Cu activity on the foil was used to determine counting efficiency for NaI #1, expressed as counts per disintegration and as counts per emitted 511 keV photon.   For both NaI #1 and #2, the 511 keV photon counting efficiency was also estimated independently, using a ^{22}Na button source counted in contact with the detector. The ^{64}Cu efficiency for NaI #2 was estimated from its 511 keV photon counting efficiency relative to NaI #1 which had known ^{64}Cu counting efficiency.

The detector efficiencies established at PNNL were used to make the initial calculations of ^{64}Cu activities on foils irradiated by Godiva-IV during the exercise. Upon review of the activity data, it became apparent that there were two distinct populations of ^{64}Cu activities, one from foils counted on NaI #1 and the other from foils counted on NaI #2. When foils that were exposed to the same energy spectrum (i.e. foils exposed at the 2 meter distance in air) had their activity results expressed as specific activity per unit fluence, A_o / Φ_{tot} (cm^2 g^{-1} min^{-1}), the mean result for NaI #2 (1.05E-06 ± 4%) was 1.58 times the mean result for NaI #1 (6.68E-07 ± 6%). The same ratio was obtained for foils exposed in air at the 4 meter distance. It was concluded that the original detector efficiencies were invalid either because of errors during the original calibration and/or because one or both instruments had drift in gain or threshold settings.

Fortunately, a subset of six copper foils exposed in air during the exercise were counted on both an HPGe system and a NaI system which made a cross comparison of HPGe activity measurement and NaI measurement on each foil possible. The comparison confirmed that the initially determined NaI efficiencies were not valid. As a result, counting efficiencies for both NaI detectors were revised using the HPGe ^{64}Cu activity data generated on the subset of copper foils that had been analyzed on both systems. The initial and revised efficiencies are shown in **Table E.1**. The cross comparison of initial NaI results with HPGe results is shown in **Table F1**.

The counting efficiencies for the two Ortec microDetective DX detectors and Canberra Falcon 5000 detector used to count the copper foils at the exercise were determined at PNNL prior to the exercise for a 1.27 cm diameter thin disk sample centered on contact with the detector housing, using a calibration source of the same dimensions. The calibration source was prepared at PNNL by uniformly depositing a liquid activity standard on a paper disk 1.27 cm in diameter .

To help validate the revised counting efficiencies assigned to NaI #1 and NaI #2, calculations were run for a 1" x 1" NaI detector using the MCNP-SuperSynth detector response modeling program developed at PNNL. The results are shown in **Figure F.1**. The revised NaI counting efficiency for NaI #1 (0.0194 counts per disintegration) is consistent with modeling results for a 1 x 1 inch NaI coupled to a Ludlum 2200 scaler with its pulse height counting threshold set at approximately 300 keV. The revised NaI counting efficiency for NaI #2 (0.0285 counts per disintegration) is consistent with modeling results for a

1 x 1.125 inch NaI and scaler with its pulse height counting threshold set at approximately 200 keV (**Figure F.2**). If the number of counts > 20 keV is taken as a first approximation for the "total counts" without threshold, then the peak-to-total ratio for the 1 x 1 inch NaI can be inferred from the SuperSynth model as approximately 37%, which is consistent with the general figure of approximately 35% for 511 keV photons interacting with a 1 x 1 NaI as interpolated from the graph in **Figure F.3** (from Knoll, 1979).

Table F.1 Calibration of NaI efficiency against HPGe Results

Dosimeter #	Uncorrected ^{64}Cu Activity		
	HPGe A_o (dpm/g)	NaI 1 A_o (dpm/g)	NaI 2 A_o (dpm/g)
65	109589	151635	
66	102135		241437
63	177987	250998	
64	168683		382094
10	44464		108757
12	47942		109606

Location	Geometry	Distance (m)	Height above floor (cm)	Given $D_p(10)_n$ (rad)
2	tree	2.0	181.8	437
2	tree	2.0	181.8	437
2	tree	2.0	189.4	724
2	tree	2.0	189.4	724
6	tree	2.5	146	156
6	tree	2.5	146	156

Given Fluence n/cm^2	Uncorrected ^{64}Cu Activity per unit fluence			Relative Response Data		
	HPGe A_o/ϕ_{tot} (cm^2 g^{-1} m^{-1})	NaI 1 A_o/ϕ_{tot} (cm^2 g^{-1} m^{-1})	NaI 2 A_o/ϕ_{tot} (cm^2 g^{-1} m^{-1})	Na1 / HPGe	Na2 / HPGe	(NaI2 / HPGe) / (NaI1 / HPGe)
2.14E+11	5.12E-07	7.09E-07		1.38		
2.14E+11	4.77E-07		1.13E-06		2.36	
3.53E+11	5.04E-07	7.11E-07		1.41		
3.53E+11	4.78E-07		1.08E-06		2.27	
8.76E+10	5.08E-07		1.24E-06		2.45	
8.76E+10	5.47E-07		1.25E-06		2.29	
mean	5.04E-07	7.10E-07	1.18E-06	1.40	2.34	1.68
stdev.s	2.59E-08	1.74E-09	8.36E-08	0.02	0.08	
C.V.	0.051	0.002	0.071	0.013	0.035	
n	6	2	4	2	4	

Hanford PNAD (5 mil)	
mean	5.08E-07
stdev.s	5.58E-09
C.V.	0.01
n	2

Hanford PNAD (10 mil)	
mean	4.78E-07
stdev.s	4.16E-10
C.V.	0.00
n	2

5 mil / 10 mil
1.06

Dosimeters 10 and 12 are PNNL PNADs. These have 10 mil foils. Dosimeter numbers 63-66 are Hanford PNADs. Dosimeters 63 and 65 have 5 mil copper foils. Dosimeters 64 and 66 have 10 mil copper foils. Thicker copper foils are expected to have less response per unit mass due to absorption self shielding of epithermal neutrons in the foil (IAEA 1982). The comparison to the right provides a measure of the impact of changing from 5 mil copper foils in the historical Hanford PNAD design to 10 mil copper foils in the new PNNL PNAD design. A similar ratio (1.08) was observed for the NaI activity results on Hanford PNADs 61-66. Because of increased mass, the thicker foils provide greater sensitivity for measuring epithermal fluence.

Figure F.1 MCNP-SuperSynth Calculation of 1" x 1" NaI Detector Response

Radius of the disk 0.635 cm (in cell H105 above, i.e., 12.7mm diameter)				
400keV to 620keV	>300 keV	>200 keV	>100 keV	>20 keV
3.80E-02 counts per gamma (cpg)	4.88E-02 counts per gamma (cpg)	6.81E-02	8.75E-02	1.03E-01
3.91E-01 gamma per disintegration (gpd)				
1.49E-02 count per disintigration (cpd)	1.91E-02	2.66E-02	3.42E-02	4.03E-02
400keV to 620keV	>300 keV	>200 keV	>100 keV	>20 keV
1.49% efficiency	1.91%	2.66%	3.42%	4.03%

For a 1inch by 1inch NaI (i.e., our 2.5cm thick by 2.5cm diameter NaI detectors)

Figure F.2 MCNP-SuperSynth Calculation of 1" x 1.125" NaI Detector Response

400 keV to 620 keV			>400 keV	>300 keV		>200 keV	>100 keV	>20 keV
4.28E-02	cpg		4.33E-02	5.39E-02		7.28E-02	9.15E-02	1.08E-01
3.91E-01	gpd							
1.67E-02	cpd		1.69E-02	2.11E-02		2.84E-02	3.58E-02	4.21E-02
400 keV to 620 keV								
1.67%	efficiency		1.69%	2.11%		2.84%	3.58%	4.21%

Cu-64 Al sandwich and NaI detector 1in x 1.125in
0.25 mm thick and 12.7mm diameter
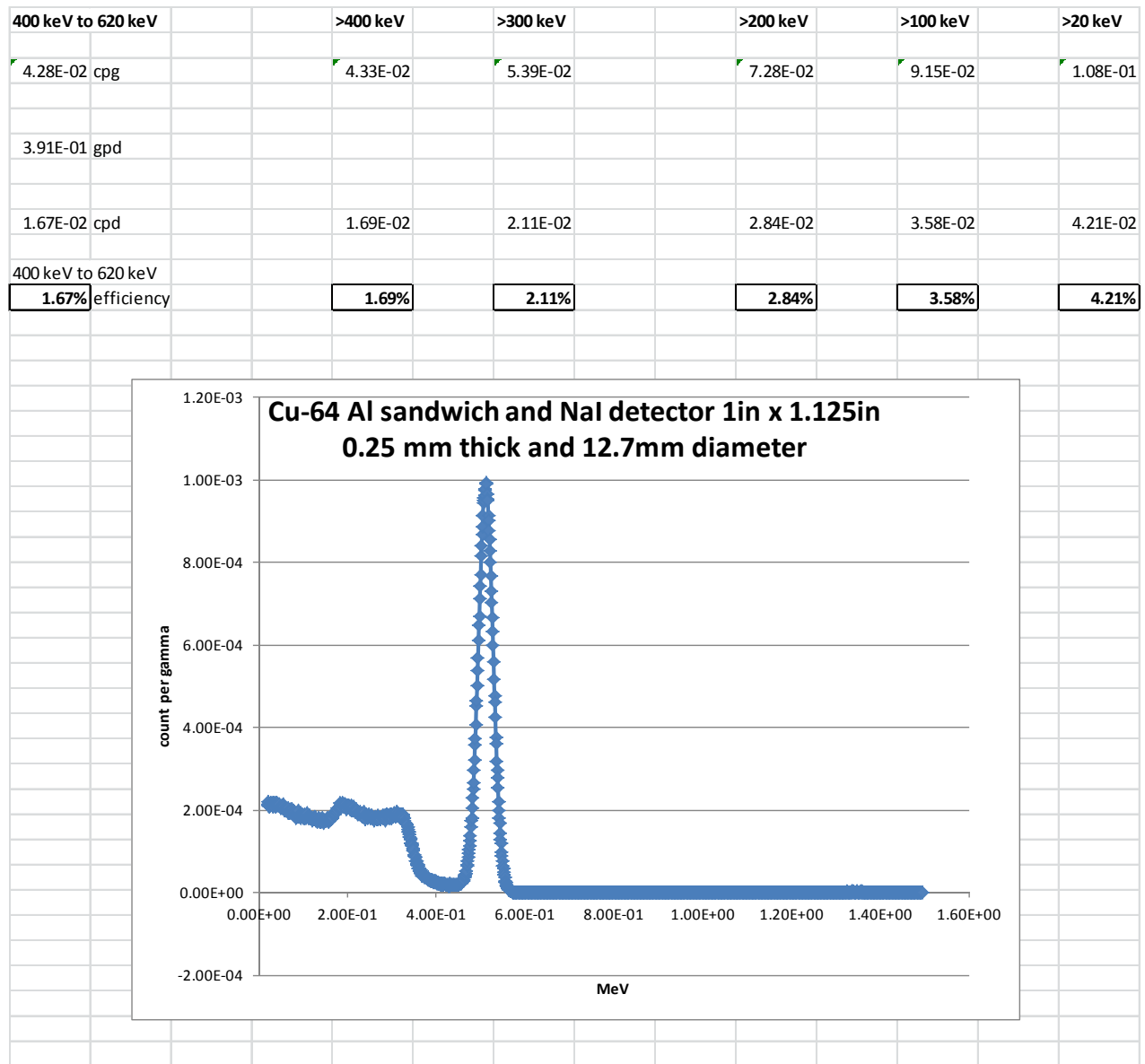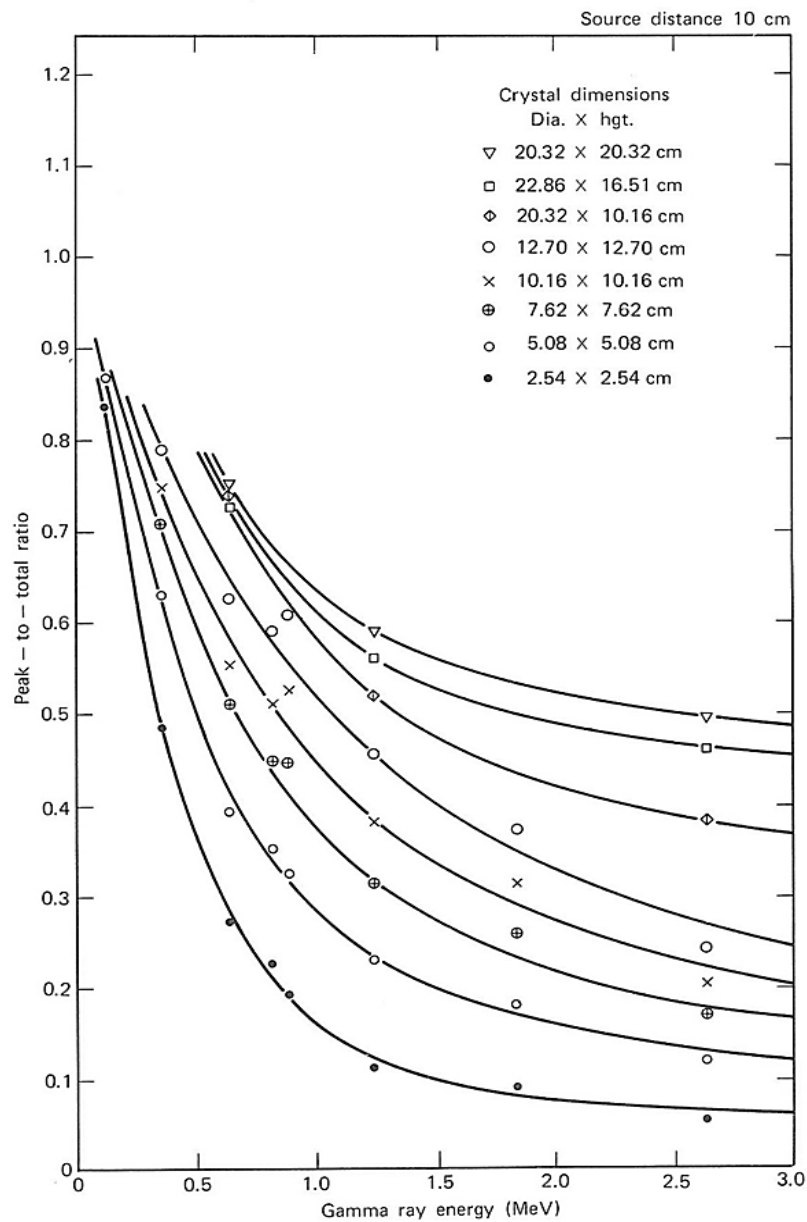
FIGURE 10-21. Peak-to-total ratio (or the "photofraction") for various solid cylinders of NaI(T1), for a point gamma ray source 10 cm from the scintillator surface. (Courtesy Harshaw Chemical Company.)

Appendix G

Activity Measurement Results for PNAD and FNAD Components

Count Rate Corrections for ^{64}Cu Measurements

The equation below was used to manually correct count rate measurements on copper foils counted with NaI detectors. The equation corrects for decay during irradiation, decay between irradiation and start of counting, and decay during counting (IAEA 1982). The same corrections were applied automatically by Genie™ 2000 software for activity measurements on copper, indium and gold foils that were counted on germanium detectors.

$$C_c = \left(\frac{C}{1-\tau C} - B_g \right) \left[\frac{\lambda t_i}{1-e^{-\lambda t_i}} \ \frac{\lambda t_c}{1-e^{-\lambda t_c}} \right] e^{\lambda t_a}$$

Where:

C_c	=	corrected count rate
C	=	observed count rate
τ	=	counter dead time
B_g	=	counter background count rate
t_i	=	irradiation time
t_a	=	time between end of irradiation and start of counting
t_c	=	count time
λ	=	decay constant for ^{64}Cu (9.0957E-04 min^{-1})

When the irradiation time and count time are much shorter than the half-life, the quantity in square brackets becomes unity. Dead time corrections were not performed on the copper foil count rate data collected in the exercise because the count rates were not large enough to warrant dead time correction. Although negligible for copper foils, the decay corrections within the square brackets *were* applied since they were already programmed into the spreadsheet application used for the exercise. This application was designed to also be used for counting NAD samples irradiated with local isotopic neutron sources such as ^{252}Cf, which typically requires relatively long (compared to product half-life) irradiation times in order to obtain readily measurable activity. Although the actual irradiation times for Pulses 1, 2 and 3 were on the order of tens of microseconds (characteristically 50 microseconds based on past exercises), the precise values were not provided to participants. Accordingly, for calculational purposes, the value for t_i was arbitrarily set equal to 1 second with no discernable effect on accuracy.

Count Rate Corrections for ^{32}P Measurements

The equation below was used to manually correct count rate measurements on sulfur pellets counted with GM or iSolo. The equation corrects for decay during irradiation, decay between irradiation and start of counting, decay during counting, and for the influence of ^{31}Si on counting results. It is based on the general equation for a single radionuclide (IAEA 1982) given on the previous page for ^{64}Cu measurements, plus the anticipated ratio of ^{31}Si and ^{32}P activities at end of irradiation, and the estimated relative counting efficiencies for ^{31}Si and ^{32}P in solid sulfur pellets.

$$C_{1o} \quad = \quad (C\, k_1\, k_2) / (R_o\, k_1 + k_2)$$

Where:

C_{1o} = theoretical net count rate at end of irradiation attributable to ^{32}P activity

C = observed net count rate at starat of sample counting

k_1 = $(\lambda_1 t_i \;\; \lambda_1 t_c \;\; e^{\lambda_1 t_a}) / (1 - e^{-\lambda_1 t_i})(1 - e^{-\lambda_1 t_c})$

k_2 = $(\lambda_2 t_i \;\; \lambda_2 t_c \;\; e^{\lambda_2 t_a}) / (1 - e^{-\lambda_2 t_i})(1 - e^{-\lambda_2 t_c})$

λ_1 = decay constant for ^{32}P   (3.3685 E-05 min^{-1})

λ_2 = decay constant for ^{31}Si   (4.4065 E-03 min^{-1})

R_o = (^{31}Si net count rate / ^{32}P net count rate) at end of irradiation (R_o = 0.432)

t_i = irradiation time (0.0167 min)

t_a = time between end of irradiation and start of counting

t_c = count time

The value for R_o used for sulfur pellet counting during the exercise (R_o = 0.432) was determined using the estimated ratio of ^{31}Si activity to ^{32}P activity at the end of irradiation, A_{2o} / A_{1o} = 0.524 and the estimated ratio of counting efficiency for ^{31}Si activity and ^{32}P activity in solid sulfur pellet packs E_2 / E_1 = 0.825. The value for ^{31}Si/^{32}P activity ratio at end of irradiation was calculated for an unmoderated Godiva-IV energy spectrum using the PNNL program SCOPER, which was developed for estimating foil activities from irradiations in well characterized radiation fields. The SCOPER program uses the same reaction rate calculation code as the STAYSL_PNNL program (Greenwood and Johnson, 2014). The value for the relative ^{31}Si/^{32}P counting efficiency is based on the estimated relative emission rate of ^{31}Si and ^{32}P beta particles from the surface of the sulfur pellet packs per disintegration. Because ^{31}Si emits essentially one 0.5957 MeV (avg.) beta particle per disintegration and ^{32}P emits exactly one 0.6947 MeV (avg.)

beta particle per disintegration, the relative emission rates for the two particles from the surface of the packet are primarily a function of the relative particle attenuation within the sulfur pellet and plastic bag wall. The relative attenuation within the packet was estimated using the computer program VARSKIN 4 (NRC 2011) using a 3D cylindrical source model. It is assumed that ^{31}Si and ^{32}P beta particles escaping from the sulfur pellet pack will be counted with nearly equal probability in the Pancake GM and iSolo PIPS detectors.

When the irradiation time and count time are much shorter than the half-life, $k_1 \approx e^{\lambda_1 t_a}$ and $k_2 \approx e^{\lambda_2 t_a}$.

By substituting a different value for R_o that is specific to the neutron energy spectrum being used, the equation above may be used for correcting count results on NAD samples irradiated with local isotopic neutron sources such as ^{252}Cf, which typically require relatively long irradiation times and count times (compared to product half-life) in order to make reliable measurements.

Although the actual irradiation times for Pulses 1, 2 and 3 were on the order of tens of microseconds (characteristically 50 microseconds based on past exercises), the precise values were not provided to participants. Accordingly, for calculational purposes, the value for t_i was arbitrarily set equal to 1 second with no discernable effect on accuracy.

Dead time corrections were not performed on the sulfur pellet gross count rate data collected during the exercise because the count rates were not large enough to warrant dead time correction.

Pulse #	Dosimeter #	form /detector	count start	count duration (min)	net counts (cts)	net countrate C (cpm)	sample mass (g)	P-32 counting efficiency (c/d)	A (dpm)	t_a (min)	t_c (min)	k_1	k_2	corrected net countrate C_{10} (cpm)	A_o (dpm)	A_o (dpm/g)
								A								
								S								
								P-32								
1	1	6pk_gm1	5/24/16 15:29	10	3965	397	2.655	0.1130	3508	318	10	1.01	4.15	363	3208	1208
1	2	6pk_gm2	5/24/16 15:29	10	3849	385	2.634	0.0974	3952	318	10	1.01	4.15	352	3615	1372
1	3	6pk_gm1	5/24/16 15:41	10	4148	415	2.608	0.1130	3669	330	10	1.01	4.38	381	3374	1294
1	4	6pk_gm2	5/24/16 15:41	10	3624	362	2.611	0.0974	3721	330	10	1.01	4.38	333	3422	1310
1	5	6pk_gm1	5/24/16 15:55	10	1954	195	2.642	0.1130	1729	344	10	1.01	4.65	181	1599	605
1	6	6pk_gm2	5/24/16 15:55	10	315	32	2.669	0.0974	323	344	10	1.01	4.65	29	299	112
1	7	6pk_gm1	5/24/16 16:08	10	2057	206	2.642	0.1130	1820	357	10	1.01	4.93	191	1692	640
1	8	6pk_gm2	5/24/16 16:08	10	316	32	2.603	0.0974	324	357	10	1.01	4.93	29	302	116
1	9	6pk_gm1	5/24/16 16:56	10	2870	287	2.643	0.1130	2539	405	10	1.01	6.09	271	2401	909
1	10	6pk_gm2	5/24/16 16:56	10	2710	271	2.635	0.0974	2783	405	10	1.01	6.09	256	2632	999
1	11	6pk_gm1	5/24/16 17:09	10	2828	283	2.627	0.1130	2502	418	10	1.01	6.45	269	2376	904
1	12	6pk_gm2	5/24/16 17:09	10	2385	239	2.591	0.0974	2449	418	10	1.01	6.45	227	2326	898
1	13	6pk_gm1	5/24/16 17:37	10	1395	140	2.640	0.1130	1234	446	10	1.02	7.30	134	1182	448
1	14	6pk_gm2	5/24/16 17:37	10	261	26	2.586	0.0974	268	446	10	1.02	7.30	25	257	99
1	15	6pk_gm1	5/24/16 18:01	10	1317	132	2.665	0.1130	1165	470	10	1.02	8.11	127	1123	421
1	16	6pk_gm2	5/24/16 18:01	10	1261	126	2.668	0.0974	1295	470	10	1.02	8.11	122	1248	468
2	17	6pk_gm1	5/25/16 14:29	10	16362	1636	2.646	0.1130	14474	287	10	1.01	3.62	1474	13044	4930
2	18	6pk_gm2	5/25/16 14:29	10	13800	1380	2.635	0.0974	14170	287	10	1.01	3.62	1244	12770	4846
2	19	6pk_gm1	5/25/16 14:49	10	17988	1799	2.649	0.1130	15913	307	10	1.01	3.95	1637	14480	5466
2	20	6pk_gm2	5/25/16 14:49	10	15900	1590	2.649	0.0974	16327	307	10	1.01	3.95	1447	14857	5609
2	21	6pk_gm1	5/25/16 15:01	10	8127	813	2.610	0.1130	7189	319	10	1.01	4.17	744	6578	2520
2	22	6pk_isolo	5/25/16 16:24	30	4357	145	2.608	0.1379	1053	402	30	1.01	6.28	138	998	383
2	23	6pk_gm1	5/25/16 15:16	10	7717	772	2.632	0.1130	6827	334	10	1.01	4.45	711	6288	2389
2	24	6pk_isolo	5/25/16 16:55	30	3972	132	2.664	0.1379	960	433	30	1.02	7.19	127	919	345
2	25	6pk_gm1	5/25/16 15:28	10	5501	550	2.628	0.1130	4866	346	10	1.01	4.70	509	4504	1714
2	26	6pk_isolo	5/25/16 17:30	30	4132	138	2.646	0.1379	999	468	30	1.02	8.39	133	965	365
2	27	6pk_gm1	5/25/16 15:41	10	11151	1115	2.643	0.1130	9864	359	10	1.01	4.97	1038	9178	3473
2	28	6pk_gm2	5/25/16 15:41	10	9800	980	2.630	0.0974	10063	359	10	1.01	4.97	912	9363	3560
2	29	6pk_gm1	5/25/16 15:54	10	4979	498	2.597	0.1130	4405	372	10	1.01	5.27	466	4118	1586
2	30	6pk_gm2	5/25/16 15:54	10	4230	423	2.568	0.0974	4344	372	10	1.01	5.27	396	4061	1581
2	31	6pk_gm1	5/25/16 16:07	10	4772	477	2.608	0.1130	4221	385	10	1.01	5.58	448	3966	1521
2	32	6pk_gm2	5/25/16 16:07	10	4079	408	2.622	0.0974	4189	385	10	1.01	5.58	383	3935	1501
3	33	6pk_gm1	5/26/16 15:48	10	7196	720	2.637	0.1130	6366	253	10	1.01	3.12	637	5633	2136
3	34	6pk_gm1	5/26/16 20:39	10	4545	455	2.639	0.1130	4021	544	10	1.02	11.24	446	3941	1493
3	35	6pk_isolo	5/26/16 20:02	30	2289	76	2.675	0.1379	553	507	30	1.02	9.97	74	539	202
3	36	6pk_isolo	5/26/16 20:34	30	2247	75	2.571	0.1379	543	539	30	1.02	11.48	73	533	207
3	37	6pk_gm1	5/26/16 16:15	10	4468	447	2.663	0.1130	3953	280	10	1.01	3.51	401	3549	1333
3	38	6pk_gm1	5/26/16 21:08	10	3015	302	2.578	0.1130	2667	573	10	1.02	12.77	297	2629	1020
3	39	6pk_isolo	5/26/16 21:06	30	1854	62	2.651	0.1379	448	571	30	1.02	13.22	61	442	167
3	40	6pk_isolo	5/26/16 17:50	30	278	9	2.649	0.1379	67	375	30	1.01	5.57	9	63	24
3	41	6pk_isolo	5/26/16 21:40	30	1906	64	2.617	0.1379	461	605	30	1.02	15.35	63	457	175
3	42	6pk_gm1	5/26/16 21:21	10	6626	663	2.650	0.1130	5862	586	10	1.02	13.52	655	5790	2185
3	43	6pk_gm1	5/26/16 16:51	10	2637	264	2.669	0.1130	2333	316	10	1.01	4.11	241	2132	799
3	44	6pk_isolo	5/26/16 22:14	30	5281	176	2.681	0.1379	1277	639	30	1.02	17.83	176	1273	475
3	45	6pk_gm1	5/26/16 17:07	10	10191	1019	2.628	0.1130	9015	332	10	1.01	4.41	938	8296	3157
3	46	6pk_gm1	5/26/16 22:06	10	2431	243	2.607	0.1130	2151	631	10	1.02	16.48	242	2140	821
1	61	1pk_isolo	5/24/16 14:52	30	2729	91	0.426	0.1438	633	281	30	1.01	3.68	82	571	1341
1	62	1pk_isolo	5/24/16 15:24	30	2600	87	0.433	0.1438	603	313	30	1.01	4.24	79	552	1276
2	63	1pk_isolo	5/25/16 14:40	30	9510	317	0.430	0.1438	2204	298	30	1.01	3.97	289	2007	4666
2	64	1pk_isolo	5/25/16 15:12	30	9551	318	0.416	0.1438	2214	330	30	1.01	4.57	294	2044	4913
3	65	1pk_isolo	5/26/16 15:58	30	5733	191	0.456	0.1438	1329	263	30	1.01	3.40	171	1189	2607
3	66	1pk_isolo	5/26/16 16:31	30	5630	188	0.432	0.1438	1305	296	30	1.01	3.93	171	1187	2747
1	71	7pk_gm1	5/24/16 18:16	10	1480	148	3.046	0.1168	1267	485	10	1.02	8.66	143	1226	402
2	72	7pk_isolo	5/25/16 15:44	30	19628	654	3.083	0.1337	4894	362	30	1.01	5.26	612	4575	1484
3	73	7pk_isolo	5/26/16 17:09	30.5	11708	384	3.070	0.1337	2871	335	31	1.01	4.67	355	2656	865

Table G.2 ^{64}Cu Specific Activity in Copper Foils

								B											
								Cu (Cd)											
								Cu-64											
Pulse #	Dosimeter #	form /detector	count start	count duration (min)	net counts (cts)	net countrate (cpm)	sample mass (g)	Counting Efficiency (c/d)	A (dpm)	λ (min-1)	t_a (min)	t_c (min)	t_i (min)	countrate corrected to end of burst (cpm)	A_o (dpm)	A_o (dpm/g)	HPGe A_o (dpm)	HPGe A_o (dpm/g)	HPGe Detector
1	1	cu_na1	5/24/16 16:25	10	1780	178	0.281	0.0194	9178	9.09E-04	374	10	0.0167	251	12955	46104			
1	2	cu_na2	5/24/16 16:20	10	2572	257	0.281	0.0285	9026	9.09E-04	369	10	0.0167	361	12682	45132			
1	3	cu_na1	5/24/16 17:00	10	1678	168	0.281	0.0194	8652	9.09E-04	409	10	0.0167	245	12608	44868			
1	4	cu_na2	5/24/16 17:00	10	2325	233	0.281	0.0285	8159	9.09E-04	409	10	0.0167	339	11889	42309			
1	5	cu_na1	5/24/16 17:34	10	1606	161	0.281	0.0194	8281	9.09E-04	443	10	0.0167	241	12446	44291			
1	6	cu_na2	5/24/16 17:32	10	1132	113	0.281	0.0285	3972	9.09E-04	441	10	0.0167	170	5959	21208			
1	7	cu_na1	5/24/16 17:50	10	1607	161	0.282	0.0194	8286	9.09E-04	459	10	0.0167	245	12636	44809			
1	8	cu_na2	5/24/16 17:47	10	1144	114	0.282	0.0285	4015	9.09E-04	456	10	0.0167	174	6105	21650			
1	9	cu_na1	5/24/16 18:05	10	1573	157	0.281	0.0194	8111	9.09E-04	474	10	0.0167	243	12539	44621			
1	10	cu_na2	5/24/16 18:01	10	2417	242	0.281	0.0285	8482	9.09E-04	470	10	0.0167	372	13064	46492	12494	44464	dx1
1	11	cu_na1	5/24/16 18:18	10	1623	162	0.281	0.0194	8369	9.09E-04	487	10	0.0167	254	13091	46587			
1	12	cu_na2	5/24/16 18:13	10	2418	242	0.282	0.0285	8485	9.09E-04	482	10	0.0167	377	13213	46855	13520	47942	dx2
1	13	cu_na1	5/24/16 18:23	10	1268	127	0.282	0.0194	6538	9.09E-04	492	10	0.0167	199	10274	36434			
1	14	cu_na2	5/24/16 18:24	10	1239	124	0.281	0.0285	4348	9.09E-04	493	10	0.0167	195	6839	24336			
1	15	cu_na1	5/24/16 18:40	10	1156	116	0.281	0.0194	5961	9.09E-04	509	10	0.0167	184	9513	33853			
1	16	cu_na2	5/24/16 18:38	10	1609	161	0.282	0.0285	5646	9.09E-04	507	10	0.0167	256	8994	31895			
2	17	cu_na1	5/25/16 16:47	10	6947	695	0.281	0.0194	35822	9.09E-04	425	10	0.0167	1027	52962	188478			
2	18	cu_na2	5/25/16 16:47	10	9256	926	0.281	0.0285	32481	9.09E-04	425	10	0.0167	1369	48024	170904			
2	19	cu_na1	5/25/16 16:59	10	6355	636	0.282	0.0194	32769	9.09E-04	437	10	0.0167	950	48981	173690			
2	20	cu_na2	5/25/16 16:59	10	8835	884	0.281	0.0285	31004	9.09E-04	437	10	0.0167	1321	46343	164921			
2	21	cu_na1	5/25/16 17:15	10	6113	611	0.281	0.0194	31521	9.09E-04	453	10	0.0167	927	47806	170128			
2	22	cu_na2	5/25/16 17:15	10	3857	386	0.280	0.0285	13535	9.09E-04	453	10	0.0167	585	20528	73314			
2	23	cu_na1	5/25/16 17:27	10	6342	634	0.282	0.0194	32702	9.09E-04	465	10	0.0167	972	50141	177805			
2	24	cu_na2	5/25/16 17:27	10	4405	441	0.281	0.0285	15458	9.09E-04	465	10	0.0167	675	23702	84348			
2	25	cu_na1	5/25/16 17:38	10	5237	524	0.282	0.0194	27004	9.09E-04	476	10	0.0167	811	41821	148301			
2	26	cu_na2	5/25/16 17:38	10	4796	480	0.281	0.0285	16830	9.09E-04	476	10	0.0167	743	26065	92758			
2	27	cu_na1	5/25/16 17:50	10	6399	640	0.281	0.0194	32996	9.09E-04	488	10	0.0167	1002	51661	183847			
2	28	cu_na2	5/25/16 17:50	10	9083	908	0.281	0.0285	31874	9.09E-04	488	10	0.0167	1422	49905	177599			
2	29	cu_na1	5/25/16 18:01	10	4548	455	0.281	0.0194	23451	9.09E-04	499	10	0.0167	719	37087	131980			
2	30	cu_na2	5/25/16 18:01	10	6088	609	0.281	0.0285	21364	9.09E-04	499	10	0.0167	963	33786	120235			
2	31	cu_na1	5/25/16 18:15	10	4425	443	0.281	0.0194	22817	9.09E-04	513	10	0.0167	709	36546	130056			
2	32	cu_na2	5/25/16 18:15	10	6061	606	0.281	0.0285	21269	9.09E-04	513	10	0.0167	971	34067	121235			
3	33	cu_na1	5/26/16 16:18	10	4370	437	0.281	0.0194	22533	9.09E-04	283	10	0.0167	568	29280	104199			
3	34	cu_na2	5/26/16 16:18	10	6005	601	0.281	0.0285	21073	9.09E-04	283	10	0.0167	780	27382	97445			
3	35	cu_na1	5/26/16 16:30	10	2002	200	0.281	0.0194	10323	9.09E-04	295	10	0.0167	263	13561	48260			
3	36	cu_na2	5/26/16 16:30	10	2979	298	0.281	0.0285	10454	9.09E-04	295	10	0.0167	391	13733	48872			
3	37	cu_na1	5/26/16 16:42	10	4154	415	0.282	0.0194	21420	9.09E-04	307	10	0.0167	552	28447	100875			
3	38	cu_na2	5/26/16 16:42	10	4895	490	0.282	0.0285	17178	9.09E-04	307	10	0.0167	650	22813	80897			
3	39	cu_na1	5/26/16 17:04	10	1555	156	0.280	0.0194	8018	9.09E-04	329	10	0.0167	211	10864	38800			
3	40	cu_na2	5/26/16 17:04	10	190	19	0.280	0.0285	667	9.09E-04	329	10	0.0167	26	903	3226			
3	41	cu_na1	5/26/16 17:16	10	547	55	0.281	0.0194	2821	9.09E-04	341	10	0.0167	75	3864	13749			
3	42	cu_na2	5/26/16 17:16	10	6458	646	0.281	0.0285	22663	9.09E-04	341	10	0.0167	885	31043	110472			
3	43	cu_na1	5/26/16 17:27	10	3155	316	0.280	0.0194	16268	9.09E-04	352	10	0.0167	437	22508	80386			
3	44	cu_na2	5/26/16 17:27	10	4205	421	0.281	0.0285	14756	9.09E-04	352	10	0.0167	582	20416	72655			
3	45	cu_na1	5/26/16 17:49	10	6153	615	0.281	0.0194	31727	9.09E-04	374	10	0.0167	868	44783	159370			
3	46	cu_na2	5/26/16 17:49	10	4369	437	0.282	0.0285	15332	9.09E-04	374	10	0.0167	617	21641	76741			
1	61	cu_na1	5/24/16 18:55	10	812	81	0.150	0.0194	4187	9.09E-04	524	10	0.0167	131	6774	45158			
1	62	cu_na2	5/24/16 18:50	10	2124	212	0.281	0.0285	7454	9.09E-04	519	10	0.0167	342	12004	42718			
2	63	cu_na1	5/25/16 18:28	10	3420	342	0.159	0.0194	17635	9.09E-04	526	10	0.0167	554	28582	179758	28300	177987	dx1
2	64	cu_na2	5/25/16 18:28	10	8070	807	0.281	0.0285	28320	9.09E-04	526	10	0.0167	1308	45898	163340	47400	168683	dx2
3	65	cu_na1	5/26/16 20:05	10	1925	193	0.146	0.0194	9926	9.09E-04	510	10	0.0167	307	15855	108597	16000	109589	dx1
3	66	cu_na2	5/26/16 20:05	10	5174	517	0.281	0.0285	18157	9.09E-04	510	10	0.0167	826	29002	103211	28700	102135	dx2
1	71	cu_falcon	5/24/16 21:39	720			0.971										36700	37796	falcon
2	72	cu_falcon	5/25/16 15:15	23.7			0.962										145000	150728	falcon
3	73	cu_falcon	5/26/16 20:50	720			0.853										73400	86049	falcon

Table G.3 ^{115m}I and ^{116m}I Specific Activity in Indium Foils

Pulse #	Dosimeter #	C In (Cd) detector	count start	count duration (min)	sample mass (g)	In-115m A_o (dpm)	In-115m A_o (dpm/g)	In-116m A_o (dpm)	In-116m A_o (dpm/g)	D In (bare) detector	count start	count duration (min)	sample mass (g)	In-115m A_o (dpm)	In-115m A_o (dpm/g)	In-116m A_o (dpm)	In-116m A_o (dpm/g)
1	1	falcon	5/24/16 15:17	32.9	0.235	2.30E+04	9.79E+04	8.90E+06	3.79E+07	dx1	5/24/16 15:40	16.1	0.230	2.23E+04	9.70E+04	2.45E+07	1.07E+08
1	2	falcon	5/24/16 16:46	18	0.238	2.36E+04	9.92E+04	9.10E+06	3.82E+07	dx2	5/24/16 19:11	21.1	0.227	2.12E+04	9.34E+04	2.25E+07	9.91E+07
1	3	dx2	5/24/16 16:59	13.5	0.228	2.03E+04	8.90E+04	7.64E+06	3.35E+07	dx1	5/24/16 19:01	19.4	0.228	2.13E+04	9.34E+04	2.08E+07	9.12E+07
1	4	falcon	5/24/16 17:08	20.1	0.228	2.36E+04	1.04E+05	7.94E+06	3.48E+07	dx1	5/24/16 19:23	15	0.230	2.21E+04	9.61E+04	2.08E+07	9.04E+07
1	5	dx2	5/24/16 17:16	31.2	0.230	1.11E+04	4.83E+04	9.60E+06	4.17E+07	falcon	5/24/16 19:24	40	0.228	1.16E+04	5.09E+04	4.36E+07	1.91E+08
1	6	falcon	5/24/16 17:37	30	0.229	1.87E+03	8.17E+03	5.14E+06	2.24E+07	dx2	5/24/16 19:34	36.7	0.230	1.72E+03	7.48E+03	2.31E+07	1.00E+08
1	7	dx1	5/24/16 17:36	20	0.226	1.02E+04	4.51E+04	9.68E+06	4.28E+07	dx1	5/24/16 19:39	28.3	0.229	1.11E+04	4.85E+04	4.28E+07	1.87E+08
1	8	dx2	5/24/16 17:50	50	0.230	1.82E+03	7.91E+03	5.90E+06	2.57E+07	falcon	5/24/16 20:06	16.7	0.229	2.22E+03	9.69E+03	3.08E+07	1.34E+08
1	9	dx1	5/24/16 17:58	15	0.227	1.54E+04	6.78E+04	8.78E+06	3.87E+07	dx1	5/24/16 20:10	16.7	0.236	1.62E+04	6.86E+04	2.55E+07	1.08E+08
1	10	falcon	5/24/16 18:09	15	0.229	1.64E+04	7.16E+04	9.35E+06	4.08E+07	dx2	5/24/16 20:12	16.7	0.228	1.50E+04	6.58E+04	2.45E+07	1.07E+08
1	11	dx1	5/24/16 18:15	20	0.227	1.48E+04	6.52E+04	9.00E+06	3.96E+07	falcon	5/24/16 20:24	15	0.230	1.65E+04	7.17E+04	2.75E+07	1.20E+08
1	12	falcon	5/24/16 18:26	20.1	0.228	1.64E+04	7.19E+04	9.72E+06	4.26E+07	dx1	5/24/16 20:28	16.7	0.227	1.46E+04	6.43E+04	2.46E+07	1.08E+08
1	13	dx1	5/24/16 18:37	22.4	0.226	7.99E+03	3.54E+04	8.32E+06	3.68E+07	dx2	5/24/16 20:30	25	0.230	7.12E+03	3.10E+04	3.48E+07	1.51E+08
1	14	dx2	5/24/16 18:43	25	0.228	1.77E+03	7.76E+03	5.98E+06	2.62E+07	dx1	5/24/16 20:46	46.7	0.229	1.69E+03	7.38E+03	2.96E+07	1.29E+08
1	15	falcon	5/24/16 16:17	26.4	0.236	8.55E+03	3.62E+04	7.43E+06	3.15E+07	dx1	5/24/16 16:30	60	0.229	8.02E+03	3.50E+04	2.01E+07	8.78E+07
1	16	falcon	5/24/16 16:49	34.3	0.236	8.66E+03	3.67E+04	7.30E+06	3.09E+07	dx2	5/24/16 20:57	lost	0.228	lost	lost	lost	lost
2	17	dx1	5/25/16 16:33	15	0.230	8.50E+04	3.70E+05	3.19E+07	1.39E+08	dx2	5/25/16 18:25	16	0.227	8.12E+04	3.58E+05	8.64E+07	3.81E+08
2	18	dx1	5/25/16 16:10	18.5	0.232	8.45E+04	3.64E+05	3.23E+07	1.39E+08	falcon	5/25/16 18:27	16	0.226	9.01E+04	3.99E+05	9.32E+07	4.12E+08
2	19	dx2	5/25/16 16:11	19	0.228	9.37E+04	4.11E+05	3.13E+07	1.37E+08	dx1	5/25/16 18:31	15.5	0.227	8.99E+04	3.96E+05	8.86E+07	3.90E+08
2	20	dx2	5/25/16 16:34	15	0.232	9.44E+04	4.07E+05	3.01E+07	1.30E+08	dx2	5/25/16 18:42	11.5	0.231	9.46E+04	4.10E+05	9.24E+07	4.00E+08
2	21	dx1	5/25/16 17:28	15.5	0.227	4.13E+04	1.82E+05	3.55E+07	1.56E+08	falcon	5/25/16 18:44	15	0.231	4.52E+04	1.96E+05	1.77E+08	7.66E+08
2	22	dx2	5/25/16 15:52	15.5	0.235	5.92E+03	2.52E+04	1.80E+07	7.66E+07	dx1	5/25/16 18:47	30.3	0.228	6.60E+03	2.89E+04	8.78E+07	3.85E+08
2	23	dx2	5/25/16 17:29	20.9	0.230	3.92E+04	1.70E+05	3.62E+07	1.57E+08	dx2	5/25/16 18:55	15.1	0.229	3.90E+04	1.70E+05	1.69E+08	7.38E+08
2	24	falcon	5/25/16 16:03	32.5	0.227	6.45E+03	2.84E+04	2.16E+07	9.52E+07	falcon	5/25/16 19:00	30.1	0.229	6.42E+03	2.80E+04	1.04E+08	4.54E+08
2	25	dx2	5/25/16 17:51	15	0.230	2.87E+04	1.25E+05	3.04E+07	1.32E+08	dx2	5/25/16 19:13	15.1	0.229	3.01E+04	1.31E+05	1.36E+08	5.94E+08
2	26	dx2	5/25/16 16:52	33.3	0.230	6.95E+03	3.02E+04	2.35E+07	1.02E+08	dx1	5/25/16 19:21	30	0.231	7.32E+03	3.17E+04	1.14E+08	4.94E+08
2	27	falcon	5/25/16 16:57	22	0.237	6.85E+04	2.89E+05	3.58E+07	1.51E+08	dx2	5/25/16 19:30	15.1	0.226	5.87E+04	2.60E+05	9.21E+07	4.08E+08
2	28	falcon	5/25/16 16:37	15.9	0.228	6.51E+04	2.86E+05	3.52E+07	1.54E+08	falcon	5/25/16 19:33	15	0.230	6.26E+04	2.72E+05	9.84E+07	4.28E+08
2	29	dx1	5/25/16 15:26	22.7	0.227	2.80E+04	1.23E+05	2.55E+07	1.12E+08	dx1	5/25/16 17:58	15	0.228	2.73E+04	1.20E+05	7.30E+07	3.20E+08
2	30	dx2	5/25/16 15:27	22.2	0.234	2.86E+04	1.22E+05	2.55E+07	1.09E+08	dx2	5/25/16 18:08	15	0.228	2.89E+04	1.27E+05	7.50E+07	3.29E+08
2	31	falcon	5/25/16 15:39	21.4	0.234	3.26E+04	1.39E+05	2.74E+07	1.17E+08	falcon	5/25/16 18:11	15	0.230	3.04E+04	1.32E+05	8.13E+07	3.53E+08
2	32	dx1	5/25/16 15:51	15	0.232	2.94E+04	1.27E+05	2.63E+07	1.13E+08	dx1	5/25/16 18:14	15	0.230	2.86E+04	1.24E+05	7.54E+07	3.28E+08
3	33	dx1	5/26/16 16:30	10	0.235	3.76E+04	1.60E+05	2.07E+07	8.81E+07	dx1	5/26/16 20:47	10.5	0.231	3.95E+04	1.71E+05	5.77E+07	2.50E+08
3	34	falcon	5/26/16 16:34	15	0.229	2.51E+04	1.10E+05	2.23E+07	9.74E+07	dx2	5/26/16 20:49	12.7	0.228	2.49E+04	1.09E+05	9.62E+07	4.22E+08
3	35	dx2	5/26/16 16:37	30	0.230	3.25E+03	1.41E+04	1.04E+07	4.52E+07	falcon	5/26/16 20:52	16	0.231	3.62E+03	1.57E+04	5.65E+07	2.45E+08
3	36	dx1	5/26/16 16:47	30	0.228	4.18E+03	1.83E+04	1.19E+07	5.22E+07	dx2	5/26/16 21:05	20	0.229	3.41E+03	1.49E+04	6.36E+07	2.78E+08
3	37	falcon	5/26/16 16:50	9.7	0.228	2.42E+04	1.06E+05	2.19E+07	9.61E+07	falcon	5/26/16 21:10	12	0.230	2.36E+04	1.03E+05	1.01E+08	4.39E+08
3	38	falcon	5/26/16 17:02	15	0.229	1.75E+04	7.64E+04	1.88E+07	8.21E+07	dx1	5/26/16 21:18	15	0.230	1.63E+04	7.09E+04	9.05E+07	3.93E+08
3	39	dx2	5/26/16 17:09	30	0.234	2.81E+03	1.20E+04	8.21E+06	3.51E+07	falcon	5/26/16 21:23	25	0.231	2.75E+03	1.19E+04	4.02E+07	1.74E+08
3	40	falcon	5/26/16 15:57	30.1	0.228	3.69E+02	1.62E+03	8.05E+05	3.53E+06	dx1	5/26/16 20:29	15	0.227	5.01E+02	2.21E+03	1.38E+07	6.08E+07
3	41	dx1	5/26/16 15:58	30	0.226	2.42E+04	1.07E+05	2.86E+06	1.27E+07	dx2	5/26/16 20:30	17.3	0.229	2.89E+04	1.26E+05	1.38E+07	6.03E+07
3	42	dx2	5/26/16 15:59	10	0.227	3.76E+04	1.66E+05	2.01E+07	8.85E+07	dx2	5/26/16 20:39	12.1	0.231	4.08E+04	1.77E+05	6.12E+07	2.65E+08
3	43	dx1	5/26/16 17:21	30	0.236	1.58E+04	6.69E+04	1.78E+07	7.54E+07	dx2	5/26/16 21:27	15	0.228	1.44E+04	6.32E+04	5.25E+07	2.30E+08
3	44	falcon	5/26/16 17:19	21.1	0.226	8.71E+03	3.85E+04	1.83E+07	8.10E+07	dx1	5/26/16 21:34	31	0.229	8.69E+03	3.79E+04	8.49E+07	3.71E+08
3	45	dx2	5/26/16 17:43	145.7	0.229	5.45E+04	2.38E+05	3.05E+07	1.33E+08	dx2	5/26/16 21:43	20	0.231	5.61E+04	2.43E+05	1.43E+08	6.19E+08
3	46	dx1	5/26/16 21:01	15	0.230	1.47E+04	6.39E+04	1.64E+07	7.13E+07	falcon	5/26/16 21:50	20.1	0.227	1.53E+04	6.74E+04	5.08E+07	2.24E+08
1	61	dx2	5/24/16 16:34	21.5	0.122	1.18E+04	9.67E+04	5.02E+06	4.11E+07	dx2	5/24/16 16:01	30	0.118	1.16E+04	9.83E+04	5.11E+06	4.33E+07
1	62	falcon	5/24/16 20:41	11.6	0.226	2.42E+04	1.07E+05	8.59E+06	3.80E+07	falcon	5/24/16 20:53	11	0.231	2.41E+04	1.04E+05	2.31E+07	1.00E+08
2	63	dx1	5/25/16 15:03	16.2	0.119	4.16E+04	3.50E+05	2.02E+07	1.70E+08	falcon	5/25/16 17:42	9.9	0.114	4.14E+04	3.63E+05	5.31E+07	4.66E+08
2	64	dx2	5/25/16 15:04	15	0.230	8.24E+04	3.58E+05	2.81E+07	1.22E+08	dx1	5/25/16 17:46	10	0.228	7.77E+04	3.41E+05	7.98E+07	3.50E+08
3	65	dx1	5/26/16 20:14	12	0.115	2.41E+04	2.10E+05	1.22E+07	1.06E+08	dx2	5/26/16 22:05	20	0.114	2.47E+04	2.17E+05	3.32E+07	2.91E+08
3	66	dx2	5/26/16 20:15	12	0.232	4.94E+04	2.13E+05	1.61E+07	6.94E+07	dx1	5/26/16 22:07	10.5	0.228	4.80E+04	2.11E+05	4.74E+07	2.08E+08
1	71	falcon	5/25/16 12:26	97.1	0.184	7.25E+03	3.94E+04	<3.5E10	n/a	dx2	5/25/16 12:33	88.4	0.188	6.04E+03	3.21E+04	<2.9E10	n/a
2	72	falcon	5/25/16 17:21	19.9	0.187	2.34E+04	1.25E+05	2.21E+07	1.18E+08	falcon	5/25/16 17:54	14.9	0.190	2.47E+04	1.30E+05	7.20E+07	3.79E+08
3	73	falcon	5/26/16 20:16	13	0.183	1.31E+04	7.16E+04	1.19E+07	6.50E+07	falcon	5/26/16 22:11	26.7	0.176	1.34E+04	7.61E+04	4.03E+07	2.29E+08

Table G.4 ^{198}Au Specific Activity in Gold Foils

Pulse #	Dosimeter #	E					
		Au (outer - bare)					
		Au-198					
		detector	count start	count duration (min)	sample mass (g)	A$_o$ (dpm)	A$_o$ (dpm/g)
1	71	falcon	5/24/16 21:09	10.2	0.255	1.78E+05	6.98E+05
2	72	dx1	5/25/16 20:11	10	0.269	6.02E+05	2.24E+06
3	73	dx1	5/26/16 10:31	10.2	0.254	3.72E+05	1.46E+06

Pulse #	Dosimeter #	F					
		Au (outer - Cd)					
		Au-198					
		detector	count start	count duration (min)	sample mass (g)	A$_o$ (dpm)	A$_o$ (dpm/g)
1	71	falcon	5/24/16 12:04	23.6	0.266	6.67E+04	2.51E+05
2	72	dx1	5/25/16 12:35	5.5	0.247	2.34E+05	9.47E+05
3	73	falcon	5/26/16 22:40	10	0.258	1.46E+05	5.66E+05

Pulse #	Dosimeter #	G					
		Au (inner - bare)					
		Au-198					
		detector	count start	count duration (min)	sample mass (g)	A$_o$ (dpm)	A$_o$ (dpm/g)
1	71	dx2	5/24/16 15:20	16.2	0.251	3.65E+05	1.45E+06
2	72	dx1	5/25/16 20:42	5	0.252	1.35E+06	5.36E+06
3	73	dx2	5/26/16 22:27	16.4	0.248	7.74E+05	3.12E+06

Table G.5 Specific Activity per Unit Fluence and per Unit Dose in PNAD Foils

Dosimeter #	Pulse #	distance (m)	Position #	phantom type	location on phantom	mounting on phantom	Given Fluence (n/cm²)	A / S / P-32	B / Cu (Cd) / Cu-64	C / In (Cd) / In-115m	C / In (Cd) / In-116m	D / In / In-115m	D / In / In-116m	Given Dose, $D_p(10)_n$ (cGy)	A / S / P-32	B / Cu (Cd) / Cu-64	C / In (Cd) / In-115m	C / In (Cd) / In-116m	D / In / In-115m	D / In / In-116m
							Measured Specific Activity per Unit Fluence A_o / ϕ_{tot} (cm² g⁻¹ min⁻¹)							**Measured Specific Activity per Unit Absorbed Dose** $A_o / D_p(10)_n$ (cGy⁻¹ g⁻¹ min⁻¹)						
1	1	2.0	1	Tree A-D	air	normal	1.01E+11	1.20E-08	4.56E-07	9.69E-07	3.75E-04	9.60E-07	1.05E-03	214	5.65E+00	2.15E+02	4.57E+02	1.77E+05	4.53E+02	4.98E+05
2	1	2.0	1	Tree A-D	air	normal	1.01E+11	1.36E-08	4.47E-07	9.82E-07	3.79E-04	9.25E-07	9.81E-04	214	6.41E+00	2.11E+02	4.63E+02	1.79E+05	4.36E+02	4.63E+05
3	1	2.0	2	Tree A-D	air	normal	9.59E+10	1.35E-08	4.68E-07	9.28E-07	3.49E-04	9.74E-07	9.51E-04	205	6.31E+00	2.19E+02	4.34E+02	1.63E+05	4.56E+02	4.45E+05
4	1	2.0	2	Tree A-D	air	normal	9.59E+10	1.37E-08	4.41E-07	1.08E-06	3.63E-04	1.00E-06	9.43E-04	205	6.39E+00	2.06E+02	5.05E+02	1.70E+05	4.69E+02	4.41E+05
62	1	2.0	2	Tree A-D	air	normal	9.59E+10	1.33E-08	4.45E-07	1.12E-06	3.96E-04	1.09E-06	1.04E-03	205	6.22E+00	2.08E+02	5.22E+02	1.85E+05	5.09E+02	4.88E+05
17	2	2.0	1	Tree A-D	air	normal	3.60E+11	1.37E-08	5.24E-07	1.03E-06	3.85E-04	9.94E-07	1.06E-03	764	6.45E+00	2.47E+02	4.84E+02	1.82E+05	4.68E+02	4.98E+05
18	2	2.0	1	Tree A-D	air	normal	3.60E+11	1.35E-08	4.75E-07	1.01E-06	3.87E-04	1.11E-06	1.15E-03	764	6.34E+00	2.24E+02	4.77E+02	1.82E+05	5.22E+02	5.40E+05
19	2	2.0	3	Tree A-D	air	normal	3.60E+11	1.52E-08	4.82E-07	1.14E-06	3.81E-04	1.10E-06	1.08E-03	761	7.18E+00	2.28E+02	5.40E+02	1.80E+05	5.20E+02	5.13E+05
20	2	2.0	3	Tree A-D	air	normal	3.60E+11	1.56E-08	4.58E-07	1.13E-06	3.60E-04	1.14E-06	1.11E-03	761	7.37E+00	2.17E+02	5.35E+02	1.70E+05	5.38E+02	5.26E+05
64	2	2.0	2	Tree A-D	air	normal	3.43E+11	1.43E-08	4.76E-07	1.04E-06	3.56E-04	9.94E-07	1.02E-03	732	6.71E+00	2.23E+02	4.89E+02	1.67E+05	4.66E+02	4.78E+05
66	3	2.0	2	Tree A-D	air	normal	2.07E+11	1.33E-08	4.99E-07	1.03E-06	3.35E-04	1.02E-06	1.00E-03	442	6.22E+00	2.34E+02	4.82E+02	1.57E+05	4.76E+02	4.70E+05
							mean	1.38E-08	4.70E-07	1.04E-06	3.70E-04	1.03E-06	1.04E-03	mean	6.48E+00	2.21E+02	4.90E+02	1.74E+05	4.83E+02	4.87E+05
							C.V.	0.07	0.05	0.07	0.05	0.07	0.06	C.V.	0.07	0.05	0.07	0.05	0.07	0.06
							n	11	11	11	11	11	11	n	11	11	11	11	11	11
61	1	2.0	2	Tree A-D	air	normal	9.59E+10	1.40E-08	4.71E-07	1.01E-06	4.29E-04	1.03E-06	4.52E-04	205	6.54E+00	2.20E+02	4.72E+02	2.01E+05	4.80E+02	2.11E+05
63	2	2.0	2	Tree A-D	air	normal	3.43E+11	1.36E-08	5.24E-07	1.02E-06	4.95E-04	1.06E-06	1.36E-03	732	6.37E+00	2.46E+02	4.78E+02	2.32E+05	4.96E+02	6.36E+05
65	3	2.0	2	Tree A-D	air	normal	2.07E+11	1.26E-08	5.25E-07	1.01E-06	5.12E-04	1.05E-06	1.41E-03	442	5.90E+00	2.46E+02	4.74E+02	2.40E+05	4.90E+02	6.59E+05
						5 mil foils	mean	1.34E-08	5.07E-07	1.01E-06	4.79E-04	1.04E-06	1.38E-03	mean	6.27E+00	2.37E+02	4.75E+02	2.24E+05	4.89E+02	6.48E+05
							C.V.	0.05	0.06	0.01	0.09	0.02	0.03	C.V.	0.05	0.06	0.01	0.09	0.02	0.02
							n	3	3	3	3	3	2	n	3	3	3	3	3	2
9	1	2.5	6	Tree A-D	air	normal	8.58E+10	1.06E-08	5.20E-07	7.91E-07	4.51E-04	8.00E-07	1.26E-03	159	5.71E+00	2.81E+02	4.27E+02	2.43E+05	4.32E+02	6.80E+05
10	1	2.5	6	Tree A-D	air	normal	8.58E+10	1.16E-08	5.42E-07	8.35E-07	4.76E-04	7.67E-07	1.25E-03	159	6.28E+00	2.92E+02	4.50E+02	2.57E+05	4.14E+02	6.76E+05
11	1	2.5	6	Tree A-D	air	normal	8.58E+10	1.05E-08	5.43E-07	7.60E-07	4.62E-04	8.36E-07	1.39E-03	159	5.69E+00	2.93E+02	4.10E+02	2.49E+05	4.51E+02	7.52E+05
12	1	2.5	6	Tree A-D	air	normal	8.58E+10	1.05E-08	5.46E-07	8.38E-07	4.97E-04	7.50E-07	1.26E-03	159	5.65E+00	2.95E+02	4.52E+02	2.68E+05	4.05E+02	6.82E+05
27	2	2.5	6	Tree A-D	air	normal	3.07E+11	1.13E-08	5.99E-07	9.41E-07	4.92E-04	8.46E-07	1.33E-03	570	6.09E+00	3.23E+02	5.07E+02	2.65E+05	4.56E+02	7.15E+05
28	2	2.5	6	Tree A-D	air	normal	3.07E+11	1.16E-08	5.78E-07	9.30E-07	5.03E-04	8.87E-07	1.39E-03	570	6.25E+00	3.12E+02	5.01E+02	2.71E+05	4.77E+02	7.51E+05
33	3	2.5	6	Tree A-D	air	normal	1.85E+11	1.15E-08	5.63E-07	8.65E-07	4.76E-04	9.24E-07	1.35E-03	344	6.21E+00	3.03E+02	4.65E+02	2.56E+05	4.97E+02	7.26E+05
42	3	2.5	6	Tree A-D	air	normal	1.85E+11	1.18E-08	5.97E-07	8.95E-07	4.79E-04	9.55E-07	1.43E-03	344	6.35E+00	3.21E+02	4.82E+02	2.57E+05	5.13E+02	7.70E+05
							mean	1.12E-08	5.61E-07	8.57E-07	4.79E-04	8.46E-07	1.33E-03	mean	6.03E+00	3.02E+02	4.62E+02	2.58E+05	4.56E+02	7.19E+05
							C.V.	0.05	0.05	0.07	0.04	0.09	0.05	C.V.	0.05	0.05	0.07	0.04	0.08	0.05
							n	8	8	8	8	8	8	n	8	8	8	8	8	8

Dosimeter #	Pulse #	distance (m)	Position #	phantom type	location on phantom	mounting on phantom	Given Fluence (n/cm²)	A — S	B — Cu (Cd)	C — In (Cd)		D — In		Given Dose, $D_p(10)_n$ (cGy)	A — S	B — Cu (Cd)	C — In (Cd)		D — In	
								P-32	Cu-64	In-115m	In-116m	In-115m	In-116m		P-32	Cu-64	In-115m	In-116m	In-115m	In-116m
15	1	4.0	8	Tree A-H	air	normal	5.33E+10	7.91E-09	6.35E-07	6.80E-07	5.91E-04	6.57E-07	1.65E-03	92	4.58E+00	3.68E+02	3.94E+02	3.42E+05	3.81E+02	9.54E+05
16	1	4.0	8	Tree A-H	air	normal	5.33E+10	8.78E-09	5.98E-07	6.88E-07	5.80E-04	N/A	N/A	92	5.08E+00	3.47E+02	3.99E+02	3.36E+05	N/A	N/A
29	2	4.0	8	Tree A-H	air	normal	1.91E+11	8.30E-09	6.91E-07	6.46E-07	5.88E-04	6.27E-07	1.68E-03	329	4.82E+00	4.01E+02	3.75E+02	3.41E+05	3.64E+02	9.73E+05
30	2	4.0	8	Tree A-H	air	normal	1.91E+11	8.28E-09	6.30E-07	6.40E-07	5.71E-04	6.64E-07	1.72E-03	329	4.81E+00	3.65E+02	3.71E+02	3.31E+05	3.85E+02	1.00E+06
31	2	4.0	8	Tree A-H	air	backward	1.91E+11	7.96E-09	6.81E-07	7.29E-07	6.13E-04	6.92E-07	1.85E-03	329	4.62E+00	3.95E+02	4.23E+02	3.56E+05	4.02E+02	1.07E+06
32	2	4.0	8	Tree A-H	air	backward	1.91E+11	7.86E-09	6.35E-07	6.63E-07	5.94E-04	6.51E-07	1.72E-03	329	4.56E+00	3.68E+02	3.85E+02	3.45E+05	3.78E+02	9.96E+05
43	3	4.0	9	Tree A-H	air	normal	1.15E+11	6.94E-09	6.99E-07	5.82E-07	6.56E-04	5.49E-07	2.00E-03	199	4.01E+00	4.04E+02	3.36E+02	3.79E+05	3.17E+02	1.16E+06
46	3	4.0	9	Tree A-H	air	normal	1.18E+11	6.96E-09	6.50E-07	5.42E-07	6.04E-04	5.71E-07	1.90E-03	199	4.12E+00	3.86E+02	3.21E+02	3.58E+05	3.39E+02	1.12E+06
							mean	7.87E-09	6.52E-07	6.46E-07	6.00E-04	6.30E-07	1.79E-03	mean	4.58E+00	3.79E+02	3.76E+02	3.49E+05	3.67E+02	1.04E+06
							C.V.	0.08	0.05	0.09	0.04	0.08	0.07	C.V.	0.08	0.05	0.09	0.04	0.08	0.08
							n	8	8	8	8	7	7	n	8	8	8	8	7	7
5	1	3.0	4	BOMAB	front	normal	6.55E+10	9.24E-09	6.76E-07	7.37E-07	6.37E-04	7.77E-07	2.92E-03	123	4.92E+00	3.60E+02	3.92E+02	3.39E+05	4.14E+02	1.55E+06
7	1	3.0	5	BOMAB	front	normal	6.77E+10	9.46E-09	6.62E-07	6.67E-07	6.33E-04	7.16E-07	2.76E-03	126	5.08E+00	3.56E+02	3.58E+02	3.40E+05	3.85E+02	1.48E+06
21	2	3.0	4	BOMAB	front	normal	2.34E+11	1.08E-08	7.27E-07	7.78E-07	6.68E-04	8.36E-07	3.27E-03	441	5.72E+00	3.86E+02	4.13E+02	3.55E+05	4.44E+02	1.74E+06
23	2	3.0	5	BOMAB	front	normal	2.42E+11	9.87E-09	7.35E-07	7.04E-07	6.50E-04	7.04E-07	3.05E-03	450	5.31E+00	3.95E+02	3.79E+02	3.50E+05	3.78E+02	1.64E+06
34	3	3.0	4	BOMAB	front	normal	1.41E+11	1.06E-08	6.91E-07	7.77E-07	6.91E-04	7.75E-07	2.99E-03	266	5.61E+00	3.66E+02	4.12E+02	3.66E+05	4.11E+02	1.59E+06
							mean	9.99E-09	6.98E-07	7.33E-07	6.56E-04	7.61E-07	3.00E-03	mean	5.33E+00	3.73E+02	3.91E+02	3.50E+05	4.06E+02	1.60E+06
							C.V.	0.07	0.05	0.07	0.04	0.07	0.06	C.V.	0.06	0.05	0.06	0.03	0.06	0.06
							n	5	5	5	5	5	5	n	5	5	5	5	5	5
38	3	4.0	7	BOMAB	front	normal	1.10E+11	9.27E-09	7.35E-07	6.95E-07	7.46E-04	6.44E-07	3.58E-03	192	5.31E+00	4.21E+02	3.98E+02	4.28E+05	3.69E+02	2.05E+06
41	3	9.0	10	BOMAB	front	normal	6.17E+10	2.83E-09	2.23E-07	1.74E-07	2.05E-04	2.05E-07	9.77E-04	85	2.06E+00	1.62E+02	1.26E+02	1.49E+05	1.48E+02	7.09E+05
45	3	2.0	3	PMMA	front	normal	2.17E+11	1.45E-08	7.34E-07	1.10E-06	6.14E-04	1.12E-06	2.85E-03	459	6.88E+00	3.47E+02	5.18E+02	2.90E+05	5.29E+02	1.35E+06

Measured Specific Activity per Unit Fluence A_o / ϕ_{tot} (cm² g⁻¹ min⁻¹) — i.e. A_o / ϕ_{tot} ($\mathrm{cm^2\,g^{-1}\,min^{-1}}$)

Measured Specific Activity per Unit Absorbed Dose $A_o / D_p(10)_n$ ($\mathrm{cGy^{-1}\,g^{-1}\,min^{-1}}$)

Dosimeter #	Pulse #	distance (m)	Position #	phantom type	location on phantom	mounting on phantom	Given Fluence (n/cm²)	A S P-32	B Cu (Cd) Cu-64	C In (Cd) In-115m	C In (Cd) In-116m	D In In-115m	D In In-116m	Given Dose, D_p(10)_n (cGy)	A S P-32	B Cu (Cd) Cu-64	C In (Cd) In-115m	C In (Cd) In-116m	D In In-115m	D In In-116m
13	1	4.0	7	PMMA	front	normal	5.10E+10	8.78E-09	7.14E-07	6.93E-07	7.22E-04	6.07E-07	2.97E-03	89	5.03E+00	4.09E+02	3.97E+02	4.14E+05	3.48E+02	1.70E+06
25	2	4.0	7	PMMA	front	normal	1.82E+11	9.42E-09	8.15E-07	6.86E-07	7.26E-04	7.22E-07	3.26E-03	319	5.37E+00	4.65E+02	3.91E+02	4.14E+05	4.12E+02	1.86E+06
							mean	9.10E-09	7.65E-07	6.89E-07	7.24E-04	6.65E-07	3.11E-03	mean	5.20E+00	4.37E+02	3.94E+02	4.14E+05	3.80E+02	1.78E+06
							C.V.	0.05	0.09	0.01	0.00	0.12	0.07	C.V.	0.05	0.09	0.01	0.00	0.12	0.06
							n	2	2	2	2	2	2	n	2	2	2	2	2	2
36	3	3.0	5	BOMAB - LAT	side	normal	1.46E+11	1.42E-09	3.35E-07	1.26E-07	3.57E-04	1.02E-07	1.90E-03	271	7.65E-01	1.80E+02	6.77E+01	1.93E+05	5.49E+01	1.02E+06
37	3	3.0	5	BOMAB - LAT	side	normal	1.46E+11	9.13E-09	6.91E-07	7.27E-07	6.58E-04	7.03E-07	3.01E-03	271	4.92E+00	3.72E+02	3.92E+02	3.54E+05	3.79E+02	1.62E+06
							mean	5.27E-09	5.13E-07	4.26E-07	5.08E-04	4.02E-07	2.45E-03	mean	2.84E+00	2.76E+02	2.30E+02	2.74E+05	2.17E+02	1.32E+06
							C.V.	1.03	0.49	1.00	0.42	1.06	0.32	C.V.	1.03	0.49	1.00	0.42	1.06	0.32
							n	2	2	2	2	2	2	n	2	2	2	2	2	2
6	1	3.0	4	BOMAB	back	normal	6.55E+10	1.71E-09	3.24E-07	1.25E-07	3.43E-04	1.14E-07	1.53E-03	123	9.11E-01	1.72E+02	6.64E+01	1.82E+05	6.08E+01	8.17E+05
8	1	3.0	5	BOMAB	back	normal	6.77E+10	1.71E-09	3.20E-07	1.17E-07	3.79E-04	1.43E-07	1.99E-03	126	9.20E-01	1.72E+02	6.28E+01	2.04E+05	7.69E+01	1.07E+06
22	2	3.0	4	BOMAB	back	normal	2.34E+11	1.64E-09	3.13E-07	1.08E-07	3.27E-04	1.24E-07	1.65E-03	441	8.68E-01	1.66E+02	5.71E+01	1.74E+05	6.56E+01	8.73E+05
24	2	3.0	5	BOMAB	back	normal	2.42E+11	1.43E-09	3.49E-07	1.17E-07	3.93E-04	1.16E-07	1.88E-03	450	7.66E-01	1.87E+02	6.31E+01	2.11E+05	6.23E+01	1.01E+06
35	3	3.0	4	BOMAB	back	normal	1.41E+11	1.43E-09	3.42E-07	1.00E-07	3.21E-04	1.11E-07	1.73E-03	266	7.58E-01	1.81E+02	5.31E+01	1.70E+05	5.89E+01	9.20E+05
							mean	1.58E-09	3.30E-07	1.13E-07	3.53E-04	1.22E-07	1.76E-03	mean	8.45E-01	1.76E+02	6.05E+01	1.88E+05	6.49E+01	9.37E+05
							C.V.	0.09	0.05	0.08	0.09	0.11	0.10	C.V.	0.09	0.05	0.09	0.10	0.11	0.11
							n	5	5	5	5	5	5	n	5	5	5	5	5	5
39	3	4.0	7	BOMAB	back	normal	1.10E+11	1.52E-09	3.53E-07	1.09E-07	3.19E-04	1.08E-07	1.58E-03	192	8.69E-01	2.02E+02	6.25E+01	1.83E+05	6.20E+01	9.06E+05
40	3	9.0	10	BOMAB	back	normal	6.17E+10	3.86E-10	5.23E-08	2.62E-08	5.72E-05	3.58E-08	9.85E-04	85	2.80E-01	3.80E+01	1.90E+01	4.15E+04	2.60E+01	7.15E+05
44	3	2.0	1	PMMA	back	normal	2.17E+11	2.19E-09	3.35E-07	1.78E-07	3.73E-04	1.75E-07	1.71E-03	461	1.03E+00	1.58E+02	8.36E+01	1.76E+05	8.23E+01	8.04E+05
14	1	4.0	9	PMMA	back	normal	5.46E+10	1.82E-09	4.46E-07	1.42E-07	4.80E-04	1.35E-07	2.37E-03	92	1.08E+00	2.65E+02	8.44E+01	2.85E+05	8.02E+01	1.40E+06
26	2	4.0	9	PMMA	back	normal	1.95E+11	1.87E-09	4.76E-07	1.55E-07	5.24E-04	1.63E-07	2.53E-03	330	1.10E+00	2.81E+02	9.16E+01	3.10E+05	9.60E+01	1.50E+06
							mean	1.84E-09	4.61E-07	1.49E-07	5.02E-04	1.49E-07	2.45E-03	mean	1.09E+00	2.73E+02	8.80E+01	2.97E+05	8.81E+01	1.45E+06
							C.V.	0.02	0.05	0.06	0.06	0.13	0.05	C.V.	0.02	0.04	0.06	0.06	0.13	0.04
							n	2	2	2	2	2	2	n	2	2	2	2	2	2

Measured Specific Activity per Unit Fluence A_o / ϕ_{tot} (cm² g⁻¹ min⁻¹)

Measured Specific Activity per Unit Absorbed Dose $A_o / D_p(10)_n$ (cGy⁻¹ g⁻¹ min⁻¹)

Table G.6 Specific Activity per Unit Fluence and per Unit Dose in PNAD Foils Grouped by Distance and Exposure Geometry

					Measured Specific Activity per Unit Fluence A_o/ϕ_{tot} (cm^2 g^{-1} min^{-1})						Measured Specific Activity per Unit Absorbed Dose $A_o/D_p(10)_n$ (cGy^{-1} g^{-1} min^{-1})					
					A	**B**	**C**		**D**		**A**	**B**	**C**		**D**	
					S	**Cu (Cd)**	**In (Cd)**		**In**		**S**	**Cu (Cd)**	**In (Cd)**		**In**	
distance (m)	phantom type	location on phantom	mounting on phantom	Foil Thickness (mil)	P-32	Cu-64	In-115m	In-116m	In-115m	In-116m	P-32	Cu-64	In-115m	In-116m	In-115m	In-116m
2.0	Tree A-D	air	normal	10	1.38E-08	4.70E-07	1.04E-06	3.70E-04	1.03E-06	1.04E-03	6.48E+00	2.21E+02	4.90E+02	1.74E+05	4.83E+02	4.87E+05
2.0	Tree A-D	air	normal	5	1.34E-08	5.07E-07	1.01E-06	4.79E-04	1.04E-06	1.38E-03	6.27E+00	2.37E+02	4.75E+02	2.24E+05	4.89E+02	6.48E+05
2.5	Tree A-D	air	normal	10	1.12E-08	5.61E-07	8.57E-07	4.79E-04	8.46E-07	1.33E-03	6.03E+00	3.02E+02	4.62E+02	2.58E+05	4.56E+02	7.19E+05
4.0	Tree A-H	air	normal	10	7.87E-09	6.52E-07	6.46E-07	6.00E-04	6.30E-07	1.79E-03	4.58E+00	3.79E+02	3.76E+02	3.49E+05	3.67E+02	1.04E+06
3.0	BOMAB	front	normal	10	9.99E-09	6.98E-07	7.33E-07	6.56E-04	7.61E-07	3.00E-03	5.33E+00	3.73E+02	3.91E+02	3.50E+05	4.06E+02	1.60E+06
4.0	BOMAB	front	normal	10	9.27E-09	7.35E-07	6.95E-07	7.46E-04	6.44E-07	3.58E-03	5.31E+00	4.21E+02	3.98E+02	4.28E+05	3.69E+02	2.05E+06
9.0	BOMAB	front	normal	10	2.83E-09	2.23E-07	1.74E-07	2.05E-04	2.05E-07	9.77E-04	2.06E+00	1.62E+02	1.26E+02	1.49E+05	1.48E+02	7.09E+05
2.0	PMMA	front	normal	10	1.45E-08	7.34E-07	1.10E-06	6.14E-04	1.12E-06	2.85E-03	6.88E+00	3.47E+02	5.18E+02	2.90E+05	5.29E+02	1.35E+06
4.0	PMMA	front	normal	10	9.10E-09	7.65E-07	6.89E-07	7.24E-04	6.65E-07	3.11E-03	5.20E+00	4.37E+02	3.94E+02	4.14E+05	3.80E+02	1.78E+06
3.0	BOMAB - LAT	side	normal	10	5.27E-09	5.13E-07	4.26E-07	5.08E-04	4.02E-07	2.45E-03	2.84E+00	2.76E+02	2.30E+02	2.74E+05	2.17E+02	1.32E+06
3.0	BOMAB	back	normal	10	1.58E-09	3.30E-07	1.13E-07	3.53E-04	1.22E-07	1.76E-03	8.45E-01	1.76E+02	6.05E+01	1.88E+05	6.49E+01	9.37E+05
4.0	BOMAB	back	normal	10	1.52E-09	3.53E-07	1.09E-07	3.19E-04	1.08E-07	1.58E-03	8.69E-01	2.02E+02	6.25E+01	1.83E+05	6.20E+01	9.06E+05
9.0	BOMAB	back	normal	10	3.86E-10	5.23E-08	2.62E-08	5.72E-05	3.58E-08	9.85E-04	2.80E-01	3.80E+01	1.90E+01	4.15E+04	2.60E+01	7.15E+05
2.0	PMMA	back	normal	10	2.19E-09	3.35E-07	1.78E-07	3.73E-04	1.75E-07	1.71E-03	1.03E+00	1.58E+02	8.36E+01	1.76E+05	8.23E+01	8.04E+05
4.0	PMMA	back	normal	10	1.84E-09	4.61E-07	1.49E-07	5.02E-04	1.49E-07	2.45E-03	1.09E+00	2.73E+02	8.80E+01	2.97E+05	8.81E+01	1.45E+06

Table G.7 Specific Activity per Unit Fluence and per Unit Dose in FNAD Foils

			Measured Specific Activity per Unit Fluence A_o/ϕ_{tot} (cm^2 g^{-1} min^{-1})								
				Outer Dosimetry Package							Inner Package
				A	B	C		D		E	F	G
				S	Cu (Cd)	In (Cd)	In (Cd)	In	In	Au	Au (Cd)	Au
Pulse #	distance (m)	Position #	Given Fluence (n/cm^2)	P-32	Cu-64	I-115m	I-116m	I-115m	I-116m	Au-198	Au-198	Au-198
1	4.0	11	5.30E+10	7.60E-09	7.14E-07	7.44E-07	N/A	6.07E-07	N/A	1.32E-05	4.73E-06	2.75E-05
2	4.0	11	1.89E+11	7.84E-09	7.96E-07	6.61E-07	6.24E-04	6.87E-07	2.00E-03	1.18E-05	5.00E-06	2.83E-05
3	4.0	11	1.14E+11	7.57E-09	7.53E-07	6.26E-07	5.69E-04	6.66E-07	2.00E-03	1.28E-05	4.95E-06	2.73E-05

			Measured Specific Activity per Unit Ambient Absorbed Dose $A_o/D^*(10)_n$ (cGy^{-1} g^{-1} min^{-1})								
				Outer Dosimetry Package							Inner Package
				A	B	C		D		E	F	G
				S	Cu (Cd)	In (Cd)	In (Cd)	In	In	Au	Au (Cd)	Au
Pulse #	distance (m)	Position #	Given Dose, $D^*(10)_n$ (cGy)	P-32	Cu-64	I-115m	I-116m	I-115m	I-116m	Au-198	Au-198	Au-198
1	4.0	11	88	4.59E+00	4.31E+02	4.49E+02	N/A	3.66E+02	N/A	7.96E+03	2.86E+03	1.66E+04
2	4.0	11	313	4.74E+00	4.82E+02	4.00E+02	3.78E+05	4.15E+02	1.21E+06	7.15E+03	3.03E+03	1.71E+04
3	4.0	11	189	4.59E+00	4.56E+02	3.79E+02	3.45E+05	4.04E+02	1.21E+06	7.76E+03	3.00E+03	1.65E+04

Appendix H

Neutron Dose Results Based on Foil Activities

Table H.1 PNAD Neutron Kerma Calculations

Dosimeter #	Pulse #	Distance (m)	Geometry	A — S / P-32 A_0 (dpm/g)	B — Cu(Cd) / Cu-64 A_0 (dpm/g)	C — In(Cd) / I-115m A_0 (dpm/g)	C — In(Cd) / I-116m A_0 (dpm/g)	D — In(bare) / I-115m A_0 (dpm/g)	D — In(bare) / I-116m A_0 (dpm/g)	Φ_{th} (cm^{-2})	Φ_{epi} (cm^{-2})	Φ_{Cu} (cm^{-2})	Φ_{In} (cm^{-2})	Φ_{S} (cm^{-2})	K_{th} (rad)	K_{epi} (rad)	K_{Cu} (rad)	$K_{In\text{-}S}$ (rad)	K_{S} (rad)	K_{total} (rad)
1	1	2.0	Tree	1.21E+03	4.61E+04	9.79E+04	3.79E+07	9.70E+04	1.07E+08	6.65E+09	2.27E+08	2.22E+10	4.02E+10	8.43E+09	1.46E-01	9.09E-04	6.35E+00	9.12E+01	3.24E+01	130
2	1	2.0	Tree	1.37E+03	4.51E+04	9.92E+04	3.82E+07	9.34E+04	9.91E+07	5.89E+09	2.29E+08	2.27E+10	4.08E+10	9.58E+09	1.30E-01	9.18E-04	6.22E+00	8.95E+01	3.68E+01	133
3	1	2.0	Tree	1.29E+03	4.49E+04	8.90E+04	3.35E+07	9.34E+04	9.12E+07	5.59E+09	2.01E+08	2.21E+10	3.66E+10	9.03E+09	1.23E-01	8.04E-04	6.18E+00	7.91E+01	3.47E+01	120
4	1	2.0	Tree	1.31E+03	4.23E+04	1.04E+05	3.48E+07	9.61E+04	9.04E+07	5.38E+09	2.09E+08	2.08E+10	4.25E+10	9.15E+09	1.18E-01	8.36E-04	5.83E+00	9.58E+01	3.51E+01	137
5	1	3.0	BOMAB front	6.05E+02	4.43E+04	4.83E+04	4.17E+07	5.09E+04	1.91E+08	1.45E+10	2.50E+08	2.18E+10	1.98E+10	4.22E+09	3.18E-01	1.00E-03	6.10E+00	4.48E+01	1.62E+01	67
6	1	3.0	BOMAB back	1.12E+02	2.12E+04	8.17E+03	2.24E+07	7.48E+03	1.00E+08	7.55E+09	1.35E+08	1.04E+10	3.36E+09	7.82E+08	1.66E-01	5.39E-04	2.92E+00	7.39E+00	3.00E+00	13
7	1	3.0	BOMAB front	6.40E+02	4.48E+04	4.51E+04	4.28E+07	4.85E+04	1.87E+08	1.39E+10	2.57E+08	2.20E+10	1.85E+10	4.47E+09	3.07E-01	1.03E-03	6.17E+00	4.04E+01	1.72E+01	64
8	1	3.0	BOMAB back	1.16E+02	2.16E+04	7.91E+03	2.57E+07	9.69E+03	1.34E+08	1.05E+10	1.54E+08	1.07E+10	3.25E+09	8.09E+08	2.32E-01	6.16E-04	2.98E+00	7.01E+00	3.11E+00	13
9	1	2.5	Tree	9.09E+02	4.46E+04	6.78E+04	3.87E+07	6.86E+04	1.08E+08	6.72E+09	2.32E+08	2.20E+10	2.79E+10	6.34E+09	1.48E-01	9.28E-04	6.15E+00	6.18E+01	2.44E+01	92
10	1	2.5	Tree	9.99E+02	4.65E+04	7.16E+04	4.08E+07	6.58E+04	1.07E+08	6.45E+09	2.45E+08	2.29E+10	2.94E+10	6.97E+09	1.42E-01	9.80E-04	6.40E+00	6.45E+01	2.68E+01	98
11	1	2.5	Tree	9.04E+02	4.66E+04	6.52E+04	3.96E+07	7.17E+04	1.20E+08	7.74E+09	2.38E+08	2.29E+10	2.68E+10	6.31E+09	1.70E-01	9.52E-04	6.42E+00	5.88E+01	2.42E+01	90
12	1	2.5	Tree	8.98E+02	4.66E+04	7.19E+04	4.26E+07	6.43E+04	1.08E+08	6.36E+09	2.56E+08	2.31E+10	2.96E+10	6.27E+09	1.40E-01	1.02E-03	6.45E+00	6.69E+01	2.41E+01	98
13	1	4.0	PMMA front	4.48E+02	3.64E+04	3.54E+04	3.68E+07	3.10E+04	1.51E+08	1.11E+10	2.21E+08	1.79E+10	1.45E+10	3.12E+09	2.44E-01	8.84E-04	5.02E+00	3.27E+01	1.20E+01	50
14	1	4.0	PMMA back	9.93E+01	2.43E+04	7.76E+03	2.62E+07	7.38E+03	1.29E+08	9.97E+09	1.57E+08	1.20E+10	3.19E+09	6.93E+08	2.19E-01	6.29E-04	3.35E+00	7.17E+00	2.66E+00	13
15	1	4.0	Tree	4.21E+02	3.39E+04	3.62E+04	3.15E+07	3.50E+04	8.78E+07	5.45E+09	1.89E+08	1.67E+10	1.49E+10	2.94E+09	1.20E-01	7.56E-04	4.66E+00	3.43E+01	1.13E+01	50
16	1	4.0	Tree	4.68E+02	3.19E+04	3.67E+04	3.09E+07	N/A	N/A	N/A	1.86E+08	1.51E+10	1.51E+10	3.27E+09	N/A	7.42E-04	4.39E+00	3.39E+01	1.25E+01	51
17	2	2.0	Tree	4.93E+03	1.88E+05	3.70E+05	1.39E+08	3.58E+05	3.81E+08	2.34E+10	8.32E+08	9.27E+10	1.52E+11	3.44E+10	5.15E-01	3.33E-03	2.60E+01	3.37E+02	1.32E+02	496
18	2	2.0	Tree	4.85E+03	1.71E+05	3.64E+05	1.39E+08	3.99E+05	4.12E+08	2.64E+10	8.35E+08	8.41E+10	1.50E+11	3.38E+10	5.82E-01	3.34E-03	2.35E+01	3.33E+02	1.30E+02	487
19	2	2.0	Tree	5.47E+03	1.74E+05	4.11E+05	1.37E+08	3.96E+05	3.90E+08	2.45E+10	8.24E+08	8.55E+10	1.69E+11	3.82E+10	5.39E-01	3.29E-03	2.39E+01	3.75E+02	1.47E+02	546
20	2	2.0	Tree	5.61E+03	1.65E+05	4.07E+05	1.30E+08	4.10E+05	4.00E+08	2.62E+10	7.78E+08	8.11E+10	1.67E+11	3.91E+10	5.76E-01	3.11E-03	2.27E+01	3.68E+02	1.50E+02	541
21	2	3.0	BOMAB front	2.52E+03	1.70E+05	1.82E+05	1.56E+08	1.96E+05	7.66E+08	5.90E+10	9.38E+08	8.37E+10	7.48E+10	1.76E+10	1.30E+00	3.75E-03	2.34E+01	1.64E+02	6.76E+01	256
22	2	3.0	BOMAB back	3.83E+02	7.33E+04	2.52E+04	7.66E+07	2.89E+04	3.85E+08	2.99E+10	4.60E+08	3.61E+10	1.04E+10	2.67E+09	6.57E-01	1.84E-03	1.01E+01	2.20E+01	1.03E+01	43
23	2	3.0	BOMAB front	2.39E+03	1.78E+05	1.70E+05	1.57E+08	1.70E+05	7.38E+08	5.62E+10	9.44E+08	8.75E+10	7.00E+10	1.67E+10	1.24E+00	3.78E-03	2.45E+01	1.53E+02	6.40E+01	243
24	2	3.0	BOMAB back	3.45E+02	8.43E+04	2.84E+04	9.52E+07	2.80E+04	4.54E+08	3.48E+10	5.71E+08	4.15E+10	1.17E+10	2.41E+09	7.65E-01	2.28E-03	1.16E+01	2.66E+01	9.24E+00	48
25	2	4.0	PMMA front	1.71E+03	1.48E+05	1.25E+05	1.32E+08	1.31E+05	5.94E+08	4.47E+10	7.93E+08	7.30E+10	5.13E+10	1.20E+10	9.83E-01	3.17E-03	2.04E+01	1.13E+02	4.59E+01	180
26	2	4.0	PMMA back	3.65E+02	9.28E+04	3.02E+04	1.02E+08	3.17E+04	4.94E+08	3.79E+10	6.13E+08	4.56E+10	1.24E+10	2.54E+09	8.33E-01	2.45E-03	1.28E+01	2.83E+01	9.77E+00	52
27	2	2.5	Tree	3.47E+03	1.84E+05	2.89E+05	1.51E+08	2.60E+05	4.08E+08	2.48E+10	9.06E+08	9.05E+10	1.19E+11	2.42E+10	5.46E-01	3.63E-03	2.53E+01	2.71E+02	9.31E+01	390
28	2	2.5	Tree	3.56E+03	1.78E+05	2.86E+05	1.54E+08	2.72E+05	4.28E+08	2.65E+10	9.26E+08	8.74E+10	1.17E+11	2.48E+10	5.82E-01	3.71E-03	2.45E+01	2.65E+02	9.54E+01	386
29	2	4.0	Tree	1.59E+03	1.32E+05	1.23E+05	1.12E+08	1.20E+05	3.20E+08	2.01E+10	6.74E+08	6.49E+10	5.07E+10	1.11E+10	4.43E-01	2.70E-03	1.82E+01	1.14E+02	4.25E+01	175
30	2	4.0	Tree	1.58E+03	1.20E+05	1.22E+05	1.09E+08	1.27E+05	3.29E+08	2.13E+10	6.54E+08	5.92E+10	5.02E+10	1.10E+10	4.68E-01	2.62E-03	1.66E+01	1.12E+02	4.24E+01	172
31	2	4.0	Tree (backward)	1.52E+03	1.30E+05	1.39E+05	1.17E+08	1.32E+05	3.53E+08	2.29E+10	7.03E+08	6.40E+10	5.73E+10	1.06E+10	5.03E-01	2.81E-03	1.79E+01	1.34E+02	4.08E+01	193
32	2	4.0	Tree (backward)	1.50E+03	1.21E+05	1.27E+05	1.13E+08	1.24E+05	3.28E+08	2.08E+10	6.80E+08	5.96E+10	5.21E+10	1.05E+10	4.57E-01	2.72E-03	1.67E+01	1.19E+02	4.02E+01	177
33	3	2.5	tree	2.14E+03	1.04E+05	1.60E+05	8.81E+07	1.71E+05	2.50E+08	1.57E+10	5.29E+08	5.13E+10	6.58E+10	1.49E+10	3.44E-01	2.11E-03	1.44E+01	1.46E+02	5.73E+01	218
34	3	3.0	BOMAB front	1.49E+03	9.74E+04	1.19E+05	9.74E+07	1.09E+05	4.22E+08	3.14E+10	5.84E+08	4.79E+10	4.50E+10	1.04E+10	6.91E-01	2.34E-03	1.34E+01	9.94E+01	4.00E+01	154
35	3	3.0	BOMAB back	2.02E+02	4.83E+04	1.41E+04	4.52E+07	1.57E+04	2.45E+08	1.93E+10	2.71E+08	2.37E+10	5.81E+09	1.41E+09	4.25E-01	1.09E-03	6.65E+00	1.26E+01	5.40E+00	25
36	3	3.0	BOMAB front (lat.)	2.07E+02	4.89E+04	1.83E+04	5.22E+07	1.49E+04	2.78E+08	2.18E+10	3.13E+08	2.40E+10	7.54E+09	1.45E+09	4.80E-01	1.25E-03	6.73E+00	1.75E+01	5.56E+00	30
37	3	3.0	BOMAB back (lat.)	1.33E+03	1.01E+05	1.06E+05	9.61E+07	1.03E+05	4.39E+08	3.32E+10	5.76E+08	4.96E+10	4.36E+10	9.30E+09	7.31E-01	2.31E-03	1.39E+01	9.85E+01	3.57E+01	149
38	3	4.0	BOMAB front	1.02E+03	8.09E+04	7.64E+04	8.21E+07	7.09E+04	3.93E+08	3.01E+10	4.93E+08	3.98E+10	3.14E+10	7.12E+09	6.63E-01	1.97E-03	1.11E+01	6.97E+01	2.73E+01	109
39	3	4.0	BOMAB back	1.67E+02	3.88E+04	1.20E+04	3.51E+07	1.19E+04	1.74E+08	1.34E+10	2.11E+08	1.91E+10	4.94E+09	1.16E+09	2.96E-01	8.42E-04	5.35E+00	1.08E+01	4.47E+00	21
40	3	9.0	BOMAB back	2.38E+01	3.23E+03	1.62E+03	3.53E+06	2.21E+03	6.08E+07	5.54E+09	2.12E+07	1.59E+09	6.65E+08	1.66E+08	1.22E-01	8.47E-05	4.44E-01	1.43E+00	6.39E-01	3
41	3	9.0	BOMAB front	1.75E+02	1.37E+04	1.07E+04	1.27E+07	1.26E+04	6.03E+07	4.61E+09	7.59E+07	6.76E+09	4.40E+09	1.22E+09	1.01E-01	3.04E-04	1.89E+00	9.13E+00	4.68E+00	16
42	3	2.5	tree	2.19E+03	1.10E+05	1.66E+05	8.85E+07	1.77E+05	2.65E+08	1.71E+10	5.31E+08	5.44E+10	6.81E+10	1.53E+10	3.76E-01	2.13E-03	1.52E+01	1.52E+02	5.86E+01	226
43	3	4.0	tree	7.99E+02	8.04E+04	6.69E+04	7.54E+07	6.32E+04	2.30E+08	1.50E+10	4.53E+08	3.95E+10	2.75E+10	5.57E+09	3.30E-01	1.81E-03	1.11E+01	6.30E+01	2.14E+01	96
44	3	2.0	PMMA back	4.75E+02	7.27E+04	3.85E+04	8.10E+07	3.79E+04	3.71E+08	2.80E+10	4.86E+08	3.57E+10	1.58E+10	3.32E+09	6.17E-01	1.94E-03	1.00E+01	3.59E+01	1.27E+01	59
45	3	2.0	PMMA front	3.16E+03	1.59E+05	2.38E+05	1.33E+08	2.43E+05	6.19E+08	4.70E+10	7.99E+08	7.84E+10	9.78E+10	2.20E+10	1.03E+00	3.20E-03	2.20E+01	2.17E+02	8.46E+01	325
46	3	4.0	tree	8.21E+02	7.67E+04	6.39E+04	7.13E+07	6.74E+04	2.24E+08	1.48E+10	4.28E+08	3.78E+10	2.63E+10	5.73E+09	3.25E-01	1.71E-03	1.06E+01	5.89E+01	2.20E+01	92
61	1	2.0	Tree	1.34E+03	4.52E+04	9.67E+04	4.11E+07	9.83E+04	4.33E+07	2.09E+08	2.47E+08	2.22E+10	3.98E+10	9.36E+09	4.59E-03	9.88E-04	6.22E+00	8.72E+01	3.59E+01	129
62	1	2.0	Tree	1.28E+03	4.27E+04	1.07E+05	3.80E+07	1.04E+05	1.00E+08	6.00E+09	2.28E+08	2.10E+10	4.40E+10	8.90E+09	1.32E-01	9.12E-04	5.88E+00	1.01E+02	3.42E+01	141
63	2	2.0	Tree	4.67E+03	1.80E+05	3.50E+05	1.70E+08	3.63E+05	4.66E+08	2.87E+10	1.02E+09	8.84E+10	1.44E+11	3.26E+10	6.30E-01	4.07E-03	2.48E+01	3.19E+02	1.25E+02	469
64	2	2.0	Tree	4.91E+03	1.63E+05	3.58E+05	1.22E+08	3.41E+05	3.50E+08	2.21E+10	7.33E+08	8.04E+10	1.47E+11	3.43E+10	4.85E-01	2.93E-03	2.25E+01	3.24E+02	1.32E+02	479
65	3	2.0	Tree	2.61E+03	1.09E+05	2.10E+05	1.06E+08	2.17E+05	2.91E+08	1.79E+10	6.37E+08	5.34E+10	8.61E+10	1.82E+10	3.94E-01	2.55E-03	1.50E+01	1.95E+02	6.99E+01	280
66	3	2.0	Tree	2.75E+03	1.03E+05	2.13E+05	6.94E+07	2.11E+05	2.08E+08	1.34E+10	4.16E+08	5.08E+10	8.75E+10	1.92E+10	2.95E-01	1.67E-03	1.42E+01	1.96E+02	7.36E+01	284

Column calibration constants (header): C_{th} = 9.68E+01 (min-g-cm^{-2}); C_{epi} = 6.00E+00 (min-g-cm^{-2}); C_{Cu} = 4.92E+05 (min-g-cm^{-2}); C_{In} = 4.11E+05 (min-g-cm^{-2}); C_{S} = 6.98E+06 (min-g-cm^{-2}); $K_{\Phi th}$ = 2.20E-11 (rad-cm^{2}); $K_{\Phi epi}$ = 4.00E-12 (rad-cm^{2}); $K_{\Phi Cu}$ = 2.80E-10 (rad-cm^{2}); $K_{\Phi (In\text{-}S)}$ = 2.87E-09 (rad-cm^{2}); $K_{\Phi S}$ = 3.84E-09 (rad-cm^{2}).

Table H.2 FNAD Neutron Kerma Calculations

(First block — Φ_{th} and Φ_{epi} based on INDIUM foils)

Dosimeter #	Pulse #	Distance (m)	Geometry	Measured specific activity in foils							Fluence within designated energy bands (Φ_{th} and Φ_{epi} based on **INDIUM** foils)					Tissue kerma from fluence within energy bands					Kerma from total fluence
				A	B	C		D		E	F	G	< 0.4 eV	0.4 eV - 2 eV	2 eV - 0.5 MeV	> 1.2 MeV	> 2.9 MeV	< 0.4 eV	0.4 eV - 2 eV	2 eV - 0.5 MeV	1.2 MeV - 2.9 MeV	> 2.9 MeV	0.025 eV - 10 MeV
				S	Cu (Cd)	In (Cd)		In (bare)		Au	Au (Cd)	Au (bot)	C_{th} (min-g-cm^{-2})	C_{epi} (min-g-cm^{-2})	C_{Cu} (min-g-cm^{-2})	C_{In} (min-g-cm^{-2})	C_{S} (min-g-cm^{-2})	$K_{\Phi th}$ (rad-cm^2)	$K_{\Phi epi}$ (rad-cm^2)	$K_{\Phi Cu}$ (rad-cm^2)	$K_{\Phi (h-S)}$ (rad-cm^2)	$K_{\Phi S}$ (rad-cm^2)	
				P-32	Cu-64	I-115m	I-116m	I-115m	I-116m	Au-198	Au-198	Au-198	9.68E+01	6.00E+00	4.92E+05	4.11E+05	6.98E+06	2.20E-11	4.00E-12	2.80E-10	2.87E-09	3.84E-09	
				$A_\circ$ (dpm/g)	$A_\circ$ (dpm/g)	$A_\circ$ (dpm/g)	$A_\circ$ (dpm/g)	$A_\circ$ (dpm/g)	$A_\circ$ (dpm/g)	$A_\circ$ (dpm/g)	$A_\circ$ (dpm/g)	$A_\circ$ (dpm/g)	Φ_{th} (cm^{-2})	Φ_{epi} (cm^{-2})	Φ_{Cu} (cm^{-2})	Φ_{In} (cm^{-2})	Φ_{S} (cm^{-2})	K_{th} (rad)	K_{epi} (rad)	K_{Cu} (rad)	K_{In-S} (rad)	K_{S} (rad)	K_{total} (rad)
71	1	4	air	4.02E+02	3.78E+04	3.94E+04	<1.9E+11	3.21E+04	< 1.5E+11	6.98E+05	2.51E+05	1.45E+06	-	-	1.86E+10	1.62E+10	2.81E+09	-	-	5.21E+00	3.84E+01	1.08E+01	54
72	2	4	air	1.48E+03	1.51E+05	1.25E+05	1.18E+08	1.30E+05	3.79E+08	2.24E+06	9.47E+05	5.36E+06	2.52E+10	7.09E+08	7.42E+10	5.14E+10	1.04E+10	5.55E-01	2.84E-03	2.08E+01	1.18E+02	3.98E+01	179
73	3	4	air	8.65E+02	8.60E+04	7.16E+04	6.50E+07	7.61E+04	2.29E+08	1.46E+06	5.66E+05	3.12E+06	1.59E+10	3.90E+08	4.23E+10	2.94E+10	6.04E+09	3.49E-01	1.56E-03	1.19E+01	6.71E+01	2.32E+01	103

(Second block — Φ_{th} and Φ_{epi} based on GOLD foils)

Dosimeter #	Pulse #	Distance (m)	Geometry	Measured specific activity in foils							Fluence within designated energy bands (Φ_{th} and Φ_{epi} based on **GOLD** foils)					Tissue kerma from fluence within energy bands					Kerma from total fluence
				A	B	C		D		E	F	G	< 0.4 eV	0.4 eV - 2 eV	2 eV - 0.5 MeV	> 1.2 MeV	> 2.9 MeV	< 0.4 eV	0.4 eV - 2 eV	2 eV - 0.5 MeV	1.2 MeV - 2.9 MeV	> 2.9 MeV	0.025 eV - 10 MeV
				S	Cu (Cd)	In (Cd)		In (bare)		Au	Au (Cd)	Au (bot)	C_{th-Au} (min-g-cm^{-2})	C_{epi-Au} (min-g-cm^{-2})	C_{Cu} (min-g-cm^{-2})	C_{In} (min-g-cm^{-2})	C_{S} (min-g-cm^{-2})	$K_{\Phi th}$ (rad-cm^2)	$K_{\Phi epi}$ (rad-cm^2)	$K_{\Phi Cu}$ (rad-cm^2)	$K_{\Phi (h-S)}$ (rad-cm^2)	$K_{\Phi S}$ (rad-cm^2)	
				P-32	Cu-64	I-115m	I-116m	I-115m	I-116m	Au-198	Au-198	Au-198	1.86E+04	1.18E+03	4.92E+05	4.11E+05	6.98E+06	2.20E-11	4.00E-12	2.80E-10	2.87E-09	3.84E-09	
				$A_\circ$ (dpm/g)	$A_\circ$ (dpm/g)	$A_\circ$ (dpm/g)	$A_\circ$ (dpm/g)	$A_\circ$ (dpm/g)	$A_\circ$ (dpm/g)	$A_\circ$ (dpm/g)	$A_\circ$ (dpm/g)	$A_\circ$ (dpm/g)	Φ_{th} (cm^{-2})	Φ_{epi} (cm^{-2})	Φ_{Cu} (cm^{-2})	Φ_{In} (cm^{-2})	Φ_{S} (cm^{-2})	K_{th} (rad)	K_{epi} (rad)	K_{Cu} (rad)	K_{In-S} (rad)	K_{S} (rad)	K_{total} (rad)
71	1	4	air	4.02E+02	3.78E+04	3.94E+04	<1.9E+11	3.21E+04	< 1.5E+11	6.98E+05	2.51E+05	1.45E+06	8.32E+09	2.96E+08	1.86E+10	1.62E+10	2.81E+09	1.83E-01	1.18E-03	5.21E+00	3.84E+01	1.08E+01	55
72	2	4	air	1.48E+03	1.51E+05	1.25E+05	1.18E+08	1.30E+05	3.79E+08	2.24E+06	9.47E+05	5.36E+06	2.40E+10	1.12E+09	7.42E+10	5.14E+10	1.04E+10	5.28E-01	4.47E-03	2.08E+01	1.18E+02	3.98E+01	179
73	3	4	air	8.65E+02	8.60E+04	7.16E+04	6.50E+07	7.61E+04	2.29E+08	1.46E+06	5.66E+05	3.12E+06	1.67E+10	6.68E+08	4.23E+10	2.94E+10	6.04E+09	3.68E-01	2.67E-03	1.19E+01	6.71E+01	2.32E+01	103

(Third block)

Dosimeter #	Pulse #	Distance (m)	Geometry	Specific Activity of sulfur pellets	Activity to absorbed dose conversion factor	Absorbed dose from sulfur pellet pack	Specific Activity of inner gold foil	Activity to tissue kerma conversion factor	Tissue kerma
				A			G		
				S			Au (bot)		
				P-32	(rad-g-min)	(rad)	Au-198	(rad-g-min)	(rad)
				$A_\circ$ (dpm/g)			$A_\circ$ (dpm/g)		
71	1	4	air	4.02E+02	8.32E-02	33	1.45E+06	4.70E-05	68
72	2	4	air	1.48E+03	8.32E-02	123	5.36E+06	4.70E-05	252
73	3	4	air	8.65E+02	8.32E-02	72	3.12E+06	4.70E-05	147

Table H.3 Kerma Response and Dose Response of PNAD Foils

Dosimeter #	Pulse #	distance (m)	Position #	phantom type	location on phantom	mounting on phantom	Given Kerma, K (cGy)	Measured Kerma, K (cGy)	M/G	Given Dose, $D_p(10)_n$ (cGy)	Reported Dose, $D_p(10)_n$ (cGy)	R/G
1	1	2.0	1	Tree A-D	air	normal	160	130	0.81	214	130	0.61
2	1	2.0	1	Tree A-D	air	normal	160	133	0.83	214	133	0.62
3	1	2.0	2	Tree A-D	air	normal	153	120	0.78	205	120	0.59
4	1	2.0	2	Tree A-D	air	normal	153	137	0.89	205	137	0.67
62	1	2.0	2	Tree A-D	air	normal	153	141	0.92	205	141	0.69
17	2	2.0	1	Tree A-D	air	normal	570	496	0.87	764	496	0.65
18	2	2.0	1	Tree A-D	air	normal	570	487	0.85	764	487	0.64
19	2	2.0	3	Tree A-D	air	normal	568	546	0.96	761	546	0.72
20	2	2.0	3	Tree A-D	air	normal	568	541	0.95	761	541	0.71
64	2	2.0	2	Tree A-D	air	normal	547	479	0.88	732	479	0.65
66	3	2.0	2	Tree A-D	air	normal	330	284	0.86	442	284	0.64
							10 mil foils	mean stdev n	0.87 0.06 11	10 mil foils	mean stdev n	0.65 0.04 11

Dosimeter #	Pulse #	distance (m)	Position #	phantom type	location on phantom	mounting on phantom	Given Kerma, K (cGy)	Measured Kerma, K (cGy)	M/G	Given Dose, $D_p(10)_n$ (cGy)	Reported Dose, $D_p(10)_n$ (cGy)	R/G
61	1	2.0	2	Tree A-D	air	normal	153	129	0.85	205	129	0.63
63	2	2.0	2	Tree A-D	air	normal	547	469	0.86	732	469	0.64
65	3	2.0	2	Tree A-D	air	normal	330	280	0.85	442	280	0.63
							5 mil foils	mean stdev n	0.85 0.01 3	5 mil foils	mean stdev n	0.64 0.01 3

Dosimeter #	Pulse #	distance (m)	Position #	phantom type	location on phantom	mounting on phantom	Given Kerma, K (cGy)	Measured Kerma, K (cGy)	M/G	Given Dose, $D_p(10)_n$ (cGy)	Reported Dose, $D_p(10)_n$ (cGy)	R/G
9	1	2.5	6	Tree A-D	air	normal	117	92	0.79	159	92	0.58
10	1	2.5	6	Tree A-D	air	normal	117	98	0.84	159	98	0.62
11	1	2.5	6	Tree A-D	air	normal	117	90	0.77	159	90	0.56
12	1	2.5	6	Tree A-D	air	normal	117	98	0.83	159	98	0.61
27	2	2.5	6	Tree A-D	air	normal	417	390	0.94	570	390	0.68
28	2	2.5	6	Tree A-D	air	normal	417	386	0.93	570	386	0.68
33	3	2.5	6	Tree A-D	air	normal	252	218	0.86	344	218	0.63
42	3	2.5	6	Tree A-D	air	normal	252	226	0.90	344	226	0.66
							10 mil foils	mean stdev n	0.86 0.06 8	10 mil foils	mean stdev n	0.63 0.04 8

Dosimeter #	Pulse #	distance (m)	Position #	phantom type	location on phantom	mounting on phantom	Given Kerma, K (cGy)	Measured Kerma, K (cGy)	M/G	Given Dose, $D_p(10)_n$ (cGy)	Reported Dose, $D_p(10)_n$ (cGy)	R/G
15	1	4.0	8	Tree A-H	air	normal	66	50	0.76	92	50	0.55
16	1	4.0	8	Tree A-H	air	normal	66	51	0.77	92	51	0.55
29	2	4.0	8	Tree A-H	air	normal	237	175	0.74	329	175	0.53
30	2	4.0	8	Tree A-H	air	normal	237	172	0.73	329	172	0.52
31	2	4.0	8	Tree A-H	air	backward	237	193	0.81	329	193	0.59
32	2	4.0	8	Tree A-H	air	backward	237	177	0.75	329	177	0.54
43	3	4.0	9	Tree A-H	air	normal	143	96	0.67	199	96	0.48
46	3	4.0	9	Tree A-H	air	normal	143	92	0.64	199	92	0.46
							10 mil foils	mean stdev n	0.73 0.06 8	10 mil foils	mean stdev n	0.53 0.04 8
5	1	3.0	4	BOMAB	front	normal	90	67	0.75	123	67	0.55
7	1	3.0	5	BOMAB	front	normal	92	64	0.70	126	64	0.51
21	2	3.0	4	BOMAB	front	normal	323	256	0.79	441	256	0.58
23	2	3.0	5	BOMAB	front	normal	329	243	0.74	450	243	0.54
34	3	3.0	4	BOMAB	front	normal	195	154	0.79	266	154	0.58
							10 mil foils	mean stdev n	0.75 0.04 5	10 mil foils	mean stdev n	0.55 0.03 5
38	3	4.0	7	BOMAB	front	normal	139	109	0.78	192	109	0.57
41	3	9.0	10	BOMAB	front	normal	27	16	0.59	85	16	0.19
45	3	2.0	3	PMMA	front	normal	343	325	0.95	459	325	0.71
13	1	4.0	7	PMMA	front	normal	64	50	0.78	89	50	0.56
25	2	4.0	7	PMMA	front	normal	230	180	0.78	319	180	0.56
							10 mil foils	mean stdev n	0.78 0.00 2	10 mil foils	mean stdev n	0.56 0.00 2

Dosimeter #	Pulse #	distance (m)	Position #	phantom type	location on phantom	mounting on phantom	Given Kerma, K (cGy)	Measured Kerma, K (cGy)	M/G	Given Dose, $D_p(10)_n$ (cGy)	Reported Dose, $D_p(10)_n$ (cGy)	R/G
36	3	3.0	5	BOMAB - LAT	side	normal	198	30	0.15	271	30	0.11
37	3	3.0	5	BOMAB - LAT	side	normal	198	149	0.75	271	149	0.55
							10 mil foils	mean stdev n	0.45 0.42 2	10 mil foils	mean stdev n	0.33 0.31 2
6	1	3.0	4	BOMAB	back	normal	90	13	0.15	123	13	0.11
8	1	3.0	5	BOMAB	back	normal	92	13	0.14	126	13	0.11
22	2	3.0	4	BOMAB	back	normal	323	43	0.13	441	43	0.10
24	2	3.0	5	BOMAB	back	normal	329	48	0.15	450	48	0.11
35	3	3.0	4	BOMAB	back	normal	195	25	0.13	266	25	0.09
							10 mil foils	mean stdev n	0.14 0.01 5	10 mil foils	mean stdev n	0.10 0.01 5
39	3	4.0	7	BOMAB	back	normal	139	21	0.15	192	21	0.11
40	3	9.0	10	BOMAB	back	normal	27	3	0.10	85	3	0.03
44	3	2.0	1	PMMA	back	normal	344	59	0.17	461	59	0.13
14	1	4.0	9	PMMA	back	normal	66	13	0.20	92	13	0.15
26	2	4.0	9	PMMA	back	normal	237	52	0.22	330	52	0.16
							10 mil foils	mean stdev n	0.21 0.01 2	10 mil foils	mean stdev n	0.15 0.01 2

Table H.4 Summary of Bias in PNAD Foil Measured Kerma and Reported Dose

distance (m)	phantom type	location on phantom	foil thickness	Kerma K		Neutron Dose $D_p(10)_n$	
				Measured / Given	B	Reported / Given	B
2.0	Tree A-D	air	10 mil	0.87	-0.13	0.65	-0.35
2.0	Tree A-D	air	5 mil	0.85	-0.15	0.64	-0.36
2.5	Tree A-D	air	10 mil	0.86	-0.14	0.63	-0.37
4.0	Tree A-H	air	10 mil	0.73	-0.27	0.53	-0.47
3.0	BOMAB	front	10 mil	0.75	-0.25	0.55	-0.45
4.0	BOMAB	front	10 mil	0.78	-0.22	0.57	-0.43
9.0	BOMAB	front	10 mil	0.59	-0.41	0.19	-0.81
2.0	PMMA	front	10 mil	0.95	-0.05	0.71	-0.29
4.0	PMMA	front	10 mil	0.78	-0.22	0.56	-0.44
3.0	BOMAB - LAT	side	10 mil	0.45	-0.55	0.33	-0.67
3.0	BOMAB	back	10 mil	0.14	-0.86	0.10	-0.90
4.0	BOMAB	back	10 mil	0.15	-0.85	0.11	-0.89
9.0	BOMAB	back	10 mil	0.10	-0.90	0.03	-0.97
2.0	PMMA	back	10 mil	0.17	-0.83	0.13	-0.87
4.0	PMMA	back	10 mil	0.21	-0.79	0.15	-0.85

Table H.5 Kerma and Dose Response of FNAD Foils

Dosimeter #	Pulse #	distance (m)	Position #	Given Kerma K (cGy)	Measured Kerma K (cGy)*	Measured / Given	Given Dose, $D*(10)_n$ (cGy)	Reported Dose, $D*(10)_n$ (cGy)*	Reported / Given
71	1	4.0	11	65	55	0.84	88	55	0.62
72	2	4.0	11	235	179	0.76	313	179	0.57
73	3	4.0	11	142	103	0.72	189	103	0.54
					mean	0.77		mean	0.58
					stdev	0.06		stdev	0.04
					n	3		n	3

* Measured kerma was the same (within 1%) whether thermal and epithermal fluence calculations were based on indium foils or gold foils.

Appendix I

microStar® **Reader Calibration Factors**

Table I.1 PNAD Reader Calibration Factors Applied to Element Readings by microStar® 5.0 Software During Exercise

PNAD InLight									
Reader Serial Number	Reader Type	Reader Environment	Calibration ID	Calibraton Name	Dose Range	Badge Type	Calibration Date/Time	Calibration Factor (counts / unit of dose)	Dose Units
11040683	Protection Level	PNAD LD	51	Co-60 (strong beam)	0.005 cGy - 10 cGy	InLight	1/5/2016 7:10 PM	12268	cGy
11040683	Protection Level	PNAD LD	52	Co-60 (weak beam)	10 cGy - 1000 cGy	InLight	1/5/2016 7:54 PM	895	cGy
14240805	Accident Level	PNAD HD	69	Co-60 (strong beam)	0.1 cGy - 75 cGy	InLight	1/4/2016 2:43 PM	639	cGy
14240805	Accident Level	PNAD HD	71	Co-60 (weak beam)	75 cGy - 10,000 cGy	InLight	1/4/2016 5:03 PM	35	cGy

Table I.2 FNAD Reader Calibration Factors Applied to Element Readings by microStar® 5.0 Software During Exercise

FNAD nanoDot									
Reader Serial Number	Reader Type	Reader Environment	Calibration ID	Calibraton Name	Dose Range	Badge Type	Calibration Date/Time	Calibration Factor (counts / unit of dose)	Dose Units
11040683	Protection Level	FNAD LD	68	Co-60 (strong beam)	0.005 cGy - 10 cGy	nanoDot	1/10/2016 7:14 PM	8420	cGy
11040683	Protection Level	FNAD LD	69	Co-60 (weak beam)	10 cGy - 1000 cGy	nanoDot	1/10/2016 7:30 PM	679	cGy
14240805	Accident Level	FNAD HD	73	Co-60 (strong beam)	0.1 cGy - 75 cGy	nanoDot	1/12/2016 1:30 PM	409	cGy
14240805	Accident Level	FNAD HD	72	Co-60 (weak beam)	75 cGy - 10,000 cGy	nanoDot	1/11/2016 9:17 PM	25	cGy

Appendix J

InLight[®] **OSLN Dosimeter Readings**

Table J.1 PNAD InLight® Readings and Calculated Doses Using Default Gamma and Neutron Calibration Factors

PNAD #	Pulse #	Distance (m)	Position #	phantom type	dosimeter location on phantom	mounting on phantom	Reader	InLight BA Case Serial Number	Reader Calibration ID	Element 1 average converted value (mrad)	Element 2 average converted value (mrad)	Element 3 average converted value (mrad)	Element 4 average converted value (mrad)	(E3+E4)/2 (mrad)	Gamma calibration factor used	Reported Gamma Dose Dp(10)γ (cGy)	Given Dp(10)γ (rad)	R/G	Co-60 equivalent neutron signal (E2-E1) (mrad)	Neutron calibration factor used	Reported Neutron Dose Dp(10)n (cGy)	Given Dp(10)n (cGy)	R/G	(E2-E1)/Dp(10)n (cGy/cGy)
1	1	2	1	Tree A-D	air	normal	LD	BA00098569H	52	28941	413772	33891	33472	33682	1.00	34	22	1.53	384830	2.73	141	214	0.66	1.80
2	1	2	1	Tree A-D	air	normal	LD	BA00099010D	52	29460	409825	32692	31177	31934	1.00	32	22	1.45	380366	2.73	139	214	0.65	1.78
3	1	2	2	Tree A-D	air	normal	LD	BA00097638L	52	29083	381087	32001	31480	31741	1.00	32	22	1.44	352005	2.73	129	205	0.63	1.72
4	1	2	2	Tree A-D	air	normal	LD	BA00130036J	52	30193	379421	32483	32025	32254	1.00	32	22	1.47	349228	2.73	128	205	0.62	1.70
5	1	3	4	BOMAB	front	normal	LD	BA00129701B	52	31349	790469	36397	34016	35206	1.00	35	14	2.51	759120	2.73	278	123	2.26	6.17
6	1	3	4	BOMAB	back	normal	LD	BA00098095W	52	19719	461072	22776	22311	22543	1.00	23	14	1.61	441353	2.73	162	123	1.32	3.59
7	1	3	5	BOMAB	front	normal	LD	BA001124983	52	29556	759712	34661	33735	34198	1.00	34	14	2.44	730156	2.73	268	126	2.12	5.79
8	1	3	5	BOMAB	back	normal	LD	BA00098462X	52	21568	570241	25820	23955	24887	1.00	25	14	1.78	548673	2.73	201	126	1.60	4.35
9	1	2.5	6	Tree A-D	air	normal	LD	BA00097716P	52	25334	436603	29337	28840	29088	1.00	29	17	1.71	411269	2.73	151	159	0.95	2.59
10	1	2.5	6	Tree A-D	air	normal	LD	BA00130514F	52	25932	431211	29183	28898	29040	1.00	29	17	1.71	405279	2.73	149	159	0.93	2.55
11	1	2.5	6	Tree A-D	air	normal	LD	BA000931090	52	25412	422957	28930	27158	28044	1.00	28	17	1.65	397545	2.73	146	159	0.92	2.50
12	1	2.5	6	Tree A-D	air	normal	LD	BA000883423	52	25404	434292	28293	27617	27955	1.00	28	17	1.64	408888	2.73	150	159	0.94	2.57
13	1	4	7	PMMA	front	normal	LD	BA00094689H	52	20861	693365	24809	24135	24472	1.00	24	11	2.22	672504	2.73	247	89	2.77	7.56
14	1	4	9	PMMA	back	normal	LD	BA00093799F	52	16261	554777	19827	19677	19752	1.00	20	11	1.80	538516	2.73	197	92	2.15	5.85
15	1	4	8	Tree A-H	air	normal	LD	BA00112043Q	52	16600	368160	18707	17764	18235	1.00	18	11	1.66	351560	2.73	129	92	1.40	3.82
16	1	4	8	Tree A-H	air	normal	LD	BA001155475	52	16371	356034	18514	17687	18101	1.00	18	11	1.65	339663	2.73	125	92	1.35	3.69
17	2	2	1	Tree A-D	air	normal	HD	BA00129695W	71	120679	1481648	123891	122371	123131	1.00	123	78	1.58	1360968	2.73	499	764	0.65	1.78
18	2	2	1	Tree A-D	air	normal	HD	BA00129074C	71	115215	1429082	125126	123526	124326	1.00	124	78	1.59	1313867	2.73	482	764	0.63	1.72
19	2	2	3	Tree A-D	air	normal	HD	BA00098763P	71	113912	1500111	128052	125297	126675	1.00	127	78	1.62	1386199	2.73	508	761	0.67	1.82
20	2	2	3	Tree A-D	air	normal	HD	BA00099789A	71	128750	1574762	129481	127446	128464	1.00	128	78	1.65	1446012	2.73	530	761	0.70	1.90
21	2	3	4	BOMAB	front	normal	HD	BA00098475Q	71	122051	2696244	133391	130613	132002	1.00	132	50	2.64	2574193	2.73	944	441	2.14	5.84
22	2	3	4	BOMAB	back	normal	HD	BA00098722V	71	72142	1561318	85345	79973	82659	1.00	83	50	1.65	1489176	2.73	546	441	1.24	3.38
23	2	3	5	BOMAB	front	normal	HD	BA00111098C	71	121136	3053913	136580	127572	132076	1.00	132	50	2.64	2932776	2.73	1075	450	2.39	6.52
24	2	3	5	BOMAB	back	normal	HD	BA000923154	71	75343	1711277	84339	82819	83579	1.00	84	50	1.67	1635934	2.73	600	450	1.33	3.64
25	2	4	7	PMMA	front	normal	HD	BA001138158	71	74051	2212348	85974	86031	86003	1.00	86	40	2.15	2138297	2.73	784	319	2.46	6.70
26	2	4	9	PMMA	back	normal	HD	BA00098366R	71	53910	1898081	68473	67215	67844	1.00	68	40	1.70	1844172	2.73	676	330	2.05	5.59
27	2	2.5	6	Tree A-D	air	normal	HD	BA00111119G	71	99211	1518822	107087	107305	107196	1.00	107	61	1.76	1419610	2.73	520	570	0.91	2.49
28	2	2.5	6	Tree A-D	air	normal	HD	BA00111701L	71	101292	1544144	107545	107853	107699	1.00	108	61	1.77	1442852	2.73	529	570	0.93	2.53
29	2	4	8	Tree A-H	air	normal	HD	BA00097672T	71	59579	1219919	67067	64392	65729	1.00	66	40	1.64	1160339	2.73	425	329	1.29	3.53
30	2	4	8	Tree A-H	air	normal	HD	BA00097708M	71	60688	1250619	66187	62529	64358	1.00	64	40	1.61	1189930	2.73	436	329	1.33	3.62
31	2	4	8	Tree A-H	air	backward	HD	BA00110981A	71	58196	1225598	67261	64643	65952	1.00	66	40	1.65	1167402	2.73	428	329	1.30	3.55
32	2	4	8	Tree A-H	air	backward	HD	BA00110998V	71	61111	1233582	67433	66712	67073	1.00	67	40	1.68	1172470	2.73	430	329	1.31	3.56
33	3	2.5	6	Tree A-D	air	normal	LD	BA00098209T	52	61690	942661	68083	65763	66923	1.00	67	37	1.81	880972	2.73	323	344	0.94	2.56
34	3	3	4	BOMAB	front	normal	LD	BA000883712	52	69381	1705978	81575	80363	80969	1.00	81	30	2.70	1636597	2.73	600	266	2.26	6.15
35	3	3	4	BOMAB	back	normal	HD	BA00098318S	71	44456	1003705	51715	49463	50589	1.00	51	30	1.69	959249	2.73	352	266	1.32	3.61
36	3	3	5	BOMAB - LAT	side	normal	HD	BA00097976012	71	45039	1066476	52789	50034	51412	1.00	51	30	1.71	1021437	2.73	375	271	1.38	3.77
37	3	3	5	BOMAB - LAT	side	normal	HD	BA00097742U	71	68541	1654981	77721	74291	76006	1.00	76	30	2.53	1586440	2.73	582	271	2.15	5.85
38	3	4	7	BOMAB	front	normal	LD	BA001113697	52	54355	1613277	66466	65880	66173	1.00	66	24	2.76	1558923	2.73	572	192	2.98	8.12
39	3	4	7	BOMAB	back	normal	LD	BA00097925M	52	33393	737482	40920	39300	40110	1.00	40	24	1.67	704087	2.73	258	192	1.34	3.67
40	3	9	10	BOMAB	back	normal	LD	BA00098804R	52	5059	80903	5752	5789	5770	1.00	6	13	0.45	75844	2.73	28	85	0.33	0.89
41	3	9	10	BOMAB	front	normal	LD	BA000911357	52	8523	246049	10510	10760	10635	1.00	11	13	0.82	237526	2.73	87	85	1.02	2.79
42	3	2.5	6	Tree A-D	air	normal	HD	BA00094794O	71	58402	907052	66484	62026	64255	1.00	64	37	1.74	848650	2.73	311	344	0.90	2.47
43	3	4	9	Tree A-H	air	normal	HD	BA000884132	71	33676	815858	37403	37723	37563	1.00	38	24	1.57	782182	2.73	287	199	1.44	3.93
44	3	2	1	PMMA	back	normal	HD	BA00114014P	71	62780	1552786	70713	70370	70542	1.00	71	47	1.50	1490006	2.73	546	461	1.19	3.23
45	3	2	3	PMMA	front	normal	HD	BA00088219U	71	103647	2411937	118439	115809	117124	1.00	117	47	2.49	2308290	2.73	846	459	1.84	5.03
46	3	4	9	Tree A-H	air	normal	HD	BA00097796H	71	35185	797724	38683	35974	37329	1.00	37	24	1.56	762538	2.73	280	199	1.40	3.83

Table J.2 PNAD InLight® Readings and Calculated Doses Using Optimal Gamma and Neutron Calibration Factors

PNAD #	Pulse #	Distance (m)	Position #	phantom type	dosimeter location on phantom	mounting on phantom	Reader	InLight BA Case Serial Number	Reader Calibration ID	Element 1 average converted value (mrad)	Element 2 average converted value (mrad)	Element 3 average converted value (mrad)	Element 4 average converted value (mrad)	(E3+E4)/2 (mrad)	Gamma calibration factor used	Reported Gamma Dose Dp(10)γ (cGy)	Given Dp(10)γ (rad)	R/G	Co-60 equivalent neutron signal (E2-E1) (mrad)	Neutron calibration factor used	Reported Neutron Dose Dp(10)n (cGy)	Given Dp(10)n (cGy)	R/G	(E2-E1)/Dp(10)n (cGy/cGy)
1	1	2	1	Tree A-D	air	normal	LD	BA00098569H	52	28941	413772	33891	33472	33682	2.59	13	22	0.59	384830	6.09	63	214	0.30	1.80
2	1	2	1	Tree A-D	air	normal	LD	BA00099010D	52	29460	409825	32692	31177	31934	2.59	12	22	0.56	380366	6.09	62	214	0.29	1.78
3	1	2	2	Tree A-D	air	normal	LD	BA00097638L	52	29083	381087	32001	31480	31741	2.59	12	22	0.56	352005	6.09	58	205	0.28	1.72
4	1	2	2	Tree A-D	air	normal	LD	BA00130036J	52	30193	379421	32483	32025	32254	2.59	12	22	0.57	349228	6.09	57	205	0.28	1.70
5	1	3	4	BOMAB	front	normal	LD	BA00129701B	52	31349	790469	36397	34016	35206	2.59	14	14	0.97	759120	6.09	125	123	1.01	6.17
6	1	3	4	BOMAB	back	normal	LD	BA00098095W	52	19719	461072	22776	22311	22543	2.59	9	14	0.62	441353	6.09	72	123	0.59	3.59
7	1	3	5	BOMAB	front	normal	LD	BA001124983	52	29556	759712	34661	33735	34198	2.59	13	14	0.94	730156	6.09	120	126	0.95	5.79
8	1	3	5	BOMAB	back	normal	LD	BA00098462X	52	21568	570241	25820	23955	24887	2.59	10	14	0.69	548673	6.09	90	126	0.71	4.35
9	1	2.5	6	Tree A-D	air	normal	LD	BA00097716P	52	25334	436603	29337	28840	29088	2.59	11	17	0.66	411269	6.09	67	159	0.42	2.59
10	1	2.5	6	Tree A-D	air	normal	LD	BA00130514F	52	25932	431211	29183	28898	29040	2.59	11	17	0.66	405279	6.09	66	159	0.42	2.55
11	1	2.5	6	Tree A-D	air	normal	LD	BA000931090	52	25412	422957	28930	27158	28044	2.59	11	17	0.64	397545	6.09	65	159	0.41	2.50
12	1	2.5	6	Tree A-D	air	normal	LD	BA000883423	52	25404	434292	28293	27617	27955	2.59	11	17	0.64	408888	6.09	67	159	0.42	2.57
13	1	4	7	PMMA	front	normal	LD	BA0094689H	52	20861	693365	24809	24135	24472	2.59	9	11	0.86	672504	6.09	110	89	1.24	7.56
14	1	4	9	PMMA	back	normal	LD	BA0093799F	52	16261	554777	19827	19677	19752	2.59	8	11	0.69	538516	6.09	88	92	0.96	5.85
15	1	4	8	Tree A-H	air	normal	LD	BA00112043Q	52	16600	368160	18707	17764	18235	2.59	7	11	0.64	351560	6.09	58	92	0.63	3.82
16	1	4	8	Tree A-H	air	normal	LD	BA001155475	52	16371	356034	18514	17687	18101	2.59	7	11	0.64	339663	6.09	56	92	0.61	3.69
17	2	2	1	Tree A-D	air	normal	HD	BA00129695W	71	120679	1481648	123891	122371	123131	2.59	48	78	0.61	1360968	6.09	223	764	0.29	1.78
18	2	2	1	Tree A-D	air	normal	HD	BA00129074C	71	115215	1429082	125126	123526	124326	2.59	48	78	0.62	1313867	6.09	216	764	0.28	1.72
19	2	2	3	Tree A-D	air	normal	HD	BA00098763P	71	113912	1500111	128052	125297	126675	2.59	49	78	0.63	1386199	6.09	227	761	0.30	1.82
20	2	2	3	Tree A-D	air	normal	HD	BA00099789A	71	128750	1574762	129481	127446	128464	2.59	50	78	0.64	1446012	6.09	237	761	0.31	1.90
21	2	3	4	BOMAB	front	normal	HD	BA00098475Q	71	122051	2696244	133391	130613	132002	2.59	51	50	1.02	2574193	6.09	422	441	0.96	5.84
22	2	3	4	BOMAB	back	normal	HD	BA00098722V	71	72142	1561318	85345	79973	82659	2.59	32	50	0.64	1489176	6.09	244	441	0.55	3.38
23	2	3	5	BOMAB	front	normal	HD	BA00111098C	71	121136	3053913	136580	127572	132076	2.59	51	50	1.02	2932776	6.09	481	450	1.07	6.52
24	2	3	5	BOMAB	back	normal	HD	BA000923154	71	75343	1711277	84339	82819	83579	2.59	32	50	0.65	1635934	6.09	268	450	0.60	3.64
25	2	4	7	PMMA	front	normal	HD	BA001138158	71	74051	2212348	85974	86031	86003	2.59	33	40	0.83	2138297	6.09	351	319	1.10	6.70
26	2	4	9	PMMA	back	normal	HD	BA00098366R	71	53910	1898081	68473	67215	67844	2.59	26	40	0.66	1844172	6.09	303	330	0.92	5.59
27	2	2.5	6	Tree A-D	air	normal	HD	BA00111119G	71	99211	1518822	107087	107305	107196	2.59	41	61	0.68	1419610	6.09	233	570	0.41	2.49
28	2	2.5	6	Tree A-D	air	normal	HD	BA00111701L	71	101292	1544144	107545	107853	107699	2.59	42	61	0.68	1442852	6.09	237	570	0.42	2.53
29	2	4	8	Tree A-H	air	normal	HD	BA00097672T	71	59579	1219919	67067	64392	65729	2.59	25	40	0.64	1160339	6.09	190	329	0.58	3.53
30	2	4	8	Tree A-H	air	normal	HD	BA00097708M	71	60688	1250619	66187	62529	64358	2.59	25	40	0.62	1189930	6.09	195	329	0.59	3.62
31	2	4	8	Tree A-H	air	backward	HD	BA00110981A	71	58196	1225598	67261	64643	65952	2.59	25	40	0.64	1167402	6.09	192	329	0.58	3.55
32	2	4	8	Tree A-H	air	backward	HD	BA00110998V	71	61111	1233582	67433	66712	67073	2.59	26	40	0.65	1172470	6.09	192	329	0.58	3.56
33	3	2.5	6	Tree A-D	air	normal	LD	BA00098209T	52	61690	942661	68083	65763	66923	2.59	26	37	0.70	880872	6.09	145	344	0.42	2.56
34	3	3	4	BOMAB	front	normal	LD	BA000883712	52	69381	1705978	81575	80363	80969	2.59	31	30	1.04	1636597	6.09	269	266	1.01	6.15
35	3	3	4	BOMAB	back	normal	HD	BA00098318S	71	44456	1003705	51715	49463	50589	2.59	20	30	0.65	959249	6.09	157	266	0.59	3.61
36	3	3	5	BOMAB - LAT	side	normal	HD	BA0009976012	71	45039	1066476	52789	50034	51412	2.59	20	30	0.66	1021437	6.09	168	271	0.62	3.77
37	3	3	5	BOMAB - LAT	side	normal	HD	BA00097742U	71	68541	1654981	77721	74291	76006	2.59	29	30	0.98	1586440	6.09	260	271	0.96	5.85
38	3	4	7	BOMAB	front	normal	LD	BA001113697	52	54355	1613277	66466	65880	66173	2.59	26	24	1.07	1558923	6.09	256	192	1.33	8.12
39	3	4	7	BOMAB	back	normal	LD	BA000097925M	52	33395	737482	40920	39300	40110	2.59	16	24	0.65	704087	6.09	116	192	0.60	3.67
40	3	9	10	BOMAB	back	normal	LD	BA00098804R	52	5059	80903	5752	5789	5770	2.59	2	13	0.17	75844	6.09	12	85	0.15	0.89
41	3	9	10	BOMAB	front	normal	LD	BA000911357	52	8523	246049	10510	10760	10635	2.59	4	13	0.32	237526	6.09	39	85	0.46	2.79
42	3	2.5	6	Tree A-D	air	normal	HD	BA0009479O	71	58402	907052	66484	62026	64255	2.59	25	37	0.67	848650	6.09	139	344	0.40	2.47
43	3	4	9	Tree A-H	air	normal	HD	BA000884132	71	33676	815858	37403	37723	37563	2.59	15	24	0.60	782182	6.09	128	199	0.64	3.93
44	3	2	1	PMMA	back	normal	HD	BA00114014P	71	62780	1552786	70713	70370	70542	2.59	27	47	0.58	1490006	6.09	244	461	0.53	3.23
45	3	2	3	PMMA	front	normal	HD	BA0088219U	71	103647	2411937	118439	115809	117124	2.59	45	47	0.96	2308290	6.09	379	459	0.83	5.03
46	3	4	9	Tree A-H	air	normal	HD	BA00097796H	71	35185	797724	38683	35974	37329	2.59	14	24	0.60	762538	6.09	125	199	0.63	3.83

Appendix K

nanoDot Dosimeter Readings

Table K.1 Hanford PNAD nanoDot Readings and Gamma Doses ($C_\gamma = 1.00$)

PNAD #	Pulse #	Reader Environment	nanoDot Serial Number	Reader Calibration ID	Beam Used	Element Sensitivity	Element1 Counts	Element 1 converted value (mrad)	Mean Reported $D_p(10)_\gamma$ (cGy)	C.V.	n
61	1	FNAD LD	DN08839586F	69	1	0.88	16684	27903			
61	1	FNAD LD	DN08839586F	69	1	0.88	16342	27331			
61	1	FNAD LD	DN08839586F	69	1	0.88	16598	27759			
61	1	FNAD LD	DN08738725L	69	1	0.87	17048	28839			
61	1	FNAD LD	DN08738725L	69	1	0.87	16395	27735			
61	1	FNAD LD	DN08738725L	69	1	0.87	16671	28202			
61	1	FNAD LD	DN09180863L	69	1	0.91	17457	28233			
61	1	FNAD LD	DN09180863L	69	1	0.91	16852	27255			
61	1	FNAD LD	DN09180863L	69	1	0.91	16771	27124	28	0.020	9
62	1	FNAD LD	DN088396798	69	1	0.88	16571	27714			
62	1	FNAD LD	DN088396798	69	1	0.88	16405	27436			
62	1	FNAD LD	DN088396798	69	1	0.88	16221	27129			
62	1	FNAD LD	DN08509689G	69	1	0.85	16975	29392			
62	1	FNAD LD	DN08509689G	69	1	0.85	16813	29111			
62	1	FNAD LD	DN08509689G	69	1	0.85	16444	28472			
62	1	FNAD LD	DN089359977	69	1	0.89	17743	29341			
62	1	FNAD LD	DN089359977	69	1	0.89	17137	28338			
62	1	FNAD LD	DN089359977	69	1	0.89	16833	27836	28	0.030	9
63	2	FNAD LD	DN08936000B	69	1	0.89	62441	103255			
63	2	FNAD LD	DN08936000B	69	1	0.89	62299	103020			
63	2	FNAD LD	DN08936000B	69	1	0.89	63002	104183			
63	2	FNAD LD	DN08932967D	69	1	0.89	64888	107301			
63	2	FNAD LD	DN08932967D	69	1	0.89	64496	106653			
63	2	FNAD LD	DN08932967D	69	1	0.89	64128	106045			
63	2	FNAD LD	DN08283273U	69	1	0.82	59559	106897			
63	2	FNAD LD	DN08283273U	69	1	0.82	58249	104546			
63	2	FNAD LD	DN08283273U	69	1	0.82	58677	105314	105	0.015	9
64	2	FNAD LD	DN08936627J	69	1	0.89	66267	109582			
64	2	FNAD LD	DN08936627J	69	1	0.89	65177	107779			
64	2	FNAD LD	DN08936627J	69	1	0.89	65809	108824			
64	2	FNAD LD	DN08936736I	69	1	0.89	64178	106127			
64	2	FNAD LD	DN08936736I	69	1	0.89	63943	105739			
64	2	FNAD LD	DN08936736I	69	1	0.89	63526	105049			
64	2	FNAD LD	DN09180887B	69	1	0.91	65838	106480			
64	2	FNAD LD	DN09180887B	69	1	0.91	65509	105948			
64	2	FNAD LD	DN09180887B	69	1	0.91	64844	104872	107	0.016	9
65	3	FNAD LD	DN08509687K	69	1	0.85	36462	63132			
65	3	FNAD LD	DN08509687K	69	1	0.85	36379	62989			
65	3	FNAD LD	DN08509687K	69	1	0.85	36208	62693			
65	3	FNAD LD	DN08839562P	69	1	0.88	37520	62750			
65	3	FNAD LD	DN08839562P	69	1	0.88	37315	62407			
65	3	FNAD LD	DN08839562P	69	1	0.88	36615	61236			
65	3	FNAD LD	DN09034080C	69	1	0.90	38009	62155			
65	3	FNAD LD	DN09034080C	69	1	0.90	38258	62562			
65	3	FNAD LD	DN09034080C	69	1	0.90	37621	61520	62	0.010	9
66	3	FNAD LD	DN08932984H	69	1	0.89	40688	67283			
66	3	FNAD LD	DN08932984H	69	1	0.89	39335	65046			
66	3	FNAD LD	DN08932984H	69	1	0.89	39623	65522			
66	3	FNAD LD	DN089360035	69	1	0.89	38116	63030			
66	3	FNAD LD	DN089360035	69	1	0.89	36614	60546			
66	3	FNAD LD	DN089360035	69	1	0.89	36553	60446			
66	3	FNAD LD	DN08736973I	69	1	0.87	38897	65800			
66	3	FNAD LD	DN08736973I	69	1	0.87	38304	64797			
66	3	FNAD LD	DN08736973I	69	1	0.87	38210	64638	64	0.037	9

Table K.2 Hanford PNAD nanoDot Gamma Doses Using Default Gamma Dose Calibration Factor $C_\gamma = 1.00$

PNAD #	Pulse #	Distance (m)	Position #	phantom type	dosimeter location on phantom	mounting on phantom	Given Gamma dose, $D_p(10)_\gamma$ (cGy)	Reported $D_p(10)_\gamma$ (cGy)	R/G
61	1	2	2	Tree A-D	air	normal	22	28	1.26
62	1	2	2	Tree A-D	air	normal	22	28	1.29
63	2	2	2	Tree A-D	air	normal	78	105	1.35
64	2	2	2	Tree A-D	air	normal	78	107	1.37
65	3	2	2	Tree A-D	air	normal	47	62	1.33
66	3	2	2	Tree A-D	air	normal	47	64	1.36

Table K.3 PNNL FNAD nanoDot Readings

FNAD #	dosimetry package	dot type	Pulse #	nanoDot Serial Number	Reader Calibration ID	Beam Used	Element 1 Sensitivity	Element1 Counts	Element 1 converted value (mrad)	average (cGy)	C.V.	n
71	outer	OSL	1	DN088396889	68	2	0.88	101658	13719			
71	outer	OSL	1	DN088396889	68	2	0.88	100060	13503			
71	outer	OSL	1	DN088396889	68	2	0.88	99143	13380	14	0.013	3
71	outer	OSLN	1	DY02603335U	69	1	0.26	72471	410225			
71	outer	OSLN	1	DY02603335U	69	1	0.26	71546	404989			
71	outer	OSLN	1	DY02603335U	69	1	0.26	71489	404666	407	0.008	3
71	inner	OSL	1	DN087387699	69	1	0.87	10354	17515			
71	inner	OSL	1	DN087387699	68	2	0.87	127739	17437			
71	inner	OSL	1	DN087387699	68	2	0.87	126801	17309			
71	inner	OSL	1	DN08738719E	68	2	0.87	129940	17737			
71	inner	OSL	1	DN08738719E	68	2	0.87	125044	17069			
71	inner	OSL	1	DN08738719E	68	2	0.87	125260	17098	17	0.015	6
71	inner	OSLN	1	DY02603364T	69	1	0.26	202832	1148139			
71	inner	OSLN	1	DY02603364T	69	1	0.26	201216	1138991			
71	inner	OSLN	1	DY02603364T	69	1	0.26	202210	1144618			
71	inner	OSLN	1	DY02603366P	69	1	0.26	223020	1262414			
71	inner	OSLN	1	DY02603366P	69	1	0.26	217627	1231886			
71	inner	OSLN	1	DY02603366P	69	1	0.26	217523	1231298	1193	0.046	6
72	outer	OSL	2	DN086070942	69	1	0.86	32176	55064			
72	outer	OSL	2	DN086070942	69	1	0.86	31612	54098			
72	outer	OSL	2	DN086070942	69	1	0.86	31986	54738	55	0.009	3
72	outer	OSLN	2	DY02603454S	69	1	0.26	252832	1431166			
72	outer	OSLN	2	DY02603454S	69	1	0.26	253262	1433600			
72	outer	OSLN	2	DY02603454S	69	1	0.26	251371	1422896	1429	0.004	3
72	inner	OSL	2	DN08839713O	69	1	0.88	40106	67075			
72	inner	OSL	2	DN08839713O	69	1	0.88	40708	68081			
72	inner	OSL	2	DN08839713O	69	1	0.88	40292	67386			
72	inner	OSL	2	DN08839566H	69	1	0.88	39098	65389			
72	inner	OSL	2	DN08839566H	69	1	0.88	39631	66280			
72	inner	OSL	2	DN08839566H	69	1	0.88	39074	65349	67	0.017	6
72	inner	OSLN	2	DY02603405V	69	1	0.26	697756	3949676			
72	inner	OSLN	2	DY02603405V	69	1	0.26	692632	3920671			
72	inner	OSLN	2	DY02603405V	69	1	0.26	690657	3909492			
72	inner	OSLN	2	DY02603504V	69	1	0.26	693829	3927447			
72	inner	OSLN	2	DY02603504V	69	1	0.26	681462	3857443			
72	inner	OSLN	2	DY02603405V	69	1	0.26	672878	3808853	3896	0.013	6
73	outer	OSL	3	DN08839709D	69	1	0.88	19136	32004			
73	outer	OSL	3	DN08839709D	69	1	0.88	19194	32101			
73	outer	OSL	3	DN08839709D	69	1	0.88	18980	31743	32	0.006	3
73	outer	OSLN	3	DY02603562T	69	1	0.26	165168	934940			
73	outer	OSLN	3	DY02603562T	69	1	0.26	162192	920392			
73	outer	OSLN	3	DY02603562T	69	1	0.26	168191	954434			
73	outer	OSLN	3	DY02603562T	69	1	0.26	167142	948482	940	0.016	4
73	inner	OSL	3	DN08936749B	69	1	0.89	23032	38087			
73	inner	OSL	3	DN08936749B	69	1	0.89	23089	38181			
73	inner	OSL	3	DN08936749B	69	1	0.89	23043	38105			
73	inner	OSL	3	DN08436471Z	69	1	0.84	22815	39974			
73	inner	OSL	3	DN08436471Z	69	1	0.84	22248	38980			
73	inner	OSL	3	DN08436471Z	69	1	0.84	22280	39036	39	0.019	6
73	inner	OSLN	3	DY02603493Q	69	1	0.26	450373	2549355			
73	inner	OSLN	3	DY02603493Q	69	1	0.26	433994	2456641			
73	inner	OSLN	3	DY02603493Q	69	1	0.26	435970	2467826			
73	inner	OSLN	3	DY02603361Z	69	1	0.26	423010	2394465			
73	inner	OSLN	3	DY02603361Z	69	1	0.26	424358	2402096			
73	inner	OSLN	3	DY02603361Z	69	1	0.26	423040	2394635	2444	0.025	6

Table K.4 PNNL FNAD OSL Gamma and OSLN Neutron Response Data

				Irradiation Data			Outer Dosimetry Package Response Data								Inner Dosimetry Package Response Data								
FNAD #	Pulse #	Distance (m)	Position #	Given Neutron Fluence (n/cm^2)	Given Gamma dose $D^*(10)_\gamma$ (cGy)	Given Neutron dose $D^*(10)n$ (cGy)	OSL γ signal (Co-60 cGy)		OSLN $\gamma + n$ signal (Co-60 cGy)		OSLN - OSL net neutron signal (Co-60 cGy)		measured gamma signal / $D^*(10)_\gamma$	measured neutron signal / $D^*(10)_n$	OSL γ signal (Co-60 cGy)		OSLN $\gamma + n$ signal (Co-60 cGy)		OSLN - OSL net neutron signal (Co-60 cGy)		measured gamma signal / $D^*(10)_\gamma$	measured neutron signal / $D^*(10)_n$
							avg (cGy)	C.V.	avg (cGy)	C.V.	avg (cGy)	C.V.			avg (cGy)	C.V.	avg (cGy)	C.V.	avg (cGy)	C.V.		
71	1	4	11	5.30E+10	11	88	14	0.01	407	0.01	393	0.01	1.23	4.48	17	0.01	1193	0.05	1176	0.05	1.58	13.4
72	2	4	11	1.89E+11	40	313	55	0.01	1429	0.00	1375	0.01	1.37	4.39	67	0.02	3896	0.01	3829	0.02	1.66	12.2
73	3	4	11	1.14E+11	24	189	32	0.01	940	0.02	908	0.02	1.33	4.81	39	0.02	2444	0.02	2405	0.03	1.61	12.7

Table K.5 PNNL FNAD OSL/OSLN Calculated Doses Using Default Dose Calibration Factors

FNAD #	Pulse #	Distance (m)	Position #	Given Neutron Fluence (n/cm^2)	Given Gamma dose D*(10)$_\gamma$ (cGy)	Given Neutron dose D*(10)n (cGy)	Outer Package OSL Gamma Dose			Inner Package OSLN Neutron Dose			
							Default C$_\gamma$	D*(10)$_\gamma$ (cGy)	R/G	Default C$_n$	net neutron signal (cGy)	D*(10)$_n$	R/G
71	1	4	11	5.30E+10	11	88	1.00	14	1.23	12.89	1176	91	1.04
72	2	4	11	1.89E+11	40	313	1.00	55	1.37	12.89	3829	297	0.95
73	3	4	11	1.14E+11	24	189	1.00	32	1.33	12.89	2405	187	0.99

Table K.6 PNNL FNAD OSL/OSLN Calculated Doses using Optimized Dose Calibration Factors

| | | | | | | | Outer Package OSL Gamma Dose | | | Inner Package OSLN Neutron Dose | | | |
FNAD #	Pulse #	Distance (m)	Position #	Given Neutron Fluence (n/cm^2)	Given Gamma dose D*(10)$_\gamma$ (cGy)	Given Neutron dose D*(10)n (cGy)	C_γ	D*(10)$_\gamma$ (cGy)	R/G	C_n	net neutron signal (cGy)	D*(10)$_n$	R/G
71	1	4	11	5.30E+10	11	88	1.31	10	0.94	12.89	1176	91	1.04
72	2	4	11	1.89E+11	40	313	1.31	42	1.04	12.89	3829	297	0.95
73	3	4	11	1.14E+11	24	189	1.31	24	1.02	12.89	2405	187	0.99

Appendix L

PNAD Performance

Table L.1 PNNL PNAD Performance Based on Foil Measured Neutron Dose and Default Gamma Dose Calibration.

	Irradiation Data					ANSI/HPS N13.3 $D_p(10)$ Reference Doses			PNAD Performance with foil calculated neutron dose ($C_\gamma = 1.00$)							
PNAD No.	Pulse No.	Distance (m)	Location No.	phantom type	Given Neutron Fluence (n/cm^2)	Given Gamma dose $D_p(10)_\gamma$ (cGy)	Given Neutron dose $D_p(10)_n$ (cGy)	Given Total dose $D_p(10)$ (cGy)	OSL Gamma Dose (cGy)	OSL Gamma R/G	Foil Neutron Dose (cGy)	Foil Neutron R/G	PNAD $\gamma + n$ Dose (cGy)	PNAD $\gamma + n$ R/G	B	Pass or Fail
45	3	2	3	PMMA	2.17E+11	47	459	506	117	2.49	325	0.71	442	0.87	-0.13	Pass
5	1	3	4	BOMAB	6.55E+10	14	123	137	35	2.51	67	0.55	103	0.75	-0.25	Fail
7	1	3	5	BOMAB	6.77E+10	14	126	140	34	2.44	64	0.51	98	0.70	-0.30	Fail
21	2	3	4	BOMAB	2.34E+11	50	441	491	132	2.64	256	0.58	388	0.79	-0.21	Pass
23	2	3	5	BOMAB	2.42E+11	50	450	500	132	2.64	243	0.54	375	0.75	-0.25	Pass
34	3	3	4	BOMAB	1.41E+11	30	266	296	81	2.70	154	0.58	234	0.79	-0.21	Pass
13	1	4	7	PMMA	5.10E+10	11	89	100	24	2.22	50	0.56	74	0.74	-0.26	Fail
25	2	4	7	PMMA	1.82E+11	40	319	359	86	2.15	180	0.56	266	0.74	-0.26	Fail
38	3	4	7	BOMAB	1.10E+11	24	192	216	66	2.76	109	0.57	175	0.81	-0.19	Pass
41	3	9	10	BOMAB	6.17E+10	5	85	90	11	2.24	16	0.19	26	0.29	-0.71	Fail

Table L.2 PNNL PNAD Performance Based on Foil Measured Neutron Dose and Optimized Gamma Dose Calibration

	Irradiation Data					ANSI/HPS N13.3 $D_p(10)$ Reference Doses			PNAD Performance with foil calculated neutron dose (C_γ = 2.59)							
PNAD No.	Pulse No.	Distance (m)	Location No.	phantom type	Given Neutron Fluence (n/cm^2)	Given Gamma dose $D_p(10)_\gamma$ (cGy)	Given Neutron dose $D_p(10)_n$ (cGy)	Given Total dose $D_p(10)$ (cGy)	OSL Gamma Dose (cGy)	OSL Gamma R/G	Foil Neutron Dose (cGy)	Foil Neutron R/G	PNAD $\gamma + n$ Dose (cGy)	PNAD $\gamma + n$ R/G	B	Pass or Fail
45	3	2	3	PMMA	2.17E+11	47	459	506	45	0.96	325	0.71	370	0.73	-0.27	Fail
5	1	3	4	BOMAB	6.55E+10	14	123	137	14	0.97	67	0.55	81	0.59	-0.41	Fail
7	1	3	5	BOMAB	6.77E+10	14	126	140	13	0.94	64	0.51	77	0.55	-0.45	Fail
21	2	3	4	BOMAB	2.34E+11	50	441	491	51	1.02	256	0.58	307	0.63	-0.37	Fail
23	2	3	5	BOMAB	2.42E+11	50	450	500	51	1.02	243	0.54	294	0.59	-0.41	Fail
34	3	3	4	BOMAB	1.41E+11	30	266	296	31	1.04	154	0.58	185	0.62	-0.38	Fail
13	1	4	7	PMMA	5.10E+10	11	89	100	9	0.86	50	0.56	59	0.59	-0.41	Fail
25	2	4	7	PMMA	1.82E+11	40	319	359	33	0.83	180	0.56	213	0.59	-0.41	Fail
38	3	4	7	BOMAB	1.10E+11	24	192	216	26	1.07	109	0.57	134	0.62	-0.38	Fail
41	3	9	10	BOMAB	6.17E+10	5	85	90	4	0.87	16	0.19	20	0.22	-0.78	Fail

Table L.3 PNNL PNAD Performance Based on OSLN Measured Neutron Dose with Optimized Gamma and Neutron Dose Calibration Factors

		Irradiation Data					ANSI/HPS N13.3 $D_p(10)$ Reference Doses			PNAD Performance with OSLN calculated neutron dose (C_γ = 2.59, C_n = 6.09)							
PNAD No.	Pulse No.	Distance (m)	Location No.	phantom type	Given Neutron Fluence (n/cm^2)		Given Gamma dose $D_p(10)_\gamma$ (cGy)	Given Neutron dose $D_p(10)_n$ (cGy)	Given Total dose $D_p(10)$ (cGy)	OSL Gamma Dose (cGy)	OSL Gamma R/G	OSLN Neutron Dose (cGy)	OSLN Neutron R/G	PNAD $\gamma + n$ Dose (cGy)	PNAD $\gamma + n$ R/G	B	Pass or Fail
45	3	2	3	PMMA	2.17E+11		47	459	506	45	0.96	379	0.83	424	0.84	-0.16	Pass
5	1	3	4	BOMAB	6.55E+10		14	123	137	14	0.97	125	1.01	138	1.01	0.01	Pass
7	1	3	5	BOMAB	6.77E+10		14	126	140	13	0.94	120	0.95	133	0.95	-0.05	Pass
21	2	3	4	BOMAB	2.34E+11		50	441	491	51	1.02	422	0.96	473	0.96	-0.04	Pass
23	2	3	5	BOMAB	2.42E+11		50	450	500	51	1.02	481	1.07	532	1.06	0.06	Pass
34	3	3	4	BOMAB	1.41E+11		30	266	296	31	1.04	269	1.01	300	1.01	0.01	Pass
13	1	4	7	PMMA	5.10E+10		11	89	100	9	0.86	110	1.24	120	1.20	0.20	Pass
25	2	4	7	PMMA	1.82E+11		40	319	359	33	0.83	351	1.10	384	1.07	0.07	Pass
38	3	4	7	BOMAB	1.10E+11		24	192	216	26	1.07	256	1.33	281	1.30	0.30	Fail
41	3	9	10	BOMAB	6.17E+10		5	85	90	4	0.87	39	0.46	43	0.48	-0.52	Fail

Table L.4 Hanford PNAD Performance Based on Foil Measured Neutron Dose and Optimized Gamma Dose Calibration

	Irradiation Data					ANSI/HPS N13.3 $D_p(10)$ Reference Doses			PNAD Performance with foil calculated neutron dose ($C_\gamma = 1.31$)							
PNAD No.	Pulse No.	Distance (m)	Location No.	phantom type	Given Neutron Fluence (n/cm^2)	Given Gamma dose $D_p(10)_\gamma$ (cGy)	Given Neutron dose $D_p(10)_n$ (cGy)	Given Total dose $D_p(10)$ (cGy)	OSL Gamma Dose (cGy)	OSL Gamma R/G	Foil Neutron Dose (cGy)	Foil Neutron R/G	PNAD $\gamma + n$ Dose (cGy)	PNAD $\gamma + n$ R/G	B	Pass or Fail
61	1	2	2	Tree A-D	9.59E+10	22	205	227	21	0.97	129	0.63	151	0.66	-0.34	Fail
62	1	2	2	Tree A-D	9.59E+10	22	205	227	22	0.98	141	0.69	163	0.72	-0.28	Fail
63	2	2	2	Tree A-D	3.43E+11	78	732	810	80	1.03	469	0.64	550	0.68	-0.32	Fail
64	2	2	2	Tree A-D	3.43E+11	78	732	810	81	1.04	479	0.65	560	0.69	-0.31	Fail
65	3	2	2	Tree A-D	2.07E+11	47	442	489	48	1.01	280	0.63	328	0.67	-0.33	Fail
66	3	2	2	Tree A-D	2.07E+11	47	442	489	49	1.04	284	0.64	333	0.68	-0.32	Fail

Appendix M

FNAD Performance

Table M.1 FNAD Performance Based on Foil Measured Neutron Dose and Optimized Gamma Dose Calibration

FNAD No.	Pulse No.	Distance (m)	Location No.	Given Neutron Fluence (n/cm^2)	Given Gamma dose D*(10)$_\gamma$ (cGy)	Given Neutron dose D*(10)$_n$ (cGy)	Given Total dose D*(10) (cGy)	OSL Gamma Dose (cGy)	OSL Gamma R/G	Foil Neutron Dose (cGy)	Foil Neutron R/G	FNAD $\gamma + n$ Dose (cGy)	FNAD $\gamma + n$ R/G	B	Pass or Fail
		Irradiation Data			**ANSI/HPS N13.3 D*(10) Reference Doses**			**FNAD Performance with foil calculated neutron dose (C$_\gamma$ = 1.31)**							
71	1	4	11	5.30E+10	11	91	102	10	0.94	55	0.60	65	0.64	-0.36	Fail
72	2	4	11	1.89E+11	40	326	366	42	1.04	179	0.55	221	0.60	-0.40	Fail
73	3	4	11	1.14E+11	24	197	221	24	1.02	103	0.52	127	0.58	-0.42	Fail

Table M.2 FNAD Performance Based on Default OSLN Measured Neutron Dose and Optimized Gamma Dose Calibration

FNAD No.	Pulse No.	Distance (m)	Location No.	Given Neutron Fluence (n/cm^2)	Given Gamma dose D*(10)$_\gamma$ (cGy)	Given Neutron dose D*(10)$_n$ (cGy)	Given Total dose D*(10) (cGy)	OSL Gamma Dose (cGy)	OSL Gamma R/G	OSLN Neutron Dose (cGy)	OSLN Neutron R/G	PNAD $\gamma + n$ Dose (cGy)	PNAD $\gamma + n$ R/G	B	Pass or Fail
		Irradiation Data			**ANSI/HPS N13.3 D*(10) Reference Doses**			**FNAD Performance with OSLN calculated neutron dose (C$_\gamma$ = 1.31, C$_n$ = 12.89)**							
71	1	4	11	5.30E+10	11	91	102	10	0.94	91	1.00	102	1.00	0.00	Pass
72	2	4	11	1.89E+11	40	326	366	42	1.04	297	0.91	339	0.93	-0.07	Pass
73	3	4	11	1.14E+11	24	197	221	24	1.02	187	0.95	211	0.96	-0.04	Pass

Appendix N

EPD Dose Response

Table N.1 Individual EPD Dose Response.

									delivered fluence at position (n/cm²)	Reported dose (cGy)	Given Dp(10) (cGy)	Reported /Given	Correction Factor
EPD Gamma Dose Response													
Dosimeter #	Dosimeter Label	Make	Model	Pulse #	distance (m)	Position #	phantom type	dosimeter location on phantom	delivered fluence at position (n/cm²)	Reported dose (cGy)	Given Dp(10) (cGy)	Reported /Given	Correction Factor
201	EPD1	Thermo	Mark 2.5	1	9	10	Tree A-H	air	2.86E+10	0.504	2.2	0.23	4.31
202	EPD2	Mirion-MGP	DMC3000	1	9	10	Tree A-H	air	2.86E+10	0.519	2.2	0.24	4.19
203	EPD3	Mirion-MGP	DMC2000S	1	9	10	Tree A-H	air	2.86E+10	0.384	2.2	0.18	5.66
204	EPD4	Mirion-MGP	DMC3000-neutron module	1	9	10	Tree A-H	air	2.86E+10	0.561	2.2	0.26	3.87
205	EPD5	Thermo	Mark 2.5	2	2	1	Tree A-D	air	3.60E+11	15.836	78	0.20	4.93
206	EPD6	Mirion-MGP	DMC3000	2	2	1	Tree A-D	air	3.60E+11	14.898	78	0.19	5.24
207	EPD7	Mirion-MGP	DMC2000S	2	2	2	Tree A-D	air	3.43E+11	13.764	78	0.18	5.67
208	EPD8	Thermo	Mark 2.5	3	4	8	Tree A-H	air	1.15E+11	5.889	24	0.25	4.08
209	EPD9	Mirion-MGP	DMC3000	3	4	8	Tree A-H	air	1.15E+11	4.818	24	0.20	4.98
210	EPD10	Mirion-MGP	DMC2000S	3	4	8	Tree A-H	air	1.15E+11	4.600	24	0.19	5.22

									delivered fluence at position (n/cm²)	Reported dose (cGy)	Given Dp(10) (cGy)	Reported /Given	Correction Factor
EPD Neutron Dose Response													
Dosimeter #	Dosimeter Label	Make	Model	Pulse #	distance (m)	Position #	phantom type	dosimeter location on phantom	delivered fluence at position (n/cm²)	Reported dose (cGy)	Given Dp(10) (cGy)	Reported /Given	Correction Factor
204	EPD4	Mirion-MGP	DMC3000-neutron module	1	9	10	Tree A-H	air	2.86E+10	2.662	39	0.068	14.65

Table N.2 EPD Gamma Dose Response Factors by Model

Dosimeter #	Dosimeter Label	Make	Model	Barcode	Serial Number	Reported γ dose (cGy)	Given $D_p(10)_Y$ (cGy)	Reported /Given	average	stdev	C.V.
203	EPD3	Mirion-MGP	DMC2000S	EDMG1-0332	86384	0.384	2.2	0.177			
207	EPD7	Mirion-MGP	DMC2000S	EDMG1-0540	832832	13.764	78	0.176	0.18	0.01	0.05
210	EPD10	Mirion-MGP	DMC2000S	EDMG1-0432	832099	4.600	24	0.192			
202	EPD2	Mirion-MGP	DMC3000	PPMG1-0186	916376	0.519	2.2	0.239			
206	EPD6	Mirion-MGP	DMC3000	PPMG1-0236	924057	14.898	78	0.191	0.21	0.03	0.12
209	EPD9	Mirion-MGP	DMC3000	PPMG1-0149	921717	4.818	24	0.201			
204	EPD4	Mirion-MGP	DMC3000-neutron module	PPMG6-0001	1968319	0.561	2.2	0.258	0.26	n/a	n/a
201	EPD1	Thermo	Mark 2.5	PPTC6-0018	295664	0.504	2.2	0.232			
205	EPD5	Thermo	Mark 2.5	PPTC6-0017	296367	15.836	78	0.203	0.23	0.02	0.10
208	EPD8	Thermo	Mark 2.5	PPTC6-0016	296383	5.889	24	0.245			

Average:	0.21	0.22
Stdev	0.03	0.03
C.V.	0.14	0.15
Min:	0.2	0.18
Max:	0.3	0.26

Table N.3 EPD Gamma Dose Response Factors

Make	Model	Gamma Dose Response		
		Average	stdev	C.V.
Mirion-MGP	DMC2000S	0.18	0.01	0.05
Mirion-MGP	DMC3000	0.21	0.03	0.12
Mirion-MGP	DMC3000-neutron module	0.26	n/a	n/a
Thermo	Mark 2.5	0.23	0.02	0.10

Appendix O

BOMAB Direct Survey Measurements

Table O.1 BOMAB Survey Instrument Measurement Data

Pulse #	Item #	Measurement Location	Instrument	Measurement	Gross cpm, mR/h or urem/h	Net cpm, mR/h or urem/h	Date MM/DD/YYYY	Time HH:MM	Measurement Date-Time MM/DD/YYY HH:MM	Burst Date-Time MM/DD/YYY HH:MM	Decay time after burst (minutes)
1	Background	NAD breakdown Room	Ludlum 26-1 pancake GM probe with dose equivalent window cover	cpm	100	0	5/24/2016	12:00	5/24/2016 12:00	5/24/2016 10:12	108
1	Background	NAD breakdown Room	Ludlum 43-93 alpha-beta scint probe	cpm (beta)	1022	0	5/24/2016	12:00	5/24/2016 12:00	5/24/2016 10:12	108
1	Background	NAD breakdown Room	Bicron microRem	urem/h	30	0	5/24/2016	12:00	5/24/2016 12:00	5/24/2016 10:12	108
1	BOMAB 4	upper torso	Ludlum 26-1 pancake GM probe with dose equivalent window cover	mR/h	1.02	0.99	5/24/2016	16:40	5/24/2016 16:40	5/24/2016 10:12	388
1	BOMAB 4	lower torso	Ludlum 26-1 pancake GM probe with dose equivalent window cover	mR/h	0.93	0.90	5/24/2016	16:40	5/24/2016 16:40	5/24/2016 10:12	388
1	BOMAB 4	upper torso	Ludlum 26-1 pancake GM probe with dose equivalent window cover	cpm	3500	3400	5/24/2016	16:41	5/24/2016 16:41	5/24/2016 10:12	389
1	BOMAB 4	lower torso	Ludlum 26-1 pancake GM probe with dose equivalent window cover	cpm	3200	3100	5/24/2016	16:41	5/24/2016 16:41	5/24/2016 10:12	389
1	BOMAB 4	upper torso	Ludlum 43-93 alpha-beta scint probe	cpm (beta)	22000	20978	5/24/2016	16:47	5/24/2016 16:47	5/24/2016 10:12	395
1	BOMAB 4	lower torso	Ludlum 43-93 alpha-beta scint probe	cpm (beta)	20000	18978	5/24/2016	16:47	5/24/2016 16:47	5/24/2016 10:12	395
1	BOMAB 4	upper torso	Bicron microRem	urem/h	500	470	5/24/2016	16:43	5/24/2016 16:43	5/24/2016 10:12	391
1	BOMAB 4	lower torso	Bicron microRem	urem/h	400	370	5/24/2016	16:43	5/24/2016 16:43	5/24/2016 10:12	391
1	BOMAB 5	upper torso*	Ludlum 26-1 pancake GM probe with dose equivalent window cover	mR/h	1.03	1.00	5/24/2016	14:37	5/24/2016 14:37	5/24/2016 10:12	265
1	BOMAB 5	lower torso*	Ludlum 26-1 pancake GM probe with dose equivalent window cover	mR/h	0.75	0.72	5/24/2016	14:37	5/24/2016 14:37	5/24/2016 10:12	265
1	BOMAB 5	upper torso*	Ludlum 26-1 pancake GM probe with dose equivalent window cover	cpm	3800	3700	5/24/2016	14:36	5/24/2016 14:36	5/24/2016 10:12	264
1	BOMAB 5	lower torso*	Ludlum 26-1 pancake GM probe with dose equivalent window cover	cpm	3200	3100	5/24/2016	14:35	5/24/2016 14:35	5/24/2016 10:12	263
1	BOMAB 5	upper torso*	Ludlum 43-93 alpha-beta scint probe	cpm (beta)	24000	22978	5/24/2016	14:40	5/24/2016 14:40	5/24/2016 10:12	268
1	BOMAB 5	lower torso*	Ludlum 43-93 alpha-beta scint probe	cpm (beta)	20000	18978	5/24/2016	14:40	5/24/2016 14:40	5/24/2016 10:12	268
1	BOMAB 5	upper torso*	Bicron microRem	urem/h	500	470	5/24/2016	14:38	5/24/2016 14:38	5/24/2016 10:12	266
1	BOMAB 5	lower torso*	Bicron microRem	urem/h	400	370	5/24/2016	14:38	5/24/2016 14:38	5/24/2016 10:12	266
1	BOMAB 5	upper torso	Ludlum 26-1 pancake GM probe with dose equivalent window cover	mR/h	0.98	0.95	5/24/2016	15:13	5/24/2016 15:13	5/24/2016 10:12	301
1	BOMAB 5	lower torso	Ludlum 26-1 pancake GM probe with dose equivalent window cover	mR/h	0.98	0.95	5/24/2016	15:13	5/24/2016 15:13	5/24/2016 10:12	301
1	BOMAB 5	upper torso	Ludlum 26-1 pancake GM probe with dose equivalent window cover	cpm	3650	3550	5/24/2016	15:10	5/24/2016 15:10	5/24/2016 10:12	298
1	BOMAB 5	lower torso	Ludlum 26-1 pancake GM probe with dose equivalent window cover	cpm	3260	3160	5/24/2016	15:10	5/24/2016 15:10	5/24/2016 10:12	298
1	BOMAB 5	upper torso	Ludlum 43-93 alpha-beta scint probe	cpm (beta)	24000	22978	5/24/2016	15:18	5/24/2016 15:18	5/24/2016 10:12	306
1	BOMAB 5	lower torso	Ludlum 43-93 alpha-beta scint probe	cpm (beta)	20000	18978	5/24/2016	15:18	5/24/2016 15:18	5/24/2016 10:12	306
1	BOMAB 5	upper torso	Bicron microRem	urem/h	500	470	5/24/2016	15:15	5/24/2016 15:15	5/24/2016 10:12	303
1	BOMAB 5	lower torso	Bicron microRem	urem/h	400	370	5/24/2016	15:15	5/24/2016 15:15	5/24/2016 10:12	303

* dissassembled
BOMAB - elipses on
bench top

Table O.1 BOMAB Survey Instrument Measurement Data (continued)

Pulse #	Item #	Measurement Location	Instrument	Measurement	Gross cpm, mR/h or urem/h	Net cpm, mR/h or urem/h	Date MM/DD/YYYY	Time HH:MM	Measurement Date-Time MM/DD/YYYY HH:MM	Burst Date-Time MM/DD/YYY HH:MM	Decay time after burst (minutes)
2	Background	NAD breakdown Room	Pancake GM	cpm	80	0	5/25/2016	12:00	5/25/2016 12:00	5/25/2016 9:43	137
2	Background	NAD breakdown Room	Ludlum 43-93 alpha-beta scint probe	cpm (beta)	900	0	5/25/2016	12:00	5/25/2016 12:00	5/25/2016 9:43	137
2	Background	NAD breakdown Room	Bicron microRem	urem/h	25	0	5/25/2016	12:00	5/25/2016 12:00	5/25/2016 9:43	137
2	BOMAB 5	upper torso	Ludlum 26-1 pancake GM probe with dose equivalent window cover	mR/h	3.21	3.19	5/25/2016	17:04	5/25/2016 17:04	5/25/2016 9:43	441
2	BOMAB 5	lower torso	Ludlum 26-1 pancake GM probe with dose equivalent window cover	mR/h	3.03	3.01	5/25/2016	17:04	5/25/2016 17:04	5/25/2016 9:43	441
2	BOMAB 5	upper torso	Ludlum 26-1 pancake GM probe with dose equivalent window cover	cpm	13000	12920	5/25/2016	17:04	5/25/2016 17:04	5/25/2016 9:43	441
2	BOMAB 5	lower torso	Ludlum 26-1 pancake GM probe with dose equivalent window cover	cpm	11000	10920	5/25/2016	17:04	5/25/2016 17:04	5/25/2016 9:43	441
2	BOMAB 5	upper torso	Ludlum 43-93 alpha-beta scint probe	cpm (beta)	75000	74100	5/25/2016	17:10	5/25/2016 17:10	5/25/2016 9:43	447
2	BOMAB 5	lower torso	Ludlum 43-93 alpha-beta scint probe	cpm (beta)	69000	68100	5/25/2016	17:10	5/25/2016 17:10	5/25/2016 9:43	447
2	BOMAB 5	upper torso	Bicron microRem	urem/h	2500	2475	5/25/2016	17:07	5/25/2016 17:07	5/25/2016 9:43	444
2	BOMAB 5	lower torso	Bicron microRem	urem/h			5/25/2016	17:07	5/25/2016 17:07	5/25/2016 9:43	444
2	BOMAB 5	upper torso	Ludlum 26-1 pancake GM probe with dose equivalent window cover	mR/h	2.8	2.78	5/25/2016	20:42	5/25/2016 20:42	5/25/2016 9:43	659
2	BOMAB 5	lower torso	Ludlum 26-1 pancake GM probe with dose equivalent window cover	mR/h	2.41	2.39	5/25/2016	20:42	5/25/2016 20:42	5/25/2016 9:43	659
2	BOMAB 5	upper torso	Ludlum 26-1 pancake GM probe with dose equivalent window cover	cpm	10300	10220	5/25/2016	20:42	5/25/2016 20:42	5/25/2016 9:43	659
2	BOMAB 5	lower torso	Ludlum 26-1 pancake GM probe with dose equivalent window cover	cpm	9420	9340	5/25/2016	20:42	5/25/2016 20:42	5/25/2016 9:43	659
2	BOMAB 5	upper torso	Ludlum 43-93 alpha-beta scint probe	cpm (beta)	64000	63100	5/25/2016	20:48	5/25/2016 20:48	5/25/2016 9:43	665
2	BOMAB 5	lower torso	Ludlum 43-93 alpha-beta scint probe	cpm (beta)	59000	58100	5/25/2016	20:48	5/25/2016 20:48	5/25/2016 9:43	665
2	BOMAB 5	upper torso	Bicron microRem	urem/h	1700	1675	5/25/2016	20:46	5/25/2016 20:46	5/25/2016 9:43	663
2	BOMAB 5	lower torso	Bicron microRem	urem/h	1500	1475	5/25/2016	20:46	5/25/2016 20:46	5/25/2016 9:43	663
3	Background	NAD breakdown Room	Pancake GM	cpm	344	0	5/26/2016	15:42	5/26/2016 15:42	5/26/2016 11:36	246
3	Background	NAD breakdown Room	Ludlum 43-93 alpha-beta scint probe	cpm (beta)	3310	0	5/26/2016	15:42	5/26/2016 15:42	5/26/2016 11:36	246
3	Background	NAD breakdown Room	Bicron microRem	urem/h		0	5/26/2016	15:42	5/26/2016 15:42	5/26/2016 11:36	246
3	BOMAB 4	upper torso	Ludlum 26-1 pancake GM probe with dose equivalent window cover	mR/h	2.08	2.08	5/26/2016	20:09	5/26/2016 20:09	5/26/2016 11:36	513
3	BOMAB 4	lower torso	Ludlum 26-1 pancake GM probe with dose equivalent window cover	mR/h	1.55	1.55	5/26/2016	20:09	5/26/2016 20:09	5/26/2016 11:36	513
3	BOMAB 4	upper torso	Ludlum 26-1 pancake GM probe with dose equivalent window cover	cpm	7440	7096	5/26/2016	20:10	5/26/2016 20:10	5/26/2016 11:36	514
3	BOMAB 4	lower torso	Ludlum 26-1 pancake GM probe with dose equivalent window cover	cpm	5820	5476	5/26/2016	20:10	5/26/2016 20:10	5/26/2016 11:36	514
3	BOMAB 4	upper torso	Ludlum 43-93 alpha-beta scint probe	cpm (beta)	43600	40290	5/26/2016	20:11	5/26/2016 20:11	5/26/2016 11:36	515
3	BOMAB 4	lower torso	Ludlum 43-93 alpha-beta scint probe	cpm (beta)	39000	35690	5/26/2016	20:11	5/26/2016 20:11	5/26/2016 11:36	515
3	BOMAB 4	upper torso	Bicron microRem	urem/h	1100	1100	5/26/2016	20:13	5/26/2016 20:13	5/26/2016 11:36	517
3	BOMAB 4	lower torso	Bicron microRem	urem/h	1000	1000	5/26/2016	20:13	5/26/2016 20:13	5/26/2016 11:36	517
3	BOMAB 5	upper torso	Ludlum 26-1 pancake GM probe with dose equivalent window cover	mR/h	0.19	0.19	5/26/2016	21:30	5/26/2016 21:30	5/26/2016 11:36	594
3	BOMAB 5	lower torso	Ludlum 26-1 pancake GM probe with dose equivalent window cover	mR/h	0.2	0.20	5/26/2016	21:30	5/26/2016 21:30	5/26/2016 11:36	594
3	BOMAB 5	upper torso	Ludlum 26-1 pancake GM probe with dose equivalent window cover	cpm	773	429	5/26/2016	21:31	5/26/2016 21:31	5/26/2016 11:36	595
3	BOMAB 5	lower torso	Ludlum 26-1 pancake GM probe with dose equivalent window cover	cpm	773	429	5/26/2016	21:31	5/26/2016 21:31	5/26/2016 11:36	595
3	BOMAB 5	upper torso	Ludlum 43-93 alpha-beta scint probe	cpm (beta)	4960	1650	5/26/2016	21:28	5/26/2016 21:28	5/26/2016 11:36	592
3	BOMAB 5	lower torso	Ludlum 43-93 alpha-beta scint probe	cpm (beta)	4550	1240	5/26/2016	21:28	5/26/2016 21:28	5/26/2016 11:36	592
3	BOMAB 5	upper torso	Bicron microRem	urem/h	140	140	5/26/2016	21:29	5/26/2016 21:29	5/26/2016 11:36	593
3	BOMAB 5	lower torso	Bicron microRem	urem/h	120	120	5/26/2016	21:29	5/26/2016 21:29	5/26/2016 11:36	593

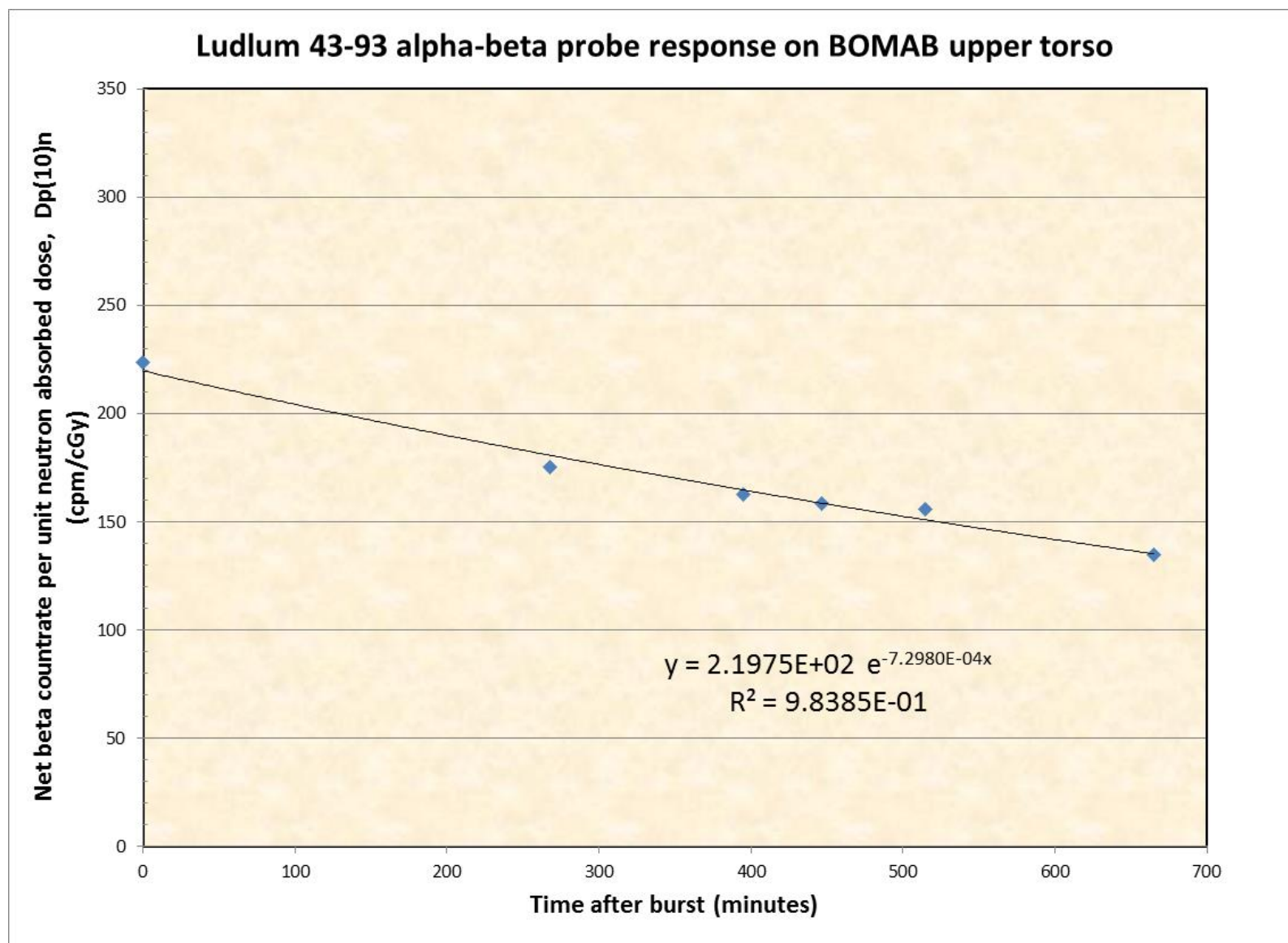**Figure O.1** Ludlum 43-93 alpha-beta probe measurements on BOMAB upper torso

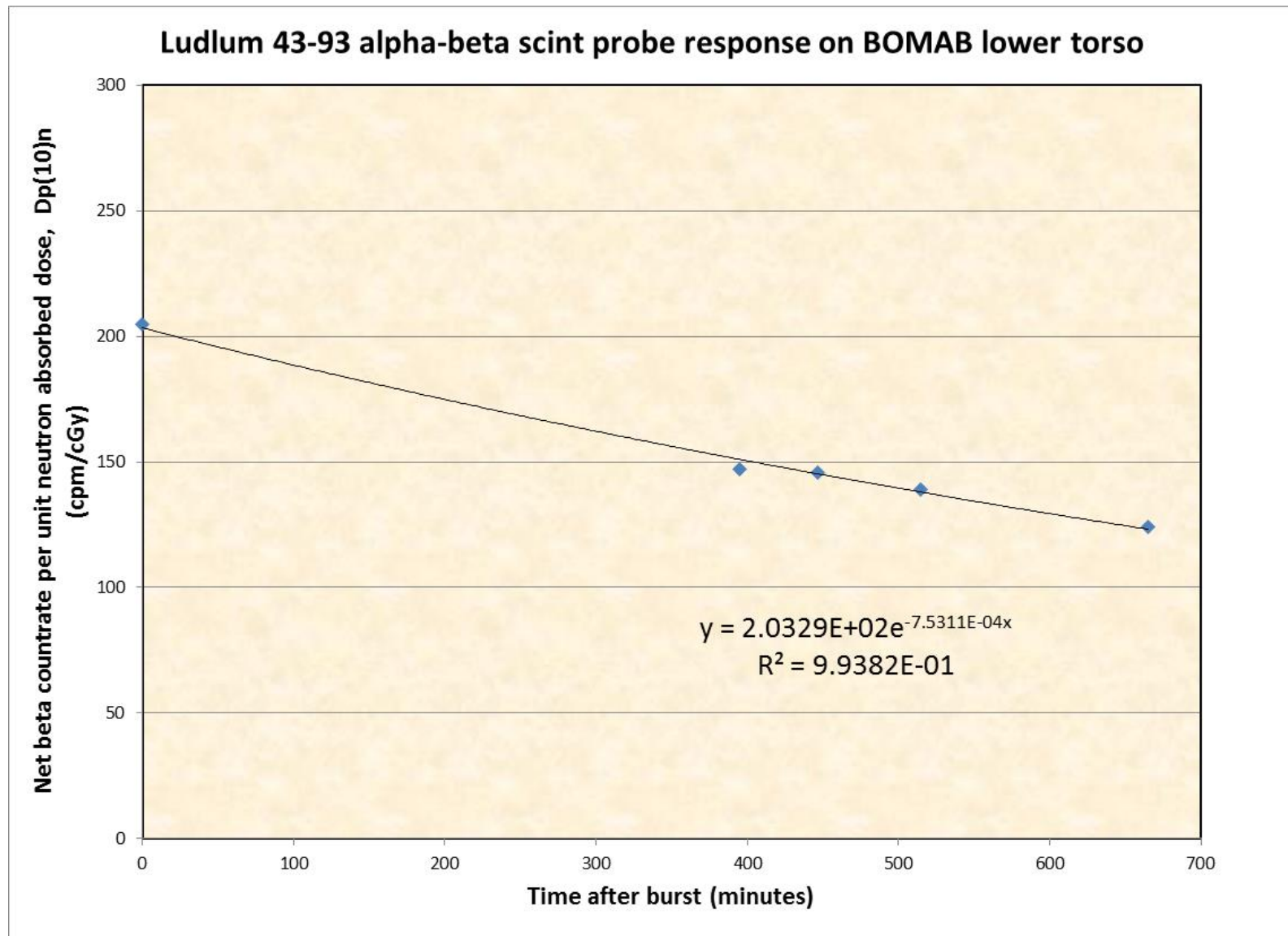**Figure O.2** Ludlum 43-93 alpha-beta probe measurements on BOMAB lower torso

Ludlum 43-93 alpha-beta scint probe response on BOMAB lower torso

$y = 2.0329E+02e^{-7.5311E-04x}$

$R^2 = 9.9382E-01$

Net beta countrate per unit neutron absorbed dose, Dp(10)n (cpm/cGy)

Time after burst (minutes)

Pancake GM probe response on BOMAB upper torso
(Ludlum 26-1 pancake GM probe with dose equivalent window cover)

$y = 3.61685E+01e^{-7.17996E-04x}$

$R^2 = 9.18883E-01$

Net countrate per unit neutron absorbed dose, Dp(10)n (cpm/cGy)
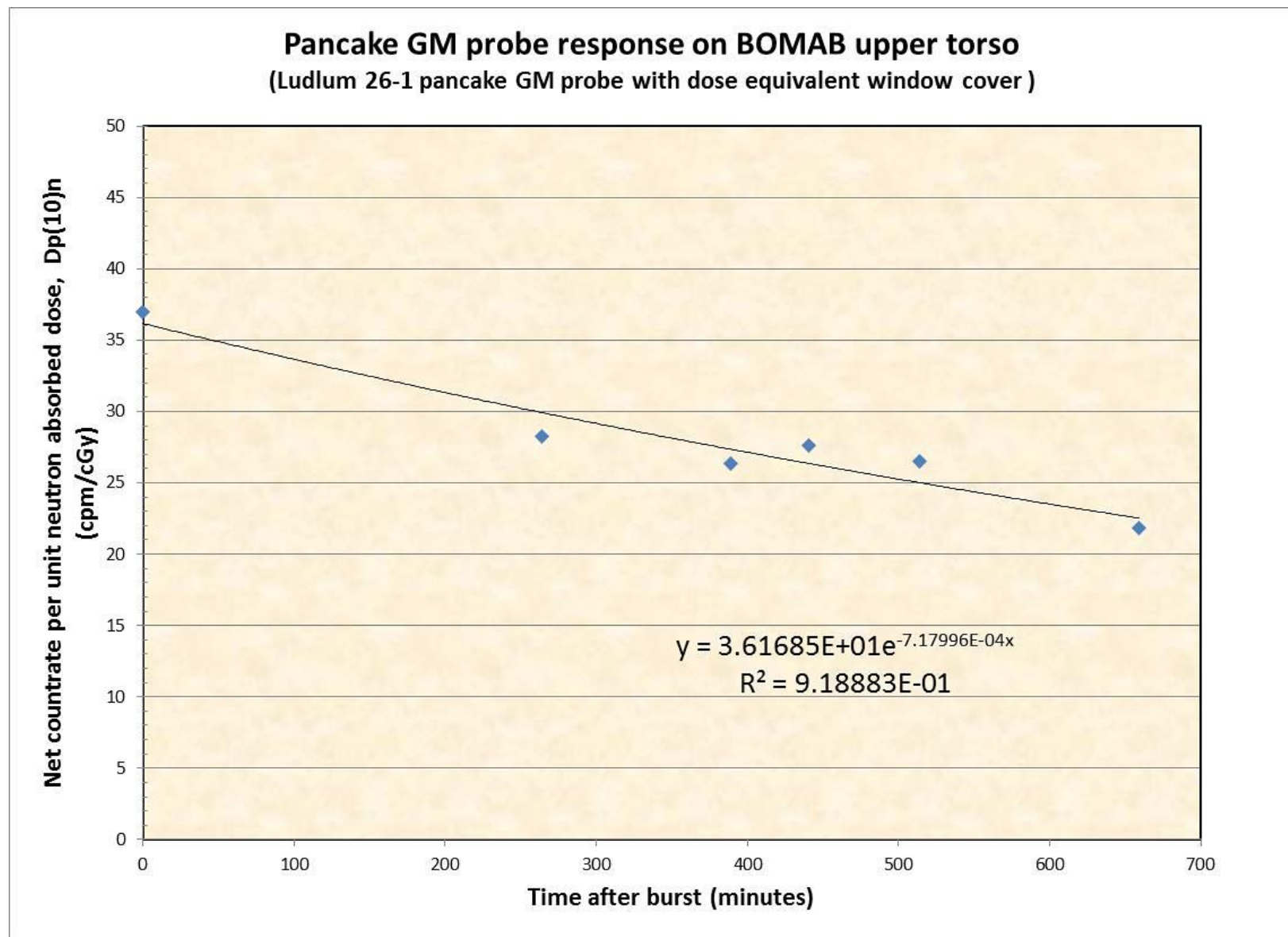
Time after burst (minutes)

Figure O.4 Pancake GM probe measurements on BOMAB lower torso

Figure O.5 Pancake GM probe measurements on BOMAB upper torso
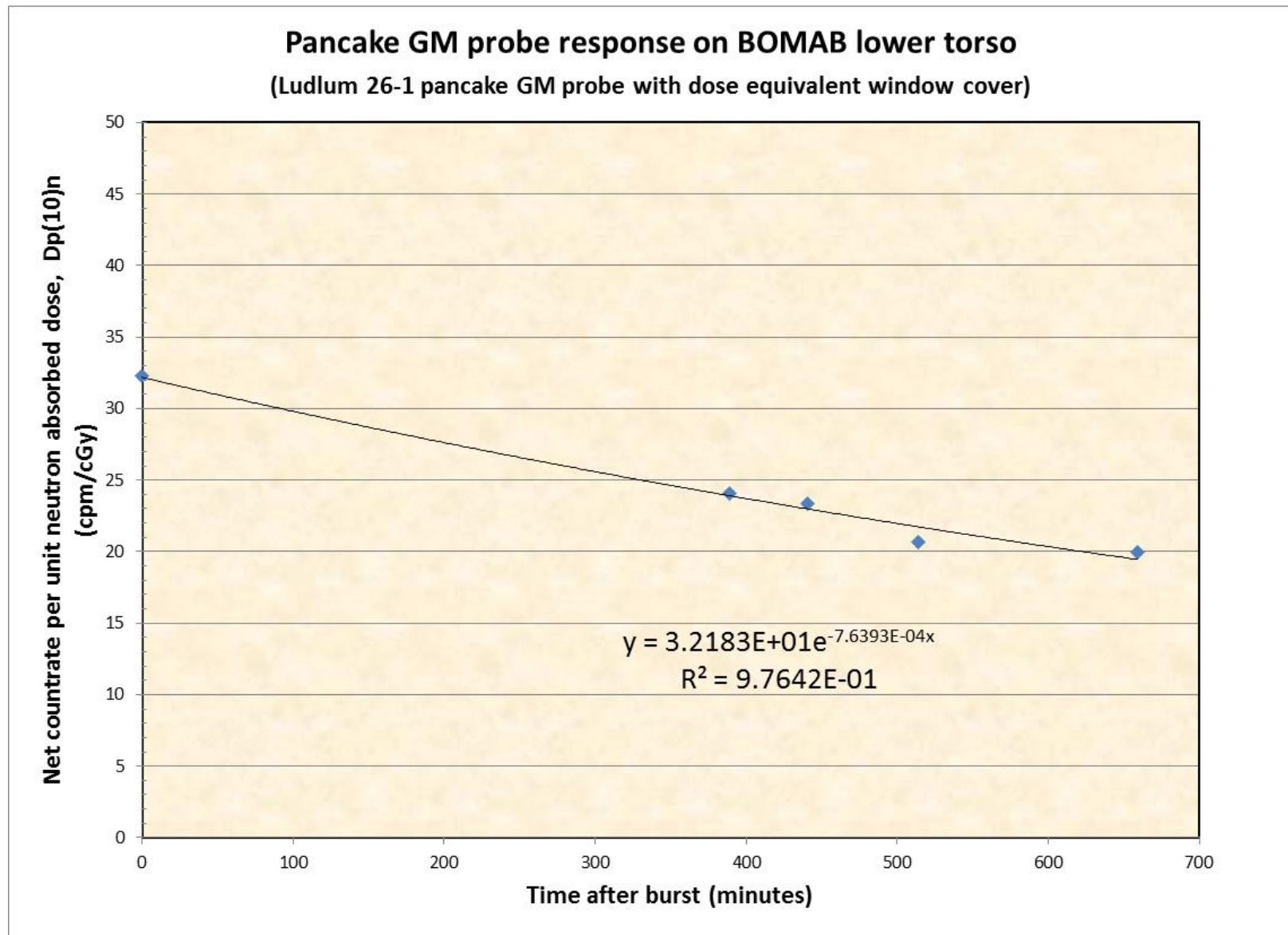

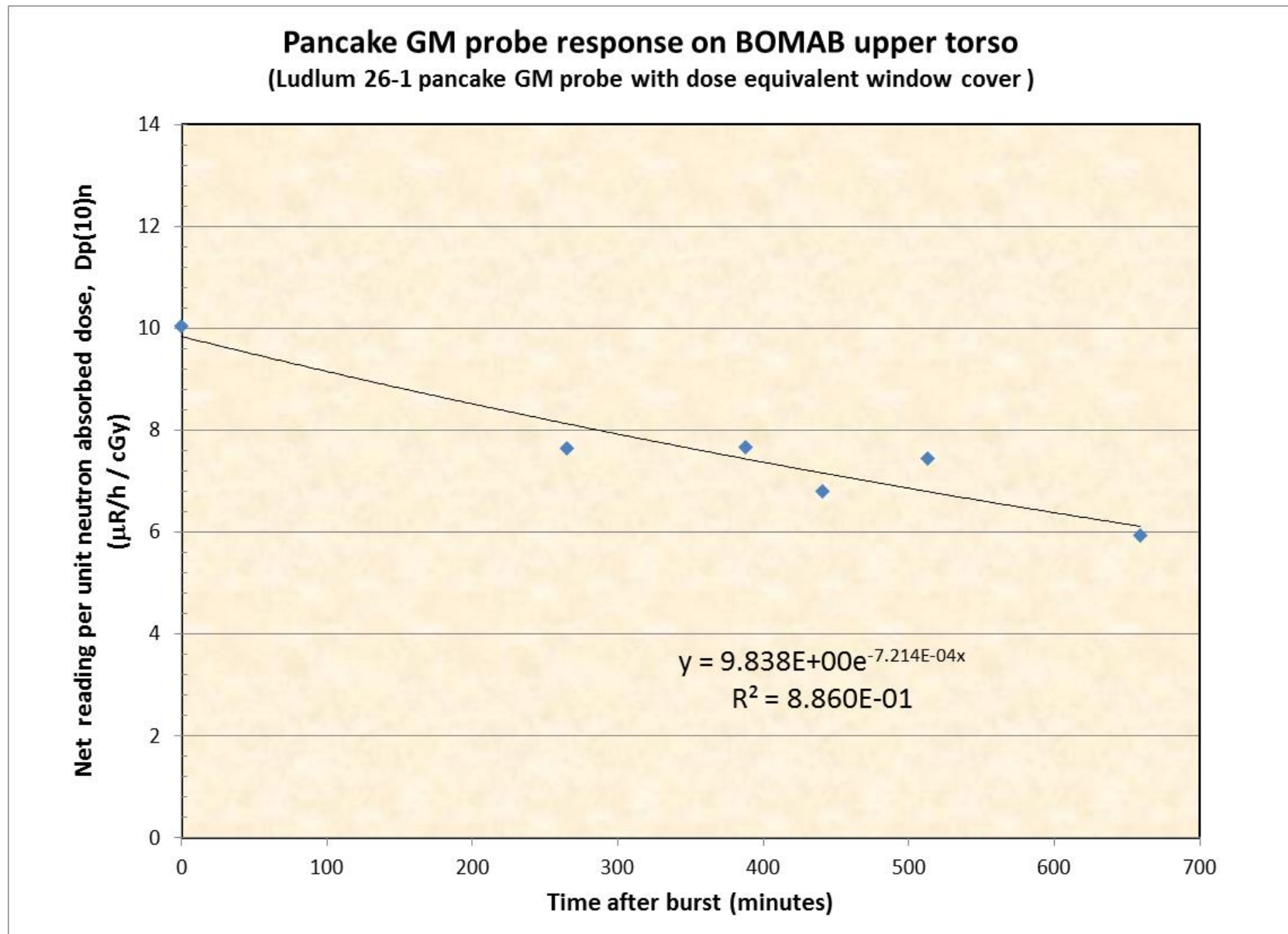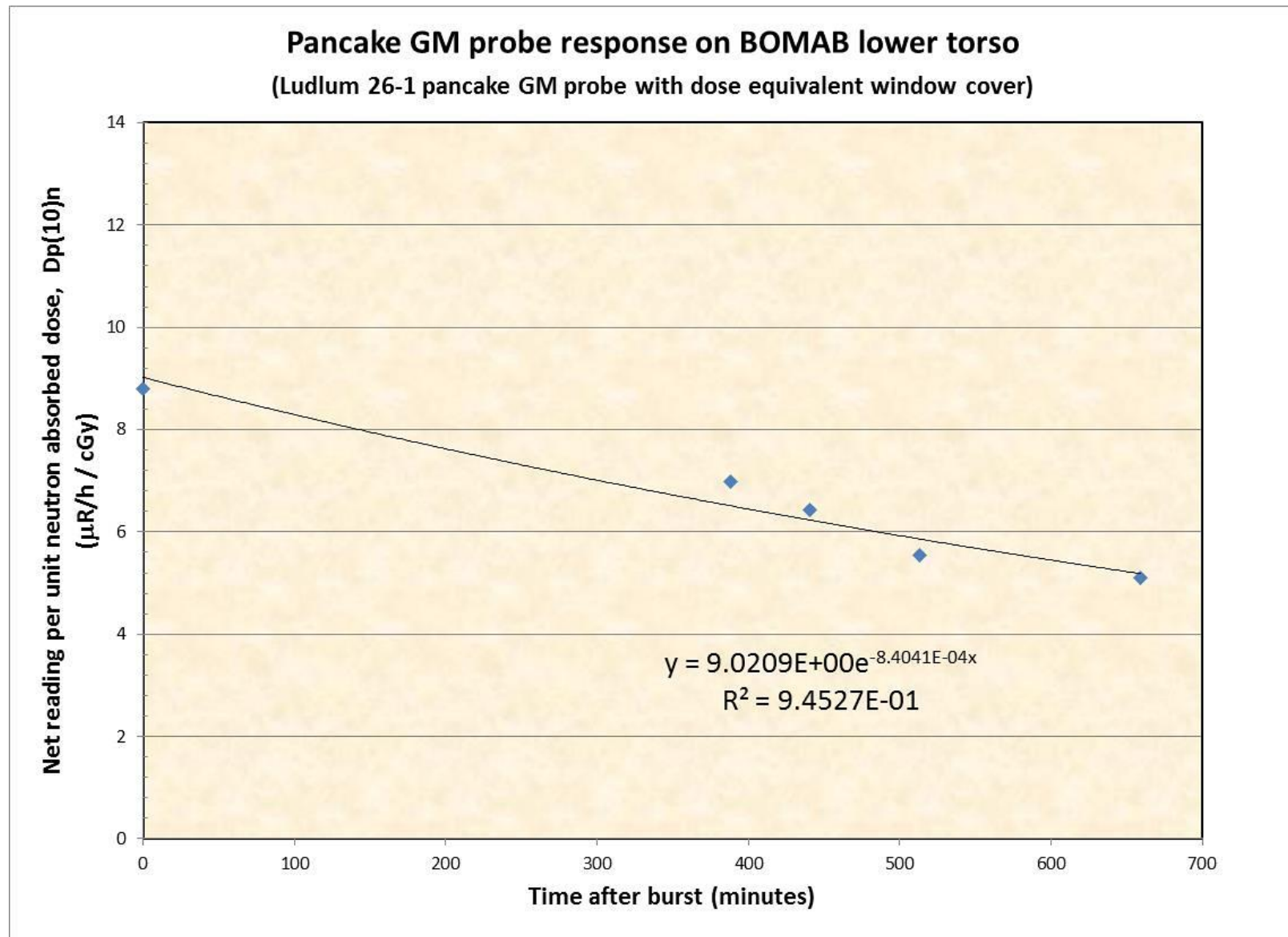**Pancake GM probe response on BOMAB upper torso**
(Ludlum 26-1 pancake GM probe with dose equivalent window cover)

$y = 9.838E+00e^{-7.214E-04x}$

$R^2 = 8.860E-01$

Figure O.6 Pancake GM probe measurements on BOMAB lower torso

Pancake GM probe response on BOMAB lower torso

(Ludlum 26-1 pancake GM probe with dose equivalent window cover)

$y = 9.0209\text{E}+00e^{-8.4041\text{E}-04x}$

$R^2 = 9.4527\text{E}-01$

Net reading per unit neutron absorbed dose, $D_p(10)n$ (μR/h / cGy)

Time after burst (minutes)

Appendix P

PNAD Direct Survey Measurements

Table P.1 PNAD Direct Survey Measurement Data

Pulse #	Item Description	Item #	Gross cpm	Net cpm	Date MM/DD/YYYY	Time HH:MM	Measurement Date-Time MM/DD/YYYY HH:MM	Burst Date-Time MM/DD/YYY HH:MM	Decay time after burst (minutes)
	Direct Survey Measurements of PNADs with Ludlum 43-93 alpha-beta scint probe								
1	NAD breakdown Room	bkg	1022	0	5/24/2016	12:00	5/24/2016 12:00	5/24/2016 10:12	108
1	Hanford PNAD	61	15000	13978	5/24/2016	14:29	5/24/2016 14:29	5/24/2016 10:12	257
1	Hanford PNAD	62	24000	22978	5/24/2016	14:30	5/24/2016 14:30	5/24/2016 10:12	258
1	PNNL PNAD front	1	20000	18978	5/24/2016	14:13	5/24/2016 14:13	5/24/2016 10:12	241
1	PNNL PNAD back	1	28000	26978	5/24/2016	14:14	5/24/2016 14:14	5/24/2016 10:12	242
1	PNNL PNAD front	2	24000	22978	5/24/2016	14:14	5/24/2016 14:14	5/24/2016 10:12	242
1	PNNL PNAD back	2	32000	30978	5/24/2016	14:15	5/24/2016 14:15	5/24/2016 10:12	243
1	PNNL PNAD front	3	22000	20978	5/24/2016	14:16	5/24/2016 14:16	5/24/2016 10:12	244
1	PNNL PNAD back	3	26000	24978	5/24/2016	14:16	5/24/2016 14:16	5/24/2016 10:12	244
1	PNNL PNAD front	4	22000	20978	5/24/2016	14:16	5/24/2016 14:16	5/24/2016 10:12	244
1	PNNL PNAD back	4	28000	26978	5/24/2016	14:17	5/24/2016 14:17	5/24/2016 10:12	245
1	PNNL PNAD front	5	34000	32978	5/24/2016	14:17	5/24/2016 14:17	5/24/2016 10:12	245
1	PNNL PNAD back	5	46000	44978	5/24/2016	14:18	5/24/2016 14:18	5/24/2016 10:12	246
1	PNNL PNAD front	6	20000	18978	5/24/2016	14:19	5/24/2016 14:19	5/24/2016 10:12	247
1	PNNL PNAD back	6	26000	24978	5/24/2016	14:20	5/24/2016 14:20	5/24/2016 10:12	248
1	PNNL PNAD front	7	34000	32978	5/24/2016	14:20	5/24/2016 14:20	5/24/2016 10:12	248
1	PNNL PNAD back	7	46000	44978	5/24/2016	14:20	5/24/2016 14:20	5/24/2016 10:12	248
1	PNNL PNAD front	8	24000	22978	5/24/2016	14:21	5/24/2016 14:21	5/24/2016 10:12	249
1	PNNL PNAD back	8	30000	28978	5/24/2016	14:21	5/24/2016 14:21	5/24/2016 10:12	249
1	PNNL PNAD front	9	24000	22978	5/24/2016	14:21	5/24/2016 14:21	5/24/2016 10:12	249
1	PNNL PNAD back	9	28000	26978	5/24/2016	14:22	5/24/2016 14:22	5/24/2016 10:12	250
1	PNNL PNAD front	10	22000	20978	5/24/2016	14:22	5/24/2016 14:22	5/24/2016 10:12	250
1	PNNL PNAD back	10	28000	26978	5/24/2016	14:22	5/24/2016 14:22	5/24/2016 10:12	250
1	PNNL PNAD front	11	22000	20978	5/24/2016	14:22	5/24/2016 14:22	5/24/2016 10:12	250
1	PNNL PNAD back	11	30000	28978	5/24/2016	14:23	5/24/2016 14:23	5/24/2016 10:12	251
1	PNNL PNAD front	12	22000	20978	5/24/2016	14:23	5/24/2016 14:23	5/24/2016 10:12	251
1	PNNL PNAD back	12	28000	26978	5/24/2016	14:24	5/24/2016 14:24	5/24/2016 10:12	252
1	PNNL PNAD front	13	28000	26978	5/24/2016	14:24	5/24/2016 14:24	5/24/2016 10:12	252
1	PNNL PNAD back	13	38000	36978	5/24/2016	14:24	5/24/2016 14:24	5/24/2016 10:12	252
1	PNNL PNAD front	14	24000	22978	5/24/2016	14:24	5/24/2016 14:24	5/24/2016 10:12	252
1	PNNL PNAD back	14	30000	28978	5/24/2016	14:25	5/24/2016 14:25	5/24/2016 10:12	253
1	PNNL PNAD front	15	18000	16978	5/24/2016	14:25	5/24/2016 14:25	5/24/2016 10:12	253
1	PNNL PNAD back	15	22000	20978	5/24/2016	14:26	5/24/2016 14:26	5/24/2016 10:12	254
1	PNNL PNAD front	16	20000	18978	5/24/2016	14:26	5/24/2016 14:26	5/24/2016 10:12	254
1	PNNL PNAD back	16	22000	20978	5/24/2016	14:27	5/24/2016 14:27	5/24/2016 10:12	255

Pulse #	Item Description	Item #	Gross cpm	Net cpm	Date MM/DD/YYYY	Time HH:MM	Measurement Date-Time MM/DD/YYY HH:MM	Burst Date-Time MM/DD/YYY HH:MM	Decay time after burst (minutes)
	Direct Survey Measurements of PNADs with Ludlum 43-93 alpha-beta scint probe								
2	NAD breakdown Room	bkg	900	0	5/25/2016	12:00	5/25/2016 12:00	5/25/2016 9:43	137
2	Hanford PNAD	63	42000	41100	5/25/2016	17:11	5/25/2016 17:11	5/25/2016 9:43	448
2	Hanford PNAD	64	63000	62100	5/25/2016	17:12	5/25/2016 17:12	5/25/2016 9:43	449
2	PNNL PNAD front	17	70000	69100	5/25/2016	17:13	5/25/2016 17:13	5/25/2016 9:43	450
2	PNNL PNAD back	17	90000	89100	5/25/2016	17:14	5/25/2016 17:14	5/25/2016 9:43	451
2	PNNL PNAD front	18	60000	59100	5/25/2016	17:15	5/25/2016 17:15	5/25/2016 9:43	452
2	PNNL PNAD back	18	85000	84100	5/25/2016	17:16	5/25/2016 17:16	5/25/2016 9:43	453
2	PNNL PNAD front	19	64000	63100	5/25/2016	17:17	5/25/2016 17:17	5/25/2016 9:43	454
2	PNNL PNAD back	19	84000	83100	5/25/2016	17:18	5/25/2016 17:18	5/25/2016 9:43	455
2	PNNL PNAD front	20	64000	63100	5/25/2016	17:19	5/25/2016 17:19	5/25/2016 9:43	456
2	PNNL PNAD back	20	80000	79100	5/25/2016	17:20	5/25/2016 17:20	5/25/2016 9:43	457
2	PNNL PNAD front	21	99000	98100	5/25/2016	17:21	5/25/2016 17:21	5/25/2016 9:43	458
2	PNNL PNAD back	21	125000	124100	5/25/2016	17:22	5/25/2016 17:22	5/25/2016 9:43	459
2	PNNL PNAD front	22	54000	53100	5/25/2016	17:23	5/25/2016 17:23	5/25/2016 9:43	460
2	PNNL PNAD back	22	69000	68100	5/25/2016	17:24	5/25/2016 17:24	5/25/2016 9:43	461
2	PNNL PNAD front	23	97000	96100	5/25/2016	17:25	5/25/2016 17:25	5/25/2016 9:43	462
2	PNNL PNAD back	23	124000	123100	5/25/2016	17:26	5/25/2016 17:26	5/25/2016 9:43	463
2	PNNL PNAD front	24	59000	58100	5/25/2016	17:27	5/25/2016 17:27	5/25/2016 9:43	464
2	PNNL PNAD back	24	76000	75100	5/25/2016	17:28	5/25/2016 17:28	5/25/2016 9:43	465
2	PNNL PNAD front	25	85000	84100	5/25/2016	17:29	5/25/2016 17:29	5/25/2016 9:43	466
2	PNNL PNAD back	25	106000	105100	5/25/2016	17:30	5/25/2016 17:30	5/25/2016 9:43	467
2	PNNL PNAD front	26	70000	69100	5/25/2016	17:31	5/25/2016 17:31	5/25/2016 9:43	468
2	PNNL PNAD back	26	91000	90100	5/25/2016	17:32	5/25/2016 17:32	5/25/2016 9:43	469
2	PNNL PNAD front	27	65000	64100	5/25/2016	17:33	5/25/2016 17:33	5/25/2016 9:43	470
2	PNNL PNAD back	27	88000	87100	5/25/2016	17:34	5/25/2016 17:34	5/25/2016 9:43	471
2	PNNL PNAD front	28	64000	63100	5/25/2016	17:35	5/25/2016 17:35	5/25/2016 9:43	472
2	PNNL PNAD back	28	79000	78100	5/25/2016	17:36	5/25/2016 17:36	5/25/2016 9:43	473
2	PNNL PNAD front	29	49000	48100	5/25/2016	17:37	5/25/2016 17:37	5/25/2016 9:43	474
2	PNNL PNAD back	29	62000	61100	5/25/2016	17:38	5/25/2016 17:38	5/25/2016 9:43	475
2	PNNL PNAD front	30	52000	51100	5/25/2016	17:39	5/25/2016 17:39	5/25/2016 9:43	476
2	PNNL PNAD back	30	63000	62100	5/25/2016	17:40	5/25/2016 17:40	5/25/2016 9:43	477
2	PNNL PNAD front	31	50000	49100	5/25/2016	17:41	5/25/2016 17:41	5/25/2016 9:43	478
2	PNNL PNAD back	31	66000	65100	5/25/2016	17:42	5/25/2016 17:42	5/25/2016 9:43	479
2	PNNL PNAD front	32	53000	52100	5/25/2016	17:43	5/25/2016 17:43	5/25/2016 9:43	480
2	PNNL PNAD back	32	64000	63100	5/25/2016	17:44	5/25/2016 17:44	5/25/2016 9:43	481

Pulse #	Item Description	Item #	Gross cpm	Net cpm	Date MM/DD/YYYY	Time HH:MM	Measurement Date-Time MM/DD/YYY HH:MM	Burst Date-Time MM/DD/YYY HH:MM	Decay time after burst (minutes)
	Direct Survey Measurements of PNADs with Ludlum 43-93 alpha-beta scint probe								
3	NAD breakdown Room	bkg	3310	0	5/26/2016	15:42	5/26/2016 15:42	5/26/2016 11:36	246
3	Hanford PNAD	65	41000	37690	5/26/2016	15:43	5/26/2016 15:43	5/26/2016 11:36	247
3	Hanford PNAD	66	60000	56690	5/26/2016	15:44	5/26/2016 15:44	5/26/2016 11:36	248
3	PNNL PNAD front	33	57000	53690	5/26/2016	15:33	5/26/2016 15:33	5/26/2016 11:36	237
3	PNNL PNAD back	33	81000	77690	5/26/2016	15:33	5/26/2016 15:33	5/26/2016 11:36	237
3	PNNL PNAD front	34	90000	86690	5/26/2016	15:33	5/26/2016 15:33	5/26/2016 11:36	238
3	PNNL PNAD back	34	111000	107690	5/26/2016	15:33	5/26/2016 15:33	5/26/2016 11:36	238
3	PNNL PNAD front	35	46000	42690	5/26/2016	15:34	5/26/2016 15:34	5/26/2016 11:36	238
3	PNNL PNAD back	35	63000	59690	5/26/2016	15:34	5/26/2016 15:34	5/26/2016 11:36	239
3	PNNL PNAD front	36	58000	54690	5/26/2016	15:34	5/26/2016 15:34	5/26/2016 11:36	239
3	PNNL PNAD back	36	65000	61690	5/26/2016	15:35	5/26/2016 15:35	5/26/2016 11:36	239
3	PNNL PNAD front	37	86000	82690	5/26/2016	15:35	5/26/2016 15:35	5/26/2016 11:36	239
3	PNNL PNAD back	37	111000	107690	5/26/2016	15:35	5/26/2016 15:35	5/26/2016 11:36	240
3	PNNL PNAD front	38	78000	74690	5/26/2016	15:36	5/26/2016 15:36	5/26/2016 11:36	240
3	PNNL PNAD back	38	100000	96690	5/26/2016	15:36	5/26/2016 15:36	5/26/2016 11:36	240
3	PNNL PNAD front	39	39000	35690	5/26/2016	15:36	5/26/2016 15:36	5/26/2016 11:36	241
3	PNNL PNAD back	39	48000	44690	5/26/2016	15:36	5/26/2016 15:36	5/26/2016 11:36	241
3	PNNL PNAD front	40	9300	5990	5/26/2016	15:37	5/26/2016 15:37	5/26/2016 11:36	241
3	PNNL PNAD back	40	8700	5390	5/26/2016	15:37	5/26/2016 15:37	5/26/2016 11:36	242
3	PNNL PNAD front	41	15200	11890	5/26/2016	15:37	5/26/2016 15:37	5/26/2016 11:36	242
3	PNNL PNAD back	41	18500	15190	5/26/2016	15:38	5/26/2016 15:38	5/26/2016 11:36	242
3	PNNL PNAD front	42	56000	52690	5/26/2016	15:38	5/26/2016 15:38	5/26/2016 11:36	242
3	PNNL PNAD back	42	72000	68690	5/26/2016	15:38	5/26/2016 15:38	5/26/2016 11:36	243
3	PNNL PNAD front	43	49000	45690	5/26/2016	15:39	5/26/2016 15:39	5/26/2016 11:36	243
3	PNNL PNAD back	43	61000	57690	5/26/2016	15:39	5/26/2016 15:39	5/26/2016 11:36	243
3	PNNL PNAD front	44	76000	72690	5/26/2016	15:39	5/26/2016 15:39	5/26/2016 11:36	244
3	PNNL PNAD back	44	89000	85690	5/26/2016	15:39	5/26/2016 15:39	5/26/2016 11:36	244
3	PNNL PNAD front	45	122000	118690	5/26/2016	15:40	5/26/2016 15:40	5/26/2016 11:36	244
3	PNNL PNAD back	45	154000	150690	5/26/2016	15:40	5/26/2016 15:40	5/26/2016 11:36	245
3	PNNL PNAD front	46	52000	48690	5/26/2016	15:40	5/26/2016 15:40	5/26/2016 11:36	245
3	PNNL PNAD back	46	64000	60690	5/26/2016	15:41	5/26/2016 15:41	5/26/2016 11:36	245

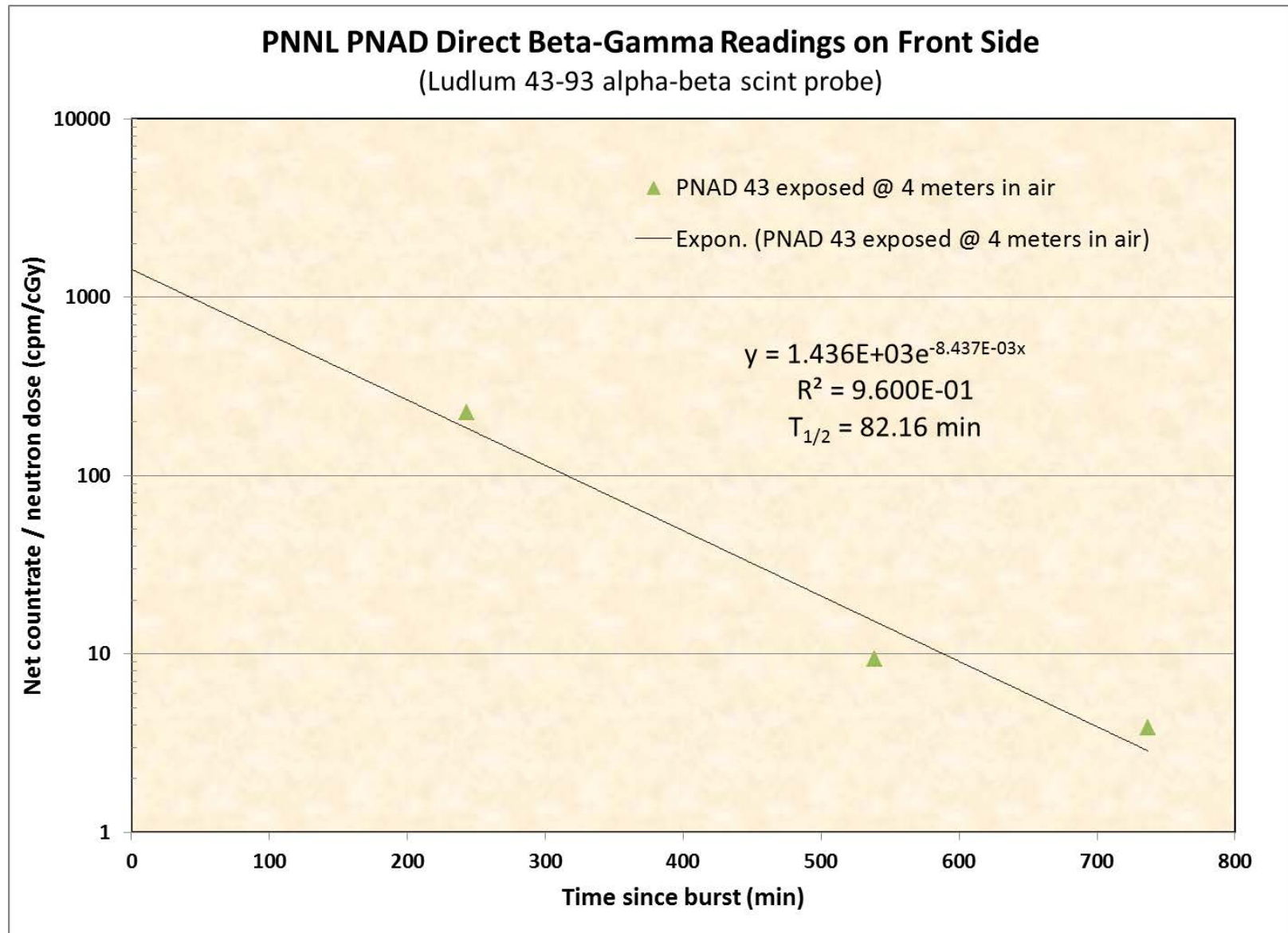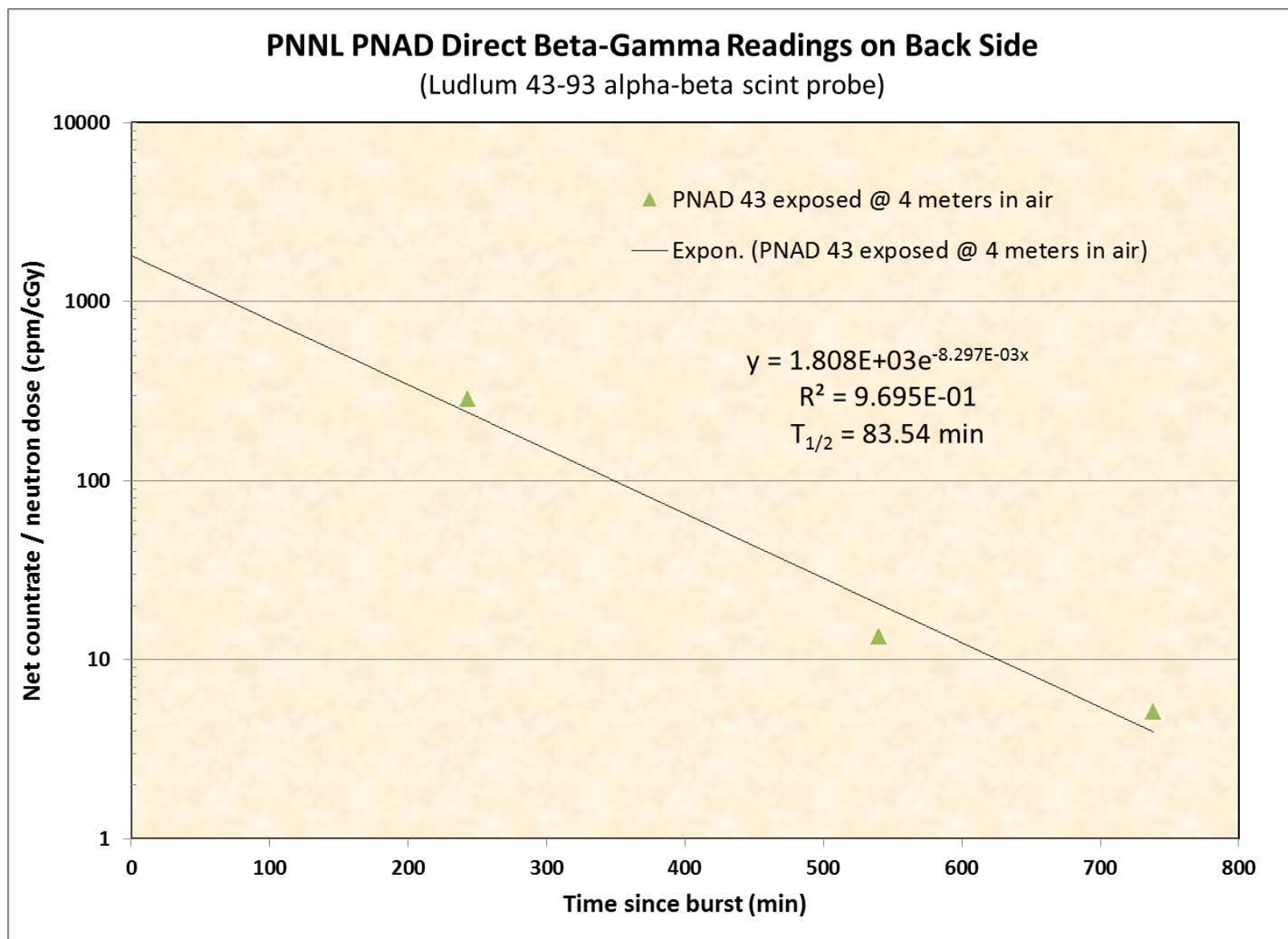**Figure P.1** Decay of PNNL PNAD Contact Readings on Front Side with Ludlum 43-93 Probe

Figure P.2 Decay of PNNL PNAD Contact Readings on Back Side with Ludlum 43-93 Probe